CANADIAN THESES ON MICROFICHE

I.S.B.N.

THESES CANADIENNES SUR MICROFICHE

National Library of Canada
Collections Development Branch

Canadian Theses on
Microfiche Service

Ottawa, Canada
K1A 0N4

Bibliothèque nationale du Canada
Direction du développement des collections

Service des thèses canadiennes
sur microfiche

NOTICE

The quality of this microfiche is heavily dependent upon the quality of the original thesis submitted for microfilming. Every effort has been made to ensure the highest quality of reproduction possible.

If pages are missing, contact the university which granted the degree.

Some pages may have indistinct print especially if the original pages were typed with a poor typewriter ribbon or if the university sent us a poor photocopy.

Previously copyrighted materials (journal articles, published tests, etc.) are not filmed.

Reproduction in full or in part of this film is governed by the Canadian Copyright Act, R.S.C. 1970, c. C-30. Please read the authorization forms which accompany this thesis.

THIS DISSERTATION
HAS BEEN MICROFILMED
EXACTLY AS RECEIVED

AVIS

La qualité de cette microfiche dépend grandement de la qualité de la thèse soumise au microfilmage. Nous avons tout fait pour assurer une qualité supérieure de reproduction.

S'il manque des pages, veuillez communiquer avec l'université qui a conféré le grade.

La qualité d'impression de certaines pages peut laisser à désirer, surtout si les pages originales ont été dactylographiées à l'aide d'un ruban usé ou si l'université nous a fait parvenir une photocopie de mauvaise qualité.

Les documents qui font déjà l'objet d'un droit d'auteur (articles de revue, examens publiés, etc.) ne sont pas microfilmés.

La reproduction, même partielle, de ce microfilm est soumise à la Loi canadienne sur le droit d'auteur, SRC 1970, c. C-30. Veuillez prendre connaissance des formules d'autorisation qui accompagnent cette thèse.

LA THÈSE A ÉTÉ
MICROFILMÉE TELLE QUE
NOUS L'AVONS REÇUE

NL-339 (r. 82/08)

Canada

154

0-315-16063-2

National Library of Canada
Bibliothèque nationale du Canada

Canadian Theses Division
Division des thèses canadiennes

Ottawa, Canada
K1A 0N4

63972

PERMISSION TO MICROFILM — AUTORISATION DE MICROFILMER

- Please print or type — Écrire en lettres moulées ou dactylographier

Full Name of Author — Nom complet de l'auteur

JAMES CRAIG MILLER

Date of Birth — Date de naissance 13 OCT 1949	Country of Birth — Lieu de naissance CANADA

Permanent Address — Résidence fixe

157A BRUNSWICK ST,
TRURO, N.S.

Title of Thesis — Titre de la thèse

LAYER MODEL OF CHROMATOGRAPHIC SOLUTE TRANSPORT THROUGH PARTIALLY FROZEN STRUCTURED SOIL

University — Université

UNIV OF ALBERTA

Degree for which thesis was presented — Grade pour lequel cette thèse fut présentée

M. Sc.

Year this degree conferred — Année d'obtention de ce grade 1983	Name of Supervisor — Nom du directeur de thèse DR. W. B. McGILL

Permission is hereby granted to the NATIONAL LIBRARY OF CANADA to microfilm this thesis and to lend or sell copies of the film.

The author reserves other publication rights, and neither the thesis nor extensive extracts from it may be printed or otherwise reproduced without the author's written permission.

L'autorisation est, par la présente, accordée à la BIBLIOTHÈQUE NATIONALE DU CANADA de microfilmer cette thèse et de prêter ou de vendre des exemplaires du film.

L'auteur se réserve les autres droits de publication; ni la thèse ni de longs extraits de celle-ci ne doivent être imprimés ou autrement reproduits sans l'autorisation écrite de l'auteur.

Date 2 FEB 1983	Signature Craig Miller

THE UNIVERSITY OF ALBERTA

Layer Model of Chromatographic Solute Transport Through Partially Frozen Structured Soil

by

(C)

JAMES CRAIG MILLER

A THESIS
SUBMITTED TO THE FACULTY OF GRADUATE STUDIES AND RESEARCH
IN PARTIAL FULFILMENT OF THE REQUIREMENTS FOR THE DEGREE
OF MASTER OF SCIENCE

DEPARTMENT OF SOIL SCIENCE

EDMONTON, ALBERTA
SPRING 1983

[illegible]

THE UNIVERSITY OF ALBERTA

RELEASE FORM

NAME OF AUTHOR JAMES CRAIG MILLER

TITLE OF THESIS Layer Model of Chromatographic Solute Transport Through Partially Frozen Structured Soil

DEGREE FOR WHICH THESIS WAS PRESENTED MASTER OF SCIENCE

YEAR THIS DEGREE GRANTED SPRING 1983

Permission is hereby granted to THE UNIVERSITY OF ALBERTA LIBRARY to reproduce single copies of this thesis and to lend or sell such copies for private, scholarly or scientific research purposes only.

The author reserves other publication rights, and neither the thesis nor extensive extracts from it may be printed or otherwise reproduced without the author's written permission.

(SIGNED) Craig Miller

PERMANENT ADDRESS:

157 A BRUNSWICK ST,
TRURO,
NOVA SCOTIA

DATED 31 JAN 1983

THE UNIVERSITY OF ALBERTA

FACULTY OF GRADUATE STUDIES AND RESEARCH

The undersigned certify that they have read, and recommend to the Faculty of Graduate Studies and Research, for acceptance, a thesis entitled Layer Model of Chromatographic Solute Transport Through Partially Frozen Structured Soil submitted by JAMES CRAIG MILLER in partial fulfilment of the requirements for the degree of MASTER OF SCIENCE.

Bill McGill

Supervisor

Frank W. Schwartz

G.R. Webster

D.S. Chanasyk

Date 31 JAN. 1983

ABSTRACT

A two-pool layer simulation model was constructed to describe solute transport through partially frozen, structured soil and a FORTRAN computer program written to implement the model. The model was based on a numerical solution of the continuity/chromatography differential equation. It can be applied to transport of non-reactive or adsorbed solutes through thawed or partially frozen soil.

Effects of soil structure were described by defining two interactive solution pools, mobile and stagnant, based on the concepts presented by Addiscott (1977). Solute transport occurs only in the mobile pool and equilibration between pools is effected between infiltration events.

Simulation experiments determined that the model was sensitive to stagnant:mobile pool size ratio, infiltration rates, adsorption coefficients and presence of a frozen layer, but not to layer thickness between 1.3 and ten cm. Simulations produced upwardly skewed solute profiles at higher solution flow rates and symmetrical profiles at lower flow rates. Frozen layers produced symmetrical profiles by reducing flow rates, thereby causing greater equilibration between pools.

Simulations were compared with results of leaching experiments performed on a Gray Luvisolic soil during spring infiltration of meltwater, using ^{3}HOH and ^{14}C-lindane as solutes. Effects of adsorption and frozen soil dominated over effects of soil structure on solute distribution.

ACKNOWLEDGMENTS

I would like to express my gratitude to my supervisor, Dr. W.B. McGill, for his help and guidance during the course of this study. Thanks are also extended to the other members of my thesis committee, Dr. D.S. Chanasyk, Dr. F.W. Schwartz, and Dr. G.R. Webster. Other members of the Department of Soil Science gave helpful comments or encouragement, in particular Dr. J.A. Robertson and Dr. S. Pawluk.

Financial assistance was provided by the Natural Sciences Engineering Research Council for chemicals and analyses and by the Department of Soil Science for computer time. The Alberta Research Council kindly provided equipment and assistance in obtaining field samples. Agriculture Canada also provided equipment.

This project could not have been started without the moral, and financial, support of my wife Kathie, and I hope that the gratitude I feel for her sacrifices is obvious without this acknowledgment.

Table of Contents

Chapter Page

I. INTRODUCTION AND LITERATURE REVIEW 1

A. INTRODUCTION 1

B. LITERATURE REVIEW 3

1. Derivation of Chromatographic Equation 3

2. Solutions to the Chromatographic Model 19

3. The Transport Model Applied to Structured Soils 30

II. MATERIALS AND METHODS 34

A. SIMULATION MODEL - DEVELOPMENT 34

1. Moisture Flux 34

2. Solute Transport (non-reactive solutes) ..37

3. Transport of Adsorbed solutes 44

4. Pesticide Decay 46

B. FIELD EXPERIMENTS 48

1. Soil 48

2. Solutes 48

3. Experimental Design 50

4. Field Measurements 52

5. Laboratory Analyses 53

III. RESULTS AND DISCUSSION 61

A. SIMULATION EXPERIMENTS 61

1. Relative Sizes of Mobile and Stagnant Pools 61

2. Rate and Pattern of Infiltration 68

3. Layer thickness 76

4. Frozen Soil 80

5. Adsorption 83
B. FIELD LEACHING EXPERIMENTS 88
Experiment 1: Leaching of Non-reactive Solute (^{3}HOH) 88
Experiment 2: Leaching of Adsorbed Solute (^{14}C-lindane) 96
C. SIMULATION OF FIELD EXPERIMENTS 101
1. Physical Properties Controlling Simulation Experiments 101
2. Comparison of Simulations and Field Observations 108
IV. SUMMARY AND CONCLUSIONS 122
A. SUMMARY 122
B. CONCLUSIONS 125
REFERENCES 128
APPENDIX A 133
APPENDIX B 134
APPENDIX C 136
APPENDIX D 138
APPENDIX E 145
APPENDIX F 154

LIST OF TABLES

Table Page

II.1 Characteristics of Breton Loam....................49

II.2 Chemical properties of lindane....................49

II.3 Preparation of liquid scintillation cocktail for direct counting of soil-borne ^{14}C-lindane and ^{3}HOH....................57

III.1 Data used in simulation experiment 1a: Influence of size of mobile and stagnant moisture pools on solute distribution....................61

III.2 Data [illegible]d in simulation experiment 1b: Infl[illegible]e of soil tension value used to assign WR [illegible] solute distribution....................66

III.3 Data used in simulation experiment 2a: Influence of infiltration rate on solute distribution....................69

III.4 Data used in simulation experiment 2b: Influence of infiltration pattern on solute distribution....................74

III.5 Data used in simulation experiment 3: Influence of layer thickness on solute distribution....................78

III.6 Data used in simulation experiment 4: Influence of frozen soil on solute distribution....................81

III.7 Data used in simulation experiment 5a: Influence of adsorption on solute distribution....84

III.8 Data used in simulation experiment 5b: Influence of infiltration rate on distribution of an adsorbed solute....................87

III.9 Physical properties of Breton Loam..............103

III.10 Volumetric moisture contents used to determine WR and WMCAP.......................................104

III.11 Infiltration measured at experimental plots 106

LIST OF FIGURES

Figure Page

I.1 Mass flow through a thin volume element............5

I.2 Hydrodynamic dispersion in a capillary tube........9

I.3 Freundlich (Giles class L) isotherm..............13

I.4 Schematic diagram of adsorption for "class L" isotherm..13

II.1 Field experiment plot layout 51

II.2 Accountability vs SCR curve for direct liquid scintillation radioassay of ^{14}C-lindane in soil-scintillation cocktail mixture...............59

II.3 Accountability vs SCR curve for direct liquid scintillation radioassay of ^{3}HOH in soil-scintillation cocktail mixture...............60

III.1 Simulation experiment 1a: Influence of relative sizes of stagnant and mobile water pools on distribution of solute added to the surface layer of a structured soil after simulated leaching by 20 cm of water.........................62

III.2 Simulation experiment 1b: Influence of soil moisture tension used to assign sizes of stagnant and mobile water pools on distribution of solute added to surface layer of a structured soil after simulated leaching by 20 cm of water.................................67

III.3 Simulation experiment 2a: Influence of infiltration rates on distribution of solute added to the surface layer of a structured soil after simulated leaching by 20 cm of water........70

III.4 Simple numerical simulations of solute transport.......................................72

III.5 Infiltration pattern used in simulation experiment 2b.....75

III.6 Simulation experiment 2b: Influence of infiltration pattern on distribution of solute applied to surface layer of a structured soil after simulated leaching by 20 cm of water.....77

III.7 Simulation experiment 3: Influence of layer thickness on distribution of solute applied to the surface layer of a structured soil after simulated leaching by 20 cm of water.....79

III.8 Simulation experiment 4: Influence of frozen layer on distribution of solute applied to the surface layer of a structured soil after simulated leaching by 12.5 cm of water.....82

III.9 Simulation experiment 5a: Influence of adsorption on distribution of solute applied to the surface layer of a structured soil after simulated leaching by 20 cm of water.....86

III.10 Simulation experiment 5b: Influence of infiltration rate on distribution of an adsorbed solute applied to the surface of structured soil after simulated leaching by 25 cm of water.....89

III.11 Tritium activity distribution observed in May, 1982, after ^{3}HOH was applied to the surface of the Ap horizon in Dec., 1981.....91

III.12 Tritium activity distribution observed in May, 1982, after ^{3}HOH was applied to the upper surface of the Bt horizon in Dec., 1981.....93

III.13 Determination of evaporation by integration between successive θ profiles on Apr. 29 and May 3, 1982.....95

III.14 Lindane adsorption isotherms.....97

III.15 ^{14}C activity distribution observed in May, 1982, after ^{14}C-lindane was applied to the surface of the Ap horizon in Dec., 1981..........98

III.16 ^{14}C activity distribution observed in May, 1982, after ^{14}C-lindane was applied to the upper surface of the Bt horizon in Dec., 1981....100

III.17 Soil moisture tension curve, Breton Loam: Ap, Bt, and BC horizons............................105

III.18 Observed and predicted spring tritium activity distribution after ^{3}HOH was applied to the Ap horizon in fall..110

III.19 Observed and predicted spring tritium activity distribution after ^{3}HOH was applied to the upper surface of Bt horizon in fall..............113

III.20 Observed and predicted spring ^{14}C activity distribution after ^{14}C-lindane was applied to the Ap horizon in fall........................118

III.21 Observed and predicted spring ^{14}C activity distribution after ^{14}C-lindane was applied to the upper surface of Bt horizon in fall..120

I. INTRODUCTION AND LITERATURE REVIEW

A. INTRODUCTION

The transport of solutes through soil is a dynamic process involving physical, chemical, and biological phenomena. Estimation of degree and extent of leaching is important in studies in pollution, soil fertility, and soil genesis.

One of the major challenges in the study of leaching through soil is determination of the quantitative relationships among the many factors which affect solute movement. In the field of chromatography the continuity equation has been applied with success to the quantitative description of solute transport through packed columns of homogeneous porous media (a list of symbols used is given in Appendix A):

$$\alpha(\partial c/\partial t) + Db(\partial a/\partial t) = -\upsilon(\partial c/\partial z) + D(\partial^2 c/\partial z^2).$$

This model of solute movement relates the rate of change in solute mass stored at depth, z, ($\alpha(\partial c/\partial t) + Db(\partial a/\partial t)$) to solute flux density due to mass flow ($-\upsilon(\partial c/\partial z)$) and diffusion ($D(\partial^2 c/\partial z^2)$). The rate of change in mass stored is divided into two components: mass dissolved in solution (c), and mass (a), held on the solid porous medium (by adsorption, electrostatic attraction, etc.). Thus the change in mass with time is expressed as the sum of partial derivatives.

Because soil is a porous medium that may adsorb solutes the soil column may be regarded as a chromatographic column in leaching studies. The model is useful because it can be used to assess the relative importance of the many factors which influence leaching. In the field, irregular patterns of leaching events and soil heterogeneity with respect to the parameters and variables used in the model make its analytical solution difficult. The chromatographic model can, however, be extended to provide a quantitative description of soil leaching, using numerical techniques and high speed computation. Further refinements can extend its use to predictive modelling.

In short the chromatographic model is a powerful unifying concept in soil leaching studies because: i) it is a general description of solute movement; and, ii) it is quantitative.

This study attempts to extend the model to solute transport studies in structured soils during spring thaw. Two major problems encountered under these conditions are the irregular "packing arrangement" of the soil medium and spatial and temporal variation in patterns of water movement. The objectives of this project are:

i) to construct a numerical model of solute transport through partially frozen structured soil, based on the theoretical chromatography equation;

ii) write a computer program to implement the model;

iii) test the sensitivity of the model to the parameters and variables it uses;

iv) compare the results of simulated experiments with results of field experiments to test whether the model simulates solute transport in the field; and,

v) determine what structural modifications are required and what further experiments are necessary to elucidate the important solute transport mechanisms which operate in soil.

B. LITERATURE REVIEW

1. Derivation of Chromatographic Equation

The continuity equation was first applied to solute transport by chemists seeking to describe the behaviour of column separations (chromatography) (DeVault, 1943; Kasten *et al*., 1952; Lapidus and Amundsen, 1952; Glueckauf, 1955). In 1941 Martin and Synge introduced column partition chromatography (Zweig and Sherma, 1972), a concept which has proven useful in describing solute transport through soil. Chromatography can be defined as the study of movement of liquid mixtures through porous media. Soil is a porous medium and the soil solution is a liquid mixture; therefore, the soil system may be analogous to a chromatographic column.

The classical theory of chromatography as it relates to soils has been reviewed by Nielsen and Biggar (1962), Frissel and Poelstra (1967), and Kirkham and Powers (1972).

Leistra (1973) and Letey and Farmer (1974) reviewed pesticide transport models based on the chromatography equation. The former review stresses the mathematical techniques employed in computational models of solute transport, while the latter stresses the physics and chemistry described by the equation. Research related to specific problems encountered in applying the classical theory to soils is the subject of this review.

The following discussion develops the theory of chromatography as it applies to soil by deriving the continuity equation and reviewing contributions to the theory from both soil science literature and sources describing conditions paralleling those in soil.

a. Mass Flow

Mass flow, sometimes called convective flow, is the most important process influencing leaching of dissolved solutes and will be considered first in developing the chromatography equation. The continuity/chromatography equation, a statement of the law of conservation of mass applied to systems of liquid mixtures flowing through porous media, states mathematically that: any change in solute mass of solution passing through a volume element of porous medium must be accounted for by a change in mass stored within the volume element. This is illustrated in the figure I.1 and in the explanation following (adapted from Kirkham and Powers, 1972):

Figure I.1. Mass flow through a thin volume element (plate):

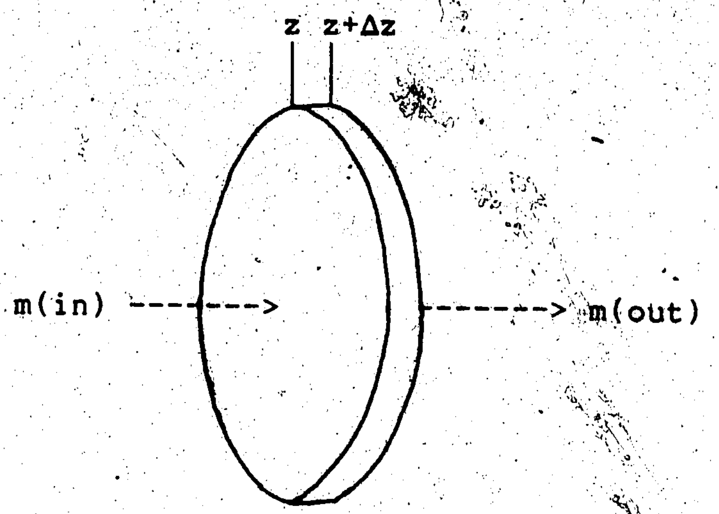

The mass, Ms, stored in the plate shown above, with thickness, Δz; cross sectional area, A; and volume $A\Delta z$, is given by:

$$Ms = m(in) - m(out).$$

Hence the change in mass stored with time is:

$$\begin{aligned} \Delta Ms/\Delta t &= \Delta[m(in)-m(out)]/\Delta t \\ &= [m(z,t+\Delta t)-m(z,t)-m(z+\Delta z,t+\Delta t)+m(z+\Delta z,t)]/\Delta t. \end{aligned}$$

The solute mass flux density, q(z), (rate of flow of mass through a unit cross sectional area of the plate) is given as:

$$q(z) = [dm(z)/dt]/A \qquad (1).$$

Therefore:

$$\begin{aligned} dMs/dt &= dm(z)/dt - dm(z+\Delta z)/dt \\ &= A[q(z) - q(z+\Delta z)] \qquad (2). \end{aligned}$$

The mass flux out of the volume element can be expressed as:

$$q(z+\Delta z) = q(z) + (dq(z)/dz)\Delta z.$$

Therefore:

$$\begin{aligned} \partial Ms/\partial t &= A[q(z) - (q(z) + \Delta z \cdot \partial q(z)/\partial z)] \\ &= -(A\Delta z)\partial q(z)/\partial z \qquad (3). \end{aligned}$$

Solute mass flux density, q, is related to liquid (solution) flux density, υ, and solute concentration, c:

$$q = \upsilon \cdot c \qquad (4).$$

So:

$$\partial Ms/\partial t = -(A\Delta z)\partial(\upsilon \cdot c)/\partial z \qquad (5).$$

Assuming that υ is constant through Δz, then:

$$\partial Ms/\partial t = -(A\Delta z)\upsilon(\partial c/\partial z) \qquad (6).$$

Ms can also be related to solute concentration:

$$Ms = V \cdot c,$$

where V = Vp (i.e. Volume = pore volume)

$$\begin{aligned} &= \alpha \cdot Vb \text{ (porosity X bulk volume)} \\ &= \alpha(A\Delta z). \end{aligned}$$

So that:

$$\partial Ms/\partial t = \alpha(A\Delta z)\partial c/\partial t,$$

if α does not change with time.

Therefore if solute is stored in solution only (substituting the above expression for the left side of equation (6)):

$$(A\Delta z)\alpha(\partial c/\partial t) = -(A\Delta z)\upsilon(\partial c/\partial z), \text{ or:}$$

$$\alpha(\partial c/\partial t) = -\upsilon(\partial c/\partial z) \qquad (7),$$

which equation describes solute transport by mass flow only and solute storage in solution only. The other main assumption is that the porous medium is homogeneous with respect to flux density, porosity and moisture content. Note that υ in this case is the liquid flux density, or Darcian velocity, and not the pore velocity, ν, as used in the equation given by Kirkham and Powers (1972). To convert to their equation, we need only note the relationship between pore velocity, ν, and Darcian velocity, υ:

$\nu = \upsilon/\alpha$, so:

$$\partial c/\partial t = -\nu(\partial c/\partial z).$$

b. Diffusion

Solute flux also occurs as a result of diffusion in response to concentration gradients. When a band of solute is applied to the soil surface, as when a pesticide is sprayed onto soil, a concentration gradient is set up and diffusion through the soil solution is induced. Fick's Law states that the diffusive flux, qd, is given by:

$$qd = -D(dC/dz),$$

where D is the diffusion coefficient of proportionality.

Diffusive and convective fluxes can be summed to express total flux, qt:

$$\begin{aligned} qt &= qc - qd \\ &= qc - D(dC/dz). \end{aligned}$$

By substituting qt for q equation (3) becomes:

$$\begin{aligned} \partial Ms/\partial t &= -(A\Delta z)\partial[qc - D(\partial c/\partial z)]/\partial z \\ &= -(A\Delta z)\partial qc/\partial z + (A\Delta z)D(\partial^2 c/\partial z^2), \end{aligned}$$

if D does not vary with z.

Recalling that convective flux, qc, is given by equation (4) ($qc = \upsilon \cdot c$) and provided υ is constant, then:

$$\alpha(\partial c/\partial t) = -\upsilon(\partial c/\partial z) + D(\partial^2 c/\partial z^2) \qquad (8).$$

Kirkham and Powers (1972) and Leistra (1973) present the form:

$$\partial c/\partial t = -\nu(\partial c/\partial z) + D'(\partial^2 c/\partial z^2),$$

which is identical to (8) if $\nu = \upsilon/\alpha$ and $D' = D/\alpha$.

The factors which influence D are given by Leistra (1973) to be volumetric moisture content (θ), geometry of the porous medium (tortuosity, etc), and partition of solute between solid and liquid phases, as well as the value of D in water (D_0). This study treats partition separately so D will be not be regarded as a function of partition parameters.

Frissel *et al*. (1970) define D as the product of D_0, θ, and tortuosity, but the theoretical basis of this expression was not given. Shearer *et al*. (1973) define D as:

$$D = (\theta/\alpha)^2 \theta^{4/3} D_0$$

The latter expression does not require determination of a tortuosity factor.

The preceeding discussion applies only to longitudinal diffusion. Transverse, or intra-aggregate (intrapedal) diffusion will be treated later under the effects of soil structure.

c. Dispersion

Spreading of the solute band is also caused by "hydrodynamic dispersion". While the term diffusion refers to the spreading of solute particles within the soil solution, dispersion refers to the longitudinal spreading caused by spatial variation in fluid flow rates.

Although the chromatographic equation deals with an average flow rate, solutions do not move at uniform rates through soil. Even in completely homogeneous media some mixing of fluid occurs because of adhesive and cohesive forces along pore walls(Figure I.2).

Figure I.2. Hydrodynamic dispersion due to "drag" in a capillary tube.

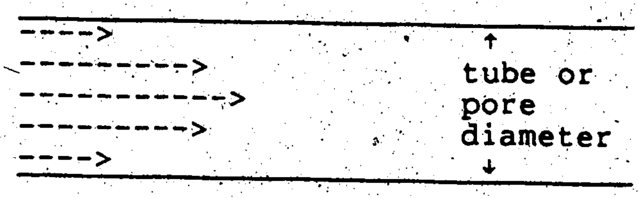

(Arrows represent the magnitude of fluid velocities and distance travelled by fluid "layers".)

This diagram represents "laminar flow" resulting from shearing of fluid in the longitudinal direction. This occurs because the attraction of the solid for the liquid retards movement close to the walls. Cohesion between liquid molecules resists flow away from the pore walls. Maximum flow rates occur at the greatest distance from the pore wall.

In the capillary bundle model (Nielsen and Bigger, 1962; Scheidegger, 1974) this is the mechanism of dispersion if flow is laminar. The degree of dispersive mixing in such a model depends on the pore radius and fluid velocity. In soil, however, the pore geometry is much more complex so pore radii cannot be well characterized by an average value. Therefore, characterizing liquid fluxes by an average value is frequently not realistic.

Amouzegar-Fard *et al*. (1982) tested the effects of probabilistic versus deterministic approaches to fluid velocity. They used normally distributed values of moisture flux to calculate 2000 separate solute concentration profiles in simulation experiments. They found that the average of the 2000 profiles differed sharply from the profile calculated using the mean value of moisture flux. This experiment provides a good illustration of the effects of dispersion on a larger scale than the capillary tube model.

Dispersion is treated in the classical equation in a manner analogous to diffusion (Kirkham and Powers, 1972):

$$q(disp) = -E(dc/dz),$$

where E is the coefficient of proportionality (cm^2/d). Because both diffusion and dispersion result in a spreading of solute they are commonly combined so that:

$$q(disp) + q(diff) = -Dspr(dc/dz).$$

Lumping D and E together as either Dspr or Da (Da = apparent diffusion or dispersion coefficient) necessitates a minor change in equation (8):

$$\alpha(\partial c/\partial t) = -\upsilon(\partial c/\partial z) + Dspr(\partial^2 c/\partial z^2) \qquad (9).$$

Diffusion perpendicular to the direction of flow reduces the effects of dispersion. Consequently dispersive and diffusive effects are not additive, making resolution of Dspr into D and E difficult. Nevertheless, Frissel *et al.* (1970) experimentally determined D and E, and defined Dspr as:

$$\mathrm{Dspr} = \upsilon \cdot E + \theta \cdot T \cdot D \qquad (10),$$

where T = tortuosity (dimensionless),

θ = volumetric moisture content (ml/cm^3).

Qualitatively, (10) states that diffusion effects are more important for low flux densities, while disperion effects are paramount for high fluxes.

d. Partition: Adsorption-Desorption

Up to this point phenomena which result in movement of solutes have been discussed. One of the main factors which cause retention or "holdback" of solute is adsorption. A substance is said to be adsorbed if the concentration of the substance (sorbate) in a boundary region (solid surface) is higher than the interior of the contiguous phase (soil solution) (Tinsley, 1979).

Chromatography utilizes the adsorptive partition of solute between mobile and stationary phases to separate solutes within or from solutions (Johnson, 1972). Separations occur in a similar fashion in soils. Soil scientists were the first to use isotherms to represent the adsorption-desorption partition (Giles, 1970).

For adsorption of many pesticides by soil the Freundlich isotherm has proven sufficiently accurate (Kay and Elrick, 1967; Oddson *et al.*, 1970; Lindstrom and Boersma, 1970). It describes an empirical relationship between amounts of adsorbed and dissolved substance at equilibrium, in which:

$$a = Kads \cdot c^{1/n} \qquad (11),$$

where a = amt of adsorbed substance (μg/g soil),
c = solution concentration (μg/ml),
k = proportionality constant (ml soln/g soil),
1/n = empirical exponent.

The exponent in this equation has been found to lie between 0.70 and 1.00 for pesticide adsorption in most soil systems (Leistra, 1973).

Giles *et al.* (1960) classified adsorption isotherms on the basis of their shape, dividing isotherm shapes into four classes and five subclasses. Freundlich iostherms fall into "class L" (Figure I.3). They hypothesized that for this type of isotherm solute particles are most likely adsorbed flat against the surface of the sorbent as in figure I.4.

Figure I.3. Freundlich (Giles Class L) isotherm.

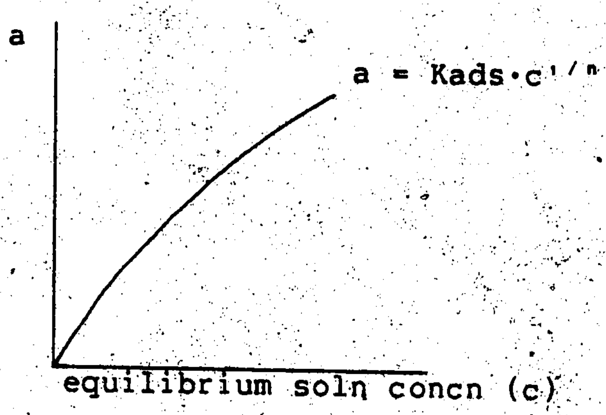

Figure I.4. Schematic diagram of adsorption for "class L" (Freundlich) isotherm.

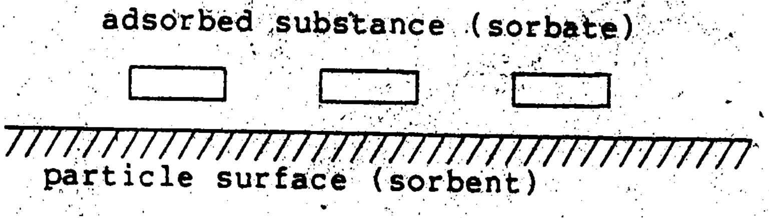

At lower concentrations the plot of a versus c in figure I.3 is almost linear. Consequently for sparingly soluble pesticides a linear isotherm is commonly used.

To accomodate adsorption-desorption in the classical equation recall (6):

$$\partial Ms/\partial t = -(A\Delta z)\upsilon(\partial c/\partial z).$$

If storage of solute occurs in the adsorbed phase as well as in solution then:

$$Ms = \alpha(A\Delta z)c + Db(A\Delta z)a,$$

where Db = dry bulk density of soil (g/cm^3) and all other symbols as previously defined.

Substituting this expression into (6):

$$\alpha(\partial c/\partial t) + Db(\partial a/\partial t) = -\upsilon(\partial c/\partial z) \qquad (12).$$

This can be converted to the equation of DeVault(1943):

$$\alpha'(\partial c/\partial V) + \partial Q'/\partial V = -\partial c/\partial z$$

where $\upsilon = 1/A(\partial V/\partial t)$, or $\partial t = \partial V/(\upsilon \cdot A)$;

$Q' = Db \cdot A \cdot a$; and

$\alpha' = \alpha \cdot A$ (porosity per unit column length).

DeVault has used dV as a convenient measure of time. This is valid when υ is constant. DeVault (1943) used the general isotherm:

$Q' = f(c)$, so that:

$$[\alpha' + \partial f(c)/\partial c]\partial c/\partial V = -\partial c/\partial z.$$

Spreading by diffusion can also be included in (12):

$$\alpha(\partial c/\partial t) + Db(\partial a/\partial t) = -\upsilon(\partial c/\partial z) + D(\partial^2 c/\partial z^2) \qquad (13).$$

Dividing through by α and allowing for the different dimensions of a used, one obtains an equation identical to that of Lapidus and Amundsen (1952).

Relating a to c by a linear isotherm ($a = Kads \cdot c$) (13) becomes:

$$\alpha(\partial c/\partial t) + Db \cdot Kads(\partial c/\partial t) = -\upsilon(\partial c/\partial z) + D(\partial^2 c/\partial z^2), \text{ or,}$$

$$(\alpha + Db \cdot Kads)\partial c/\partial t = -\upsilon(\partial c/\partial z) + D(\partial^2 c/\partial z^2) \qquad (14).$$

Again dividing by α to change dimensions (14) can be altered to the equation used by Kay and Elrick (1967). Equation (14) has been developed for saturated flow, that is, $\theta = \theta s = \alpha$. For unsaturated flow θ should be substituted for α. Substituting Dspr for D, as in (9), the chromatographic equation becomes:

$$(\theta + Db \cdot Kads)\partial c/\partial t = -\upsilon(\partial c/\partial z) + Dspr(\partial^2 c/\partial z^2) \quad (15).$$

So far the kinetics of the adsorption-desorption reaction have been ignored. It has been assumed that rates of adsorption and desorption are high enough, relative to the liquid flux, to permit transverse equilibrium between adsorbed and dissolved solute. This may not always be a valid assumption. Lapidus and Amundsen (1952) dealt with rates of mass transfer between phases, and Kasten *et al.* (1952) described the case in which rates of diffusion to adsorption sites within solid particles limited adsorption-desorption, which may be a more realistic model to describe leaching in soils. Rao *et al.* (1980), Addiscott (1981) and Nkedi-Kizza *et al.* (1982) have developed numerical models describing the effects of finite intra-aggregate diffusion rates on solute transport.

e. Sinks and Sources

The continuity equation can be written to include sink or source terms:

$$\partial(a + \theta c)/\partial t = -\partial(\upsilon c)/\partial z + S \quad (16),$$

where S = sink or source term due to salt precipitation or dissolution (Magdoff and Bresler, 1973).

Rolland and Frissel (1974) used a first-order decay reaction rate law to describe pesticide decomposition in soils:

$$dc/dt = -k \cdot c \quad (17),$$

where k is the decay rate constant (1/d).

This is an approximation of the Michaelis-Menton equation for very low concentration, as is usually the case for pesticides in soil. They have also used a first order decay rate law to describe irreversible adsorption of pesticides.

Equation (17) can be solved for $c(t+\Delta t)$:

$$c(t+\Delta t) = c(t)\exp(-k\cdot\Delta t).$$

Therefore a simple way to deal with decay of pesticides is to multiply the solution obtained from the chromatographic model by the factor $\exp(-k\cdot\Delta t)$ at the end of each time period, Δt.

The non-equilibrium case for adsorption-desportion was described in a similar manner by Lapidus and Amundsen (1952):

$$da/dz = k_1 c - k_2 a \qquad (18).$$

where k_1 = rate constant for adsorption,

k_2 = rate constant for desorption.

f. Soil Heterogeneity

Effects of soil heterogeneity on leaching were mentioned in the subsections on diffusion and dispersion. The most obvious feature of heterogeneity is the vertical stratification which characterizes all soils. This stratification results in variation in the physical and chemical parameters used in the chromatographic model. Many of the parameters were assumed to be constant during derivation of the model described in previous subsections. The situation in soil is better described by the following general model (Leistra, 1973):

$$\partial Ms/\partial t = -\partial(\upsilon \cdot c)/\partial z + \partial(D \cdot \partial c/\partial z)/\partial z$$
$$+ \partial(E \cdot \partial c/\partial z)/\partial z - (\partial M/\partial t)cons \qquad (19),$$

where $(\partial M/\partial t)cons$ = consumptive term which describes affects of assimilation, decomposition, and fixation;

$$\partial Ms/\partial t = \partial(\theta \cdot c)/\partial t + \partial(Db \cdot a)/\partial t;$$

and where θ, Db, υ, D, and E can vary with depth. Solving this equation is one of the current challenges to research in soil physics.

Vertical stratification is not the only aspect of soil heterogeneity of concern, however. Structural heterogeneity (pore distribution) influences diffusion and dispersion. Channelling of solution through macropores which represent only a fraction of the total porosity, results in greater depth of solute penetration than is estimated on the basis of total porosity (Tyler and Thomas, 1981).

The soil solution may also exhibit variability. Smiles and Gardiner (1982) have dealt with heterogeneity of the soil solution as it affects anion transport. They divided the soil solution into two pools: one accessible, and one inaccessible to anions. In this way they describe anion exclusion in the solution very near to the surface of negatively charged soil particles; inaccessible water was defined as a layer 9A° thick. Their model appears as:

$$\partial(\theta a \cdot ca)/\partial t = \partial(E \cdot \partial ca/\partial z)/\partial z - \partial(\upsilon \cdot ca)/\partial z \qquad (20),$$

where the subscript "a" refers to values for accessible water only.

Addiscott (1977) has used a similar approach to treat anion exclusion in structured soil. The case where a solute is excluded from a region is a simple illustration of heterogeneity of the soil solution. Although this study does not consider anion transport, the idea that the soil solution can be divided into separate phases, or pools, in order to treat the effects of soil structure on solute transport is central to the model which is developed herein.

Where intra-aggregate diffusion rates exert a kinetic influence on adsorption-desorption (as in the case of relatively high υ) radial diffusion within aggregates must be considered separately from inter-aggregate rates. Kasten *et al.* (1952) considered this phenomenon. They solved an equation parallel to the classical model of vertical solute transport for radial (intra-particle) transport. Addiscott (1977) has simplified the treatment of diffusion rates into and out of aggregates in his two-phase model of the soil solution. He assumes that during infiltration events there is no (diffusional) mass transfer between mobile (inter-aggregate) and stagnant (intra-aggegate) solution phases. Between infiltration events, however, complete transverse equilibration of solute between phases occurs. These simplifying assumptions avoid the problems of determining aggregate sizes and diffusivities (D) which vary with depth and, in the case of D, with moisture content. It is necessary, however, to examine the validity of these assumptions, since in the range of intermediate flow both may be invalid.

Skopp *et al.* (1981) have used an approach similar to Addiscott (1977), in that they defined two regions of soil solution but regard both as mobile. Each solution pool moves at a different rate and a small degree of solute mass transfer occurs between them. Their model would best described cases where soil solution flows around and through soil aggregates, while that of Addiscott (1977) describes cases where solution flows around aggregates.

The chromatography equation can be used to describe the effects of mass flow, dispersion, diffusion, adsorption, and decomposition on solute transport. For solute transport in soil, heterogeneity resulting from stratification, and pore geometry (soil structure) require modifications of the basic equation. The information and assumptions required for solution of various forms of the model are discussed in the next section.

2. Solutions to the Chromatographic Model

a. Analytical solutions

The techniques of differential and integral calculus can be employed to solve some forms of the chromatographic equation. These solutions are exact and usually simple to use. Use of analytical methods to solve the model, however, is severely limited by the complexity of leaching problems encountered in the field.

For instance equation (19), which is general, is too complex for analytical techniques. Most analytical solutions assume that υ, θ, and Dspr are constant so that (19) is greatly simplified. Further simplifications concerning boundary conditions and feed functions are necessary for application of analytical solutions (Leistra, 1973). In light of the complex situations which occur in soil these simplifying assumptions cannot be justified and numerical solutions must be sought.

Analytical solutions are nevertheless instructive. They can be used to analyze the effects of variation of parameters (e.g., Dspr, partition coefficient), soil physical properties (θ, Db, α), and feed variables (c(t), υ). They are also useful in assessing the error introduced by numerical methods. This can be done by using the same values for all variables and parameters in solutions which are available in both numerical and analytical forms. Concentration profiles can be calculated from analytical solutions with the assistance of only a pocket calculator and mathematical tables, whereas numerical solutions require computer assistance to accomplish the volume of computation involved.

Kirkham and Powers (1972) derive solutions for some simple cases described by the classical model, such as the general solution for a one-dimensional dispersion model ($\partial c/\partial t_1 = E(\partial^2 c/\partial z_1^2)$). This equation is solved for a moving coordinate system (t_1,z_1) and then transformed to the fixed coordinate system ($t=t_1$, $z=z_1+\nu t$), that is, the dispersion model is superimposed on the piston-flow model of mass flow. They apply this solution to two elementary boundary conditions: (i) dispersion of a displacing front; (ii) dispersion of a "slug" (narrow band) of solution. They also provide the Carslaw-Jaeger solution for the mass flow - diffusion equation ($\partial c/\partial t = -\nu(\partial c/\partial z) + D(\partial^2 c/\partial z^2)$).

Both D and E can be calculated from experimental breakthrough curves using analytical solutions (Kirkham and Powers, 1972). The solutions mentioned above illustrate the differential and integral calculus required to solve the model analytically. Neither of these equations considers partition between solution and adsorbed phases and therefore applies only for non-reactive solutes, such as chloride ion or tritiated water.

DeVault (1943) provides an analytical solution for the model describing mass flow with adsorption-desorption (non-linear isotherm). Instantaneous transverse adsorption-desorption equilibrium is assumed and spreading by diffusion or dispersion is neglected. The solution would be valid only for a range of fluid velocities for which diffusive spreading is insignificant in the lower limit of ν and dispersive spreading is insignificant in the upper limit of ν. Fluid velocities must also be low enough to exert no kinetic influence over adsorption-desorption.

Lapidus and Amundsen (1952) consider an apparent contradiction in DeVault's assumptions, namely, no diffusion and instantaneous adsorption-desorption equilibrium. They reasoned that when mass flow rates were low enough for point-wise equilibrium at all levels in the column, then longitudinal diffusion rates would be significant. Similarly, at higher flow rates which eliminate the effects of diffusion, point-wise equilibrium in the column is a questionable assumption. Therefore they solved the model:

$$\partial c/\partial t + (1/\alpha)\partial n/\partial t = -\nu(\partial c/\partial z) + D(\partial^2 c/\partial z^2)$$

where $\partial n/\partial t$ is the rate of exchange of mass between solution and adsorbed phases. They solved this equation for equilibrium and non-equilibrium conditions.

Kasten *et al.* (1952) considered the case in which finite intraparticle diffusion rates limited adsorption-desorption. They defined $\partial n/\partial t$ in terms of the rate of intraparticle radial diffusion.

All of the above analytical solutions apply to boundary conditions and solution feed functions which can be carefully controlled *in vitro*. Research in soil under field conditions allows no such luxury. Moisture flux under field conditions is a variable function of time while severe discontinuities may occur in soil properties. The analytical techniques used in the above solutions are based on continuous functions. Any rigorous treatment of solute transport through soils must be capable of treating the complex variation which occurs in the field.

b. Numerical Solutions

Numerical solutions permit consideration of more complex soil properties and leaching conditions than can be treated by analytical techniques. The first step in most numerical approaches is to divide the soil column into discrete layers so that a difference equation can be written:

$$Db(\partial a/\partial t) + \theta(\partial c/\partial t) = -\upsilon\Delta c/\Delta z + Dspr\Delta^2 c/\Delta z^2 \qquad (21).$$

For non-reactive solutes:

$$\theta(dc/dt) = -\upsilon\Delta c/\Delta z + Dspr\Delta^2 c/\Delta z^2.$$

If Δz is set = 1, then:

$$dc = (1/\theta)(-\upsilon\Delta c + Dspr\Delta^2 c)dt; \text{ or,}$$

$$\int_t^{t+\Delta t} dc = \int_t^{t+\Delta t} (1/\theta)(-\upsilon\Delta c + Dspr\Delta^2 c)dt$$

where $\Delta c = c(t,z) - c(t,z-1)$,

and $\Delta^2 c = c(t,z+1) - 2\,c(t,z) + c(t,z-1)$.

So that:

$$c(t+1,z) = c(t,z) - \int_t^{t+\Delta t}(1/\theta)[c(t,z+1) - c(t,z)]dt \qquad (22).$$

Frissel *et al*. (1970) have used this approach, solving the integral using a 4th order Runge-Kutta formula. This formula is very accurate but is based on the presence of very smooth concentration versus time curves (feed functions). For discontinuous feed functions other numerical integration techniques can be used to solve (22), of which rectangular integration, though less accurate, is the simplest:

$$\int_t^{t+\Delta t} c\,dt = c\int_t^{t+\Delta t}dt$$

$$= c\Delta t$$

Leistra (1973) developed a finite difference equation based on rectangular integration for the classical model describing leaching of non-reactive solutes:

$$
\begin{aligned}
c(t+1,z) = c(t,z) + \Delta t/\Delta z\{&\nu\cdot c(t,z-1) - \nu\cdot c(t,z) \\
&- \mathrm{Dspr}[c(t,z) - c(t,z-1)]/\Delta z \\
&+ \mathrm{Dspr}[c(t,z+1) - c(t,z)]/\Delta z\} \qquad (23).
\end{aligned}
$$

In a solution of this type initial conditions define $c(t_0,z)$ for all z. Next $c(t_1,z)$ is determined from $c(t_0,z)$ at each layer and υ from equation (23). This process is repeated for each time step for the period of time for which the solution is desired.

Variations in soil properties and flow rate are often important in leaching studies. Recall the essential differences between equations (15) and (19):

$$(\theta + \mathrm{Db}\cdot\mathrm{Kads})\partial c/\partial t = -\upsilon(\partial c/\partial z) + \mathrm{Dspr}(\partial^2 c/\partial z^2) \qquad (15);$$

$$
\begin{aligned}
\partial(\theta\cdot c)/\partial t + \partial(\mathrm{Db}\cdot\mathrm{Kads}\cdot c)/\partial t = \\
-\partial(\upsilon\cdot c)/\partial z + \partial(\mathrm{D}\cdot\partial c/\partial z)/\partial z \\
+ \partial(\mathrm{E}\cdot\partial c/\partial z)/\partial z + (\partial M/\partial t)\mathrm{cons} \qquad (19).
\end{aligned}
$$

Equation (15) is specific for columns in which θ, Db, Kads, υ, and Dspr are constants and can be handled with analytical methods. The general equation (19) describes vertical heterogeneity with regard to these properties, but requires numerical methods to yield a solution.

Leistra (1973) solves the general equation for leaching of non-reactive solutes:

$$\partial(\theta\cdot c)/\partial t = -\partial(\nu\cdot c)/\partial z + \partial(\mathrm{Dspr}\cdot\partial c/\partial z)/\partial z - k\mathrm{cons}\cdot\theta\cdot c,$$

where $k\mathrm{cons}\cdot\theta\cdot c$ is a decay sink term. Four coefficients (θ,

ν, Dspr, and $k$cons) can vary with depth.

The finite difference solution is:

$$c(t+1,z) = [r_1/\theta(z) + r_2(z-1)/\theta(z)]c(t,z-1)$$
$$+ [1 - r_1/\theta(z) - r_2(z-1)/\theta(z) - r_2(z)/\theta(z)]c(t,z)$$
$$+ (r_2(z)/\theta(z))c(t,z+1),$$

where $r_1 = \nu\Delta t/\Delta z$,

$r_2(z) = \mathrm{Dspr}(z)\Delta t/\Delta z^2$.

c(t+1,z) can therefore be determined at any time, t+1, from c(t,z), the concentration profile at time, t, and the necessary soil properties defined for each horizontal layer, z, of the soil column.

The numerical solution of Frissel *et al*. (1970) treats variable θ and Dspr, but deals only with constant water flux. Addiscott's (1977) model of a structured soil system allows for variation in flux but only very limited variation in θ. Burns' (1974) model solves the solute transport problem for variable θ and flux. Dispersion and diffusion in the models of Burns and Addiscott are effected by numerical spreading only. Leistra's (1973) model deals with vertical stratification but not with soil structure.

Published information about simulation models is frequently insufficient to assess the numerical techniques or to reproduce the simulation experiments. De Wit and van Keulen (1972) and Frissel and Reiniger (1974) published detailed manuals and programs describing a variety of simulation models of transport processes in soil written in CSMP. The former include solutions of the moisture flow distribution, while the latter require that the flux be known from other solutions or can be controlled.

c. Plate Models and Rate Models

Most of the models mentioned above are based on rigorous physical laws. Some assume that there are no rate limiting steps (DeVault, 1943). Others include specific rate laws (Kasten *et al.* 1952; Lapidus and Amundsen, 1952) to describe the effects of diffusion, dispersion, finite adsorption-desorption rates and chemical reaction rates. Those models which contain rate laws to describe kinetic effects are called "rate theories" by Frissel and Poelstra (1967).

There is another important chromatographic model which relies on the theoretical number of plates in a chromatographic column, or the "height equivalent to a theoretical plate" (HETP), to determine the solute distribution. Frissel and Poelstra (1967) call models of this type "plate theories". The number of theoretical plates is equivalent to the number of theoretical equilibrations, "n". This value can be used to calculate the solute distribution in the column as follows (Johnson, 1972):

$$c_i = (n!/i!(n-i)!)[1/(B+1)]^{(n-i)} \cdot [B/(B+1)]^i \qquad (24),$$

where c_i = concentration in the ith plate,

B = effective partition coefficient ($Db \cdot k/\theta$),

n = number of theoretical plates or equilibrations.

The above expression is the ith term in the binomial expansion of $[1/(B+1) + B/(B+1)]^n$, where n can be calculated as follows (Johnson, 1972):

$$n = 8p(L-p)/w^2,$$

where p = position of the solute peak concentration,

L = length of column (depth of penetration of leaching solution),

w = width of solute band at point where the solute concentration is 36.8% (1/e) of the maximum concentration.

In this context n, or HETP = L/n, is used as a parameter of the leaching system. Glueckauf (1955) developed the plate theory for continuous feed functions (liquid flux) and showed that HETP is a measure of the spreading coefficient. A theoretical value of Δz which when used in the models of Johnson (1972) and Glueckauf (1955) accurately predicts spreading of the solute band for a particular set of conditions.

For finite difference models, such as those of Leistra (1973), the value chosen for Δz also influences the calculated spreading of the solute band. In finite difference models, where concentrations are uniform within each layer, spreading will be greater when calculated on the basis of larger Δz. This effect is known as "pseudo dispersion" (Leistra, 1973) or "numerical dispersion" (Frissel and Reiniger, 1974). Numerical dispersion can be reduced by using relatively small values of Δz, which technique requires more computations. Alternatively Δz can be chosen so that the numerical dispersion produced by the simulation model corresponds to actual spreading produced in leaching experiments. This value of Δz can is determined from the results of a leaching experiment. Using Δz values in place of rate laws to describe spreading is invocation of the plate theory. It is sometimes difficult to apply plate models to soil because the HETP requires approximately constant values of flow rates and spreading coefficients.

It is also possible to prevent numerical spreading by selecting the time step of the simulation so that the solute concentration profile is shifted down exactly one layer thickness, Δz, at each time step (Leistra, 1973). This allows the modeller to introduce an accurately known amount of spreading. For field situations this method would require a variable time increment.

Values of Δz used in simulation models may also exert a pseudo-kinetic effect on simulation experiments. The case where flow rates exert a kinetic effect on partition of solute has already been discussed (Lapidus and Amundsen, 1952). In the layer model of Addiscott (1977) this effect is simulated by using two different leaching routines. A slow leaching routine (SLR) allows local equilibrium within each layer of thickness Δz. A fast leaching routine (FLR), which simulates intense rainfall events, limits the interaction between mobile and stagnant solution pools, thus simulating the kinetic effects of flow rates on partition between solute pools. Entry into the fast leaching routine depends on the quantitative relationship between Δz and the rainfall input, ΔV (which depends on Δt). Therefore Δt must be compatible with Δz for the simulation model to correctly predict depth of leaching.

Normally Δz is determined by a leaching experiment. One requirement that Addiscott (1977) sets for simulation models of leaching, however, is that no prior leaching experiment be required. He gives no *a priori* criteria for his choice of Δz. He has, however, determined the Δz for the best fit between calculated and experimental values, thus, in effect performing a leaching experiment to test his choice of Δz.

In a later version of the model Addiscott (1981) included a specific rate law for diffusion between mobile and stagnant solute pools. Thus he transformed the model into a rate model, and precluded the need for a prior leaching experiment to determine Δz. The specific rate law can define mobile-stagnant solute partition for any Δz and Δt (or ΔV).

The above discussion illustrates the effects Δz can have on simulation models. To avoid numerical dispersion, Δz must be relatively small. HETP can be used in place of a rate law where leaching can be characterized by an average HETP. When leaching is slow relative to partition rates, Δz need be chosen with regard to its effect on numerical dispersion only.

Addiscott (1977) assessed the sensitivity of his model of leaching through structured soils to Δz values from 3.25 to 13 cm using time steps of one day and concluded that little benefit was gained by reducing Δz below 3.25 cm.

Thoma *et al.* (1978) determined that their plate model for tritium leaching through sand dunes was insensitive to HETP variation for HETP values below ten cm. Burns (1974) assumed instantaneous equilibration between stagnant and mobile solute pools. A Δz value of 3.75 cm. yielded simulation results which were in good agreement with experimental patterns of chloride leaching.

Thornthwaite *et al.* (1960) used the analytical plate model presented above (24) to determine radiostrontium leaching patterns in laboratory columns of four texturally different soils. They used an HETP value of 1.27 cm. for all four soils. Their predicted profiles showed a good correlation with measured concentration profiles.

Numerical solutions of the chromatographic equation are better suited to solute transport in soil than analytical solutions because they can be applied to the complex variation which occurs in the field. Use of numerical solutions requires special attention to the error introduced. Error can arise from both the time step and layer thickness and sensitivity of numerical models must be assessed for both sources.

3. The Transport Model Applied to Structured Soils

The structural organization (aggregation) of soil particles controls pore size distribution which in turn influences flux distribution. The Hagen-Poiseuille equation states that volume flux through a pore is proportional to the fourth power of the pore radius (Scheidegger, 1974). This relationship between flux and pore radii indicates that water contained in small pores may remain nearly stationary while water nearby is moving rapidly. Some of the water present in the field, therefore, may not participate directly in leaching (Addiscott, 1977).

The pore distribution of strongly aggregated soils may be defined by two distinct size ranges: intra-aggregate pores, or micropores, and inter-aggregate pores, or macropores. Zimmerman *et al*. (1965) approached soil structure as a simplified dispersion problem; that is, they characterized the flux distribution by two fluxes, $\upsilon_1=0$, and $\upsilon_2>0$. The weighted average of υ_1 and υ_2 would be the mean volume flux.

Addiscott (1977, 1978) treated solute transport in structured soils by defining two solution phases on the basis of their mobility: mobile, or inter-aggregate solution; and retained, or intra-aggregate solution. A fraction of the solute in each layer is considered to move at each infiltration event and the remainder to be retained within its respective layer. After each downward displacement of solution an equilibrium is established within each layer by equalizing the concentration between pools. The assumption of complete equilibration between intra- and inter-aggregate solution may not be justified in all cases, however. In a later model Addiscott (1981) defines interaction between moble and retained pools by incorporating a diffusion rate law (Fick's law) into the model. Solute exchange between pools is controlled by diffusivity, aggregate size, and intra-aggregate concentration gradients. Rao *et al.* (1980) dealt with soil micropore regions as a diffusion sink/source so that movement into or out of aggregates is defined by a sink/source term in the classical chromatographic equation, which they solve numerically. The sink/source term is defined by radial diffusion rates.

The problem in using the two pool concept is development of a criterion to define the pore size range for each pool, or the volumes assigned to each pool. Addiscott (1977) divides the pools at the 200 kPa soil moisture tension, with the upper limit of the mobile water pool set at field capacity (5 kPa) and the lower limit of retained water at the volumetric midpoint between wilting point (1500 kPa) and dryness. Thus he implies the existence of a third pool which does not interact with the other two. His reasoning is that this fraction of soil water is associated with extremely fine pores and diffusion within these pores is slow. Since he was modelling anion transport he assumed that this pool excluded the solute.

Addiscott (1977) presents the 200 kPa division as strictly empirical, though he states that it should be the same for all soils, but may vary with the solute. He does not indicate why he has used five kPa moisture tension for field capacity, rather than the conventional ten or 33 kPa.

Nkedi-Kizza *et al*. (1982) mark the division between mobile and immobile water at eight kPa soil moisture tension. Zimmerman *et al*. (1965) assign the volumetric ratio of 3:1 for immobile:mobile water. A theoretical basis for assigning immobile and mobile solution pools has not yet been presented.

Solute transport through structured soil cannot be adequately described by a longitudinal spreading coefficient (Dspr) in the chromatography equation. The numerical approach of dividing the soil solution into two phases, or pools, in order to account for holdback of solute in the micropore region has been successful in studies of leaching in structured soil and the mobile-stagnant pool model is the simplest example of this.

In summary, the chromatography differential equation provides a theoretical framework for solute transport studies in soils, however, the equation must be adapted for leaching studies on structured soils. The two solution pool concept has proven useful in describing transport under these conditions.

In this study the interactive mobile-stagnant phase model of Addiscott (1977) is being tested in simulation and field experiments on an Alberta Gray Luvisol. Modifications to account for variation in θ and υ with depth and time, and for the effects of frozen soil must be incorporated to describe the conditions under study. The model is also extended to describe transport of adsorbed solutes.

II. MATERIALS AND METHODS

A. SIMULATION MODEL - DEVELOPMENT

The simulation model described in the following sections is based on a numerical solution of the chromatographic equation. The soil column is divided into discrete layers and water flux between the layers is defined by a water balance equation. The solute transport equation is then solved using rectangular integration.

1. Moisture Flux

Moisture flux through the soil column is defined at each layer by the following water balance equation:

$$WL = WA - \text{storage} \qquad (25),$$

where WA = water entering layer I from above,

WL = water displaced from layer I by WA,

= WA entering layer I+1,

storage = water absorbed by the layer, I.

WA added at layer one is determined as the difference between the water input and evaporation (WA = W - E).

This equation is similar to that used by Burns (1974) in his layer model of solute transport in non-structured soils. The storage available in each layer is defined as the difference between field capacity (33 kPa soil moisture tension) and the water present in the layer. Water will accumulate in each layer until field capacity is reached, after which an amount of water, WL, defined by the water balance, will be displaced into the next layer. In terms of the symbolism used in the model available storage is determined as:

$$XSWMCP(I) = WMCAP(I) + WR(I) - WT(I) \qquad (26),$$

where WMCAP(I) = storage capacity of the mobile water pool,
WR(I) = storage capacity of the stagnant water pool
WT(I) = total water present at time, J.
I = layer number.

Total water present in layer I can be expressed as the sum of mobile and stagnant water present in the layer:

$$WT(I) = WR(I) + WM(I) \qquad (27),$$

where WM(I) = water present in mobile pool.

In its present form the model does not deal with solute transport at θ less than the capacity of the stagnant pool. The amount of water present in the stagnant pool (WR) is, therefore, constant and storage capacity can be expressed in terms of WMCAP and WM only:

$$\begin{aligned} XSWMCP(I) &= WMCAP(I) + WR(I) - WT(I) \\ &= WMCAP(I) + WR(I) - (WR(I) + WM(I)) \\ &= WMCAP(I) - WM(I) \qquad (28). \end{aligned}$$

The relationship between WA and XSWMCP(I) defines three different leaching conditions:

i) $WA \leq XSWMCP(I)$ in which case all of WA is absorbed by the available storage capacity in layer I;

ii) $WMCAP(I) \geq WA > XSWMCP(I)$, in which case an amount of water, $WL = WA - XSWMCP(I)$ is displaced into layer

I+1; WA is then reset to WL and applied to layer I+1;

iii) WA > WMCAP(I), in which case all of WM(I) is displaced; WM(I) is reset to WMCAP(I); WL = WA - XSWMCAP(I); and WA is reset as in ii) and applied to layer I+1.

Slow leaching is defined by cases i) and ii), while fast leaching is defined by iii). The differences between the two will be discussed in the following section.

The program parameter M defines the size of the soil system. Layer M+1 is regarded as a sink, so that water, WL, displaced from layer M is lost to the system.

Frozen layer routine

A frozen layer is regarded as an impermeable barrier to water movement so that infiltrating water encountering a frozen layer must be stored above it. This requires definition of a third water pool, WGRAV(I), or gravity water, and its storage capacity, WGRCAP(I), and available storage, XSWGCP(I). The relationship among these terms is similar to that defined for the mobile water pool:

$$\text{XSWGCP}(I) = \text{WGRCAP}(I) - \text{WGRAV}(I),$$

where WGRCAP = total porosity - WMCAP - WR.

The available storage in each layer, I, above the frozen layer is determined as:

$$\text{storage} = \text{XSWMCP}(I) + \text{XSWGCP}(I) \qquad (29).$$

The frozen layer number, FLNR, is read by the simulation program at each time step, before the water inputs are read. If the soil is completely thawed a value of 0 is entered. If FLNR moves downward between successive time steps then the amount of WGRAV above FLNR is redistributed. WA is set to WGRAV(FLNRT-1), where FLNRT is the previous value of FLNR and FLNRT-1 is the next higher layer. WA is then transported downward according to the water balance equation (25). The program then moves upward though the soil column redistributing WGRAV contained in each successively higher layer.

When the program encounters a layer, I, such that I=0, or WGRAV(I) = 0, redistribution ceases and water inputs are read for the current time step. If a frozen layer causes ponding of water above the surface layer the amount of water ponded, WPOND, is added to WA applied to layer one at the beginning of the next time step.

2. Solute Transport (non-reactive solutes)

Transport of non-reactive solutes through heterogeneous media can be written (neglecting spreading effects) in terms of the classical chromatographic equation as:

$$\partial(\theta \cdot c)/\partial t = - \partial(\upsilon \cdot c)/\partial z \qquad (30).$$

Both θ and υ can vary with depth and time.

A finite difference equation parallel to (30) can be written as:

$$\Delta(\theta \cdot c)/\Delta t = - \Delta(\upsilon \cdot c)/\Delta z \qquad (31).$$

The left side of equation (31) can be expanded to:

$$\Delta(\theta \cdot c)/\Delta t = \theta \Delta c/\Delta t + c\Delta\theta/\Delta t + \Delta c\Delta\theta/\Delta t$$

If changes in c and θ with time are small relative to c and θ then the last term can be neglected. The values of the terms outside the difference operators can be set to:

$\theta\text{-ave} = \frac{1}{2}(\theta(t,z) + \theta(t+1,z))$; and

$c\text{-ave} = \frac{1}{2}(c(t,z) + c(t+1,z))$.

Then:

$$\begin{aligned}\Delta(\theta\cdot c) &= \theta\text{-ave}\Delta c + c\text{-ave}\Delta\theta\\ &= \theta\text{-ave}[c(t+1,z) - c(t,z)] + c\text{-ave}[\theta(t,z) - \theta(t+1,z)]\\ &= c(t+1,z)\cdot\theta(t+1,z) - c(t,z)\cdot\theta(t,z).\end{aligned}$$

Therefore the left side of equation (31) can be written as:

$$\Delta(\theta\cdot c)/\Delta t = (c(t+1,z)\cdot\theta(t+1,z) - c(t,z)\cdot\theta(t,z))/\Delta t \quad (32).$$

The right side of (31) can be expanded similarly (if $\Delta\upsilon$ and Δc are small relative to υ and c):

$$\Delta(\upsilon\cdot c)/\Delta z = (\upsilon\text{-ave}\Delta c + c\text{-ave}\Delta\upsilon)/\Delta z,$$

where $\upsilon\text{-ave} = \frac{1}{2}[\upsilon(t,z) + \upsilon(t,z-1)]$;

$c\text{-ave} = \frac{1}{2}[c(t,z) + c(t,z-1)]$;

$\Delta c = c(t,z) - c(t,z-1)$;

$\Delta\upsilon = \upsilon(t,z) - \upsilon(t,z-1)$.

Therefore the right side can be written as:

$$-\Delta(\upsilon\cdot c)/\Delta z = -\,[c(t,z)\cdot\upsilon(t,z) - c(t,z-1)\cdot\upsilon(t,z-1)]/\Delta z \quad (33).$$

Each of these expressions, (32) and (33), can be written in terms of solute masses, M, and water volumes, V:

$c = M/Vw$;

$\upsilon = \Delta V/(A\cdot\Delta t)$;

$\theta = Vw/Vb = Vw/(A\cdot\Delta z)$;

where, Vw = volume of water in layer of thickness Δz,

and, Vb = total volume of plate of thickness Δz.

Therefore:

$$L.S. = \frac{1}{\Delta t}\left[\frac{M(t+1,z)}{Vw(t+1,z)}\cdot\frac{Vw(t+1,z)}{A\Delta z} - \frac{M(t,z)}{Vw(t,z)}\cdot\frac{Vw(t,z)}{A\Delta z}\right]$$

$$= \frac{M(t+1,z) - M(t,z)}{A\Delta z\Delta t} ;$$

and:

$$R.S. = \frac{1}{\Delta z}\left[\frac{M(t,z)}{Vw(t,z)}\cdot\frac{\Delta V(t,z)}{A\Delta t} - \frac{M(t,z-1)}{Vw(t,z-1)}\cdot\frac{\Delta V(t,z-1)}{A\Delta t}\right]$$

$$= \frac{1}{A\Delta z\Delta t}\left[M(t,z)\cdot\frac{\Delta V(t,z)}{Vw(t,z)} - M(t,z-1)\cdot\frac{\Delta V(t,z-1)}{Vw(t,z-1)}\right] .$$

Putting L.S. and R.S. together:

$$M(t+1,z) - M(t,z) = -M(t,z)\cdot\frac{\Delta V(t,z)}{Vw(t,z)} + M(t,z-1)\cdot\frac{\Delta V(t,z-1)}{Vw(t,z-1)} \quad (34)$$

The symbolism used in the simulation model is as follows:

I = layer number (vertical coordinate);

J = time coordinate ($t/\Delta t$);

ST(I) = M(z,t) = total dissolved solute mass in layer I;

WT(I) = Vw(z,t) = total water in layer I;

WM(I) = water in mobile water pool in layer I;

SM(I) = solute mass in WM(I);

WR(I) = water in stationery pool in layer I;

SR(I) = solute mass in WR(I);

WGRAV(I) = water in excess of field capacity, stored above a frozen layer;

SGRAV(I) = solute mass in WGRAV(I).

WA = water entering layer I at time J;
WL = water dispaced from layer I at time J.
The rationale behind the two-pool system is explained in the literature review.

WA is determined at each layer, I, and time step, J, from the section of the model describing water movement (section III.A.1., above).

Equation (34) can be written in terms of the symbols defined above for non-reactive solutes:

$$\Delta ST(I) = WA*ST(I-1)/WT(I-1) - WL*ST(I)/WT(I) \qquad (35).$$

The solute concentrations in each pool are equilibrated within each layer at the completion of each time step so that:

$$SM(I)/WM(I) = SR(I)/WR(I) = SGRAV(I)/WGRAV(I) = ST(I)/WT(I) \qquad (36).$$

Since movement of solute occurs in the mobile phase only, equation (35) can be written as:

$$\Delta ST(I) = WA*SM(I-1)/WM(I-1) - WL*SM(I)/WM(I) \qquad (35a).$$

where the first term on the right side of the solution defines the amount of solute added to layer I from the layer above (I-1) and the second term defines the solute lost from I to the layer below (I+1). It can be seen from (35a) that the mass of solute transported between layers is proportional to the volume of water moving between layers and the solute concentration in the water. Equation (35a) is equivalent to the slow leaching algorithm used by Addiscott (1977).

For redistribution of SGRAV following movement of a frozen layer I is set at FLNRT, WA is set at WGRAV(I-1) and (35) is used to determine solute flux between layers. The program moves up, decrementing I, until WGRAV is exhausted or the soil surface is reached.

Fast leaching

Equation (35a) describes solute flux for the cases in which WA $\leq$ WMCAP(I) (slow leaching). When WA > WMCAP(I) (fast leaching), however, the solute added to layer I is not given by (35a). In this case the amount of water added to I is equal to WMCAP(I) and SM(I) is determined as WMCAP(I)*SA/WA, where SA is the solute mass in WA. The water added to layer I+1 is determined as WA = WA - XSWMCP(I) and solute added to I+1 is determined as SA plus solute displaced from I, less solute left in I. This method for resetting SA results in mixing at each layer and differs from Addiscott's (1977) fast leaching routine which pushes solute through as a plug to the layer n, such that Σ_1^nWMCAP(I) $\geq$ WA, and then sums the water and solute displaced and applies them at layer n. This results in a rather discontinuous mixing of infiltrating solution with displaced solution.

In summary the simulation program works as follows:

i) volume of water entering layer I is determined from the water flux routines;

ii) mass of solute entering layer I (in WA) is determined from the appropriate leaching routine;

iii) WL is determined from the water balance equation;

iv) mass of solute leaving I in WL is determined;

v) ST(I) is reset according to equation (35), (35a), or the fast leaching routine;

vi) solute mass is redistributed between mobile and stationary pools (SM and SR, respectively, and SGRAV, if necessary) according to equation (36);

vii) when ST(I) has been determined for all I the program is updated (J=J+1), WA at I=1 is determined as the net infiltration at J=J+1, and i) to vi) are repeated.

Evaporation

The simulation model adopts the approach of Burns (1974) in that it allows the soil to dry out to a moisture content defined as the "evaporation limit", θel. It extends the model of Burns to describe transport of volatile solutes.

The net infiltration or net evaporation is determined at each time step as WA = W - E, where W is the precipitation or water input and E is the potential evaporation. When net evaporation occurs the uppermost layer can dry to θel. Any evaporation in excess of this amount must be replenished by capillary movement (in the liquid phase) from below. Water lost from the surface, WE(1), is set equal to net evaporation. If net evaporation exceeds WT(1) then WE(1) is set to WT(1) and evaporation requirements in excess of WT(1) are stored. The evaporation routine is then repeated as many times as necessary to satisfy the evaporation requirements (-WA). If the amount of water (WT(1)) remaining in layer one is less than θel this deficit ((θel - WT(1)) is replenished by water from layer 2, so that water lost from layer two is defined as:

$$WE(2) = \theta el(1) - WT(1).$$

The equation defining water loss induced by evaporation for I > one is:

$$WE(I) = \theta el(I-1) - WT(I-1).$$

This value is assigned until net evaporation loss is satisfied, that is, for all I, such that $WT(I) < \theta el(I)$.

The mass of solute lost from each layer, SE(I), is the product of the water lost and the solute concentration in the solution phase:

$$SE(I) = WE(I)*ST(I)/WT(I).$$

Water and solute mass balances are written for each layer for which loss occurs:

$$\Delta WT(I) = -WE(I) + WE(I+1);$$

$$\Delta ST(I) = -SE(I) + SE(I+1).$$

After WT(I) and ST(I) are reset solution within each layer is equilibrated according to equation (36). This achieves a continuous mixing of solution as it moves upward, similar to that which occurs during slow leaching.

This model extends that of Burns (1974) to the description of behavior of volatile solutes, such as ammonia and many pesticides. Volatilization losses of solute mass, SV, occur from the first layer only and are approximated as:

SV = SE(1) = WE(1)*ST(1)/WT(1).

As a working approximation the evaporation limit of this model is set at the 200 kPa soil moisture tension water content. Water in excess of this amount can be lost to replenish moisture deficits above. A moisture deficit is defined as any θ less than θ at 200 kPa. The soil is not allowed to dry to tensions greater than 200 kPa. For arid soils a lower value for the evaporation limit may be neccesary. Alternatively, it might be desirable to allow θel to vary, depending on the overall moisture status of the soil profile.

The evaporation routine was included to make the model more general. Due to time constraints no attempt has been made to determine a more appropriate value of θel. The definition of SV is valid for tritiated water but may not be for other solutes. Further theoretical and experimental investigations are necessary to improve this routine.

3. Transport of Adsorbed solutes

Partition of solute mass between solution and adsorbed phases in soil can be described by a linear isotherm for lindane and other pesticides:

$a = Kads \cdot c$.

Changing to the symbols and dimensions used in the simulation model involves the following relationships:

$a = Q/(Db\Delta z)$; and,

$c = ST/WT$,

where Q = adsorbed solute mass (per layer) per unit cross-sectional area;

Db = dry bulk density;

Δz = layer thickness;

ST = dissolved solute mass (per layer) per unit cross-sectional area;

WT = total water (per layer) per unit area.

The adsorption isotherm can be defined in terms of Q and ST:

$$Q = (Db\Delta z \cdot Kads)ST/WT$$

$$= B \cdot ST \qquad 37,$$

where B is the effective partition coefficient defined by:

$$B = (Db\Delta z/WT)Kads.$$

The adsorbed solute mass, Q(I), in layer, I, can also be expressed in terms of the total solute mass, MS(I), and total dissolved solute mass, ST(I), in layer, I:

$$Q(I) = MS(I) - ST(I) \qquad (38).$$

Therefore:

$$ST(I) = MS(I)/(1+B) \qquad (39);$$

and,

$$Q(I) = B*MS(I)/(1+B) \qquad (40).$$

A change in MS(I) resulting from mass flow into and/or out of I can be defined by an equation parallel to (35):

$$\Delta MS(I) = SA - SL,$$

where SA = solute mass entering I

$$= WA*ST(I-1)/WT(I-1);$$

and SL = solute mass displaced from I by WA

= WL*ST(I)/WT(I).

Any change in MS(I) causes a change in Q(I) and ST(I) so that:

$$ST(I)_j = MS(I)_j/(1+B)$$

$$= (MS(I)_{j-1} + \Delta MS(I))/(1+B) \qquad (39a);$$

$$Q(I)_j = MS(I)_j/(1+B)$$

$$= B(MS(I)_{j-1} + \Delta MS(I))/(1+B) \qquad (40a),$$

where $_{j-1}$ and $_j$ denote successive time steps.

Equations (39a) and (40a) define the partition of solute mass between dissolved (ST(I)) and adsorbed (Q(I)) phases at layer, I, for solution moving through I. The simulation program functions as follows:

(i) change in solute mass in layer, I, is determined as $\Delta MS(I) = SA - SL$;

(ii) $ST(I)_j$ is determined from (39a);

(iii) $Q(I)_j$ is determined from (40a);

(iv) J is updated and continue.

For non-adsorbed solutes Kads, and therefore B, are set at 0 so that $ST(I)_j = MS(I)_{j-1} + \Delta MS$ and $Q(I) = 0$.

4. Pesticide Decay

Decay of solutes can be treated as a sink term. Biological degradation of many pesticides can be treated as a first order decay reaction at low concentrations (Hiltbold, 1974). Nash and Woolson (1967) determined that loss of lindane in soil followed a first order decay rate law. For first order reaction kinetics the sink term can be expressed as:

$$dS/dt = -r \cdot S \qquad (41),$$

where S = the amount or concentration of pesticide,

r = decay rate constant $(1/t)$.

Using this sink term involves subtracting a constant fraction (r) from the total amount present (MS) at every time step. It may be argued that adsorbed solute is protected from decompostion and that only the dissolved solute is subject to decay, If this is true then the decay rate equation would apply to ST (dissolved solute mass) rather than MS. The decay rate constant, r, given above is an averaged value which defines the overall decay rate in all phases and, therefore must by applied to MS rather than ST. For lindane r is less than 0.001/d (Hiltbold, 1974), so that 1/1000 X ST is lost each day.

If time steps are small enough then $\Delta S = -r\Delta t \cdot S$. The analytical solution for (41) is straightforward, however:

$$S(t+\Delta t) = S(t) \cdot \exp(-r\Delta t).$$

Decay of solutes can be effected in a finite difference model by multiplying the solute mass by the factor $\exp(-r\Delta t)$ at each time step.

For the period of the experiments performed lindane decay was not a factor in solute distribution and a decomposition term was not included in the simulation program.

B. FIELD EXPERIMENTS

1. Soil

Field experiments were performed on untilled barley stubble on Breton Loam, an orthic Gray Luvisol. The experimental site was located on the University of Alberta Breton Plots, two km southeast of the village of Breton, Alberta, NE-25-47-4-W5. The soil was formed on medium fine textured till and posseses moderate internal drainage (Howitt, 1981).

The physical and chemical properties of this soil were described by Howitt (1981). It is characterized by a clay enriched Bt horizon (18 - 60 cm) with a strong blocky primary structure and weak prismatic secondary structure. The Ap horizon is low in organic carbon (1.4 %) and possesses a weak platy structure (Crown and Greenlee, 1978). The BC horizon (65 cm -) has a weak coarse blocky structure. Soil characteristics are summarized in table II.1.

2. Solutes

The solutes used in the field experiments were ^{3}HOH (tritiated water) and ^{14}C-labelled "lindane". Tritiated water was treated as an infinitely soluble, nonreactive solute. Lindane (γ-hexachlorocyclohexane, also known, incorrectly, as γ-benzene hexachloride or γ-BHC) is an insecticidal ingredient in some seed treatments used in

Western Canada. It is a sparingly soluble, strongly adsorbed, and persistent chemical and, therefore, assessment of its mobility in soil is an environmental concern. Chemical properties of lindane, pertinent to this study, are given in table II.2.

Table II.1. Characteristics of Breton Loam (Orthic Gray Luvisol)

		Particle size analysis		
Horizon	Org. C(%)	%sand	%silt	%clay
[2]Ap	1.4	33	55	12
[1]Bt	0.4	26	40	33
[1]BC	0.2	30	42	28

[1]-Howitt (1981)
[2]-Crown and Greenlee (1978).

Table II.2. Chemical properties of lindane.

		[2]Adsorption [3]Kd			
IUPAC name	[1]aqueous solubility	[4]montmorillonite	[5]Breton L Ap	Bt	[2]Half life in soil
γ-hexachlorocyclohexane	10 ppm	2.5	13	5	2 yr

[1]-Green (1974),
[2]-Hiltbold (1974),
[3]-Kd expressed as (μmoles lindane/kg adsorbent)/(μmoles lindane/l solution) for equilibrium solution concentration of: 10 μmoles/l for [4]montmorillonite, and 4 μmoles/l for [5]Breton Loam.

3. Experimental Design

Tritiated water and solutions of ^{3}HOH and ^{14}C-lindane were each applied to the Ap and Bt horizons. The isotope solutions were mixed with air-dry, ground and seived (2 mm mesh) soil in the laboratory, using a pastry blender. In the first treatment 6.25 μCi of ^{3}HOH alone were added with 250 ml of water to each of 1.3 kg of Ap horizon soil and 2.0 kg of Bt horizon soil.

A second treatment of ^{3}HOH-^{14}C-lindane solution was also mixed with soil. In this case 2.0 μCi ^{14}C-lindane and 10.0 μCi ^{3}HOH dissolved in 200 ml of water were mixed with each of 1.0 kg of Ap and 1.5 kg of Bt soil.

The soil-water-isotope mixtures were applied to the soil on Nov.26 and Dec. 6, 1981, after the soil surface had frozen. At 12 sites approximately 2½ cm depth by 30 cm diameter of Ap horizon was removed and replaced by the Ap-isotope mixtures. Another twelve sites were excavated to the upper surface of the Bt horizon and Bt-isotope mixtures were added, lightly tamped and covered with Breton Loam Ap horizon soil.

The isotope mixtures were laterally contained within 30 cm diameter open cylindrical heating ducts pressed into each respective horizon to a depth of two to three cm. The heating ducts marked the sites for sampling. The 24 points of application of the isotope mixtures were spread out evenly over a rectangular plot area eight m X 14 m, as shown in figure II.1. Gamma-densitometer access tubes were

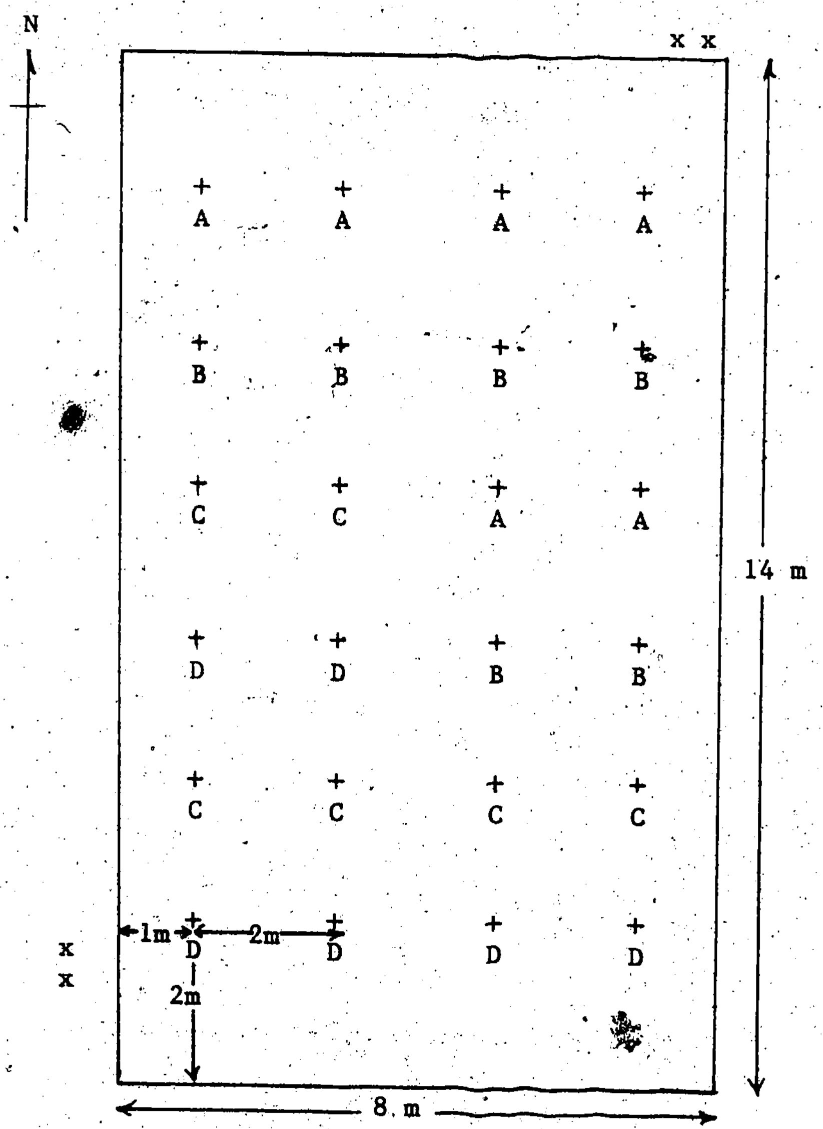
N
x x
A
A
A
A
B
B
B
B
C
C
A
A
D
D
B
B
C
C
C
C
1m
2m
D
D
D
D
x
x
2m
14 m
8 m

+ = Site of tracer application.

A = 6.25 uCi ^{3}HOH applied to Ap horizon (0-2½ cm).

B = 6.25 uCi ^{3}HOH applied to Bt horizon (17-20 cm).

C = 10 uCi ^{3}HOH and 2 uCi ^{14}C-lindane applied to Ap horizon (0-2½ cm).

D = 10 uCi ^{3}HOH and 2 uCi ^{14}C-lindane applied to Bt horizon (17-25 cm).

x x = Site of gamma densitometry twin probe access tubes.

Figure II.1. Field experiments, plot layout.

inserted near the N-E and S-W corners of the plot area.

The plot was sampled between May 5 and May 12, 1982, after the snowpack had completely melted. Two 4-cm diameter columns were taken from within each cylinder to depths of 100 to 120 cm using a hydraulic powered core sampler. The columns were sectioned into 2.5 cm layers from 0 to 75 cm and five cm layers from 75 to 120 cm depth. Solute activities were measured by liquid scintillation counting as described in section 4.b), below.

4. Field Measurements

a. Infiltration/Evaporation

i) γ-Densitometry

Wet bulk densities, Dt, were determined by the γ-densitometry method using a *Troxler Model 2376* two probe density gauge. The method and theory of operation are given by van Bavel (1958), Smith *et al*. (1967), and Troxler Electronic Laboratories (1976). Dry bulk densities, Db, and volumetric moisture contents, θ, were also determined from data obtained from γ-densitometry, as described below.

Net infiltration or net evaporation were determined as the net difference in θ between successive θ profiles determined by rectangular integration, as illustrated in figure III.13 in the next chapter.

ii) Snow survey

Total potential infiltration was determined by a snow survey on Mar.25, 1982, after the last precipitation event before the field experiment ended. Snow cores were taken near the four corners of the plot area using a tube of known diameter; snow was weighed and height equivalent of water determined as the weight over the cross-sectional area of the tube.

b. Volumetric Moisture Contents, θ

Volumetric moisture contents were calculated as the difference between Dt and Db. Ten θ profiles were measured between Mar.9, 1982, before spring thaw began, and May 15, 1982, after sampling was completed.

c. Depth of Frost

Frozen layers were determined by probing with a sampling tool. It was found that frozen layers determined in this way corresponded approximately to bulges in the difference between successive θ profiles.

5. Laboratory Analyses

a. Soil Physical Properties

i) Dry bulk density, Db

Dry bulk densities, Db, were calculated from wet densities, Dt, and gravimetric soil moisture contents, w, according to the equation:

$$Db = Dt/(1+w).$$

Gravimetric moisture contents were determined from two samples taken within one m of the access tubes in Nov. 1981, and one composite sample taken from between the tubes in

Sept. 1982. Samples were removed from the field in sealed moisture tins and dried at 105°C. w was calculated as weight of water in the samples divided by the weight of the oven-dry soil. Bulk density profiles were determined on Nov.20, 1981, and Sept.16, 1982, and the mean Db calculated at 2.5 cm increments to a depth of 110 cm.

ii) Porosity, a

Porosities were calculated from Db and particle densities, Dp, as:

$$a = 1 - Db/Dp.$$

Particle densities were determined by the method described by Blake (1965), using volumetric flasks. A porosity profile was determined for the same depth and resolution (110 cm and 2.5 cm, respectively) as for Db profiles.

iii) Moisture retention curve

Soil moisture retention curves were determined by the pressure plate method described by the manufacturer of the apparatus used (Soilmoisture Equipment Corp.). Intact soil cores were used in order to preserve the pore structure. Steel rings, 3.0 cm high by 4.8 cm in diameter were pressed into the soil, dug out and trimmed with a trowel. The same cores were used for moisture determinations at all tensions. Weights of moist soil were measured between runs and oven dry weights measured after the last equilibration. Gravimetric moisture contents were determined for Ap (8 samples), Bt (7 samples), and BC (4 samples) horizons at 5, 33, 100, 200, 500 and 1500 kPa moisture tensions, in the order given. Volumetric moisture contents at these points were obtained from the gravimetric according to the equation:

$$\theta = Db \cdot w.$$

5. Chemical Analyses

i)Adsorption

Adsorption rates and isotherms were determined for lindane adsorption to Breton Loam Ap and Bt horizon soil. Experimental methods were similar to those of Kay and Elrick (1967), except ^{14}C-labelled lindane was used and measurement was by liquid scintillation counting (LSC) rather than by gas chromatography.

Two gram soil samples, air dried and ground to pass a one mm mesh seive, were shaken in centrifuge bottles with 50 ml of ^{14}C-lindane solution of known concentration and activity. Samples were then centrifuged at 27,500 X gravity for 30 minutes. ^{14}C-lindane activity in solution was determined by LSC of two ml of the supernatant. Activity per unit volume was converted to lindane concentration by dividing by the specific activity. The amount of adsorbed lindane was calculated as the difference between the original and final amounts of dissolved lindane, less lindane adsorbed to the centrifuge bottles, determined from the isotherm for lindane adsorption to the bottles.

Adsorption isotherms were determined by shaking soil samples in incremental solutions containing 0.005 ppm to 2.5

ppm lindane for two hours. Adsorption isotherm experiments were duplicated and the adsorption coefficients determined as the slope of the regression line of adsorbed versus dissolved lindane for the combined sets of data.

Adsorption rates were determined by shaking triplicate soil samples in 1.5 ppm lindane solutions for time periods ranging from 0.25 to four hours. Adsorption equilibrium was attained in less than one hour for both Ap and Bt horizon samples.

Liquid Scintillation Counting (LSC)

Isotope activities were measured by liquid scintillation counting in *Fisher ™Scintivers* scintillation cocktail on a *Searle Isocap/300 System* after dark adaptation for two hours. Counting efficiencies were determined from sample channels ratios (SCR) as described in the instrument manual (Searle Analytic Inc., 1974) and by Vose (1980). Net counting rates (sample cpm - background cpm) were converted to actual counting rates (dpm) by dividing by the efficiency.

ii) Field sample assay

Activity of field samples was counted directly in the soil samples by a method similar to that described by Lavy *et al.* (1972). A non-gelling scintillation cocktail (table II.3) was used so that soil in the mixture would settle to ensure that fluorescence produced by scintillations would be transmitted through the cocktail. It was determined in separate experiments that addition of 15% methanol (by weight) to the scintillation cocktail was sufficient to dissolve up to two ml water in 16 ml of cocktail at the operating temperature of the scintillation counting system. The cocktail used could, therefore, dissolve all the soil solution in three gram samples of gravimetric moisture contents (*w*) up to 2.0.

Table II.3. Preparation of liquid scintillation cocktail for direct counting of soil-borne ^{14}C-lindane and ^{3}HOH.

Component	Amount
dioxane	1000 ml
xylene	600 ml
methanol	400 ml
[1]PPO	15 gm
[1]POPOP	0.1875 gm
naphthalene	240 gm

[1]-Scintillants added in a concentrate preparation, *Fisher* ™*Scintiprep 2*, in which PPO and POPOP are dissolved in xylene.

Three grams of moist soil sample were added to 16 ml of the scintillation cocktail. Vials containing the mixtures were shaken for one to three minutes on a vortex mixer. Vials were then shaken for one hour at three cps on a reciprocating shaker, allowed to settle in the dark for two hours and counted by LSC.

Sample accountabilities, determined as the net counting rate in moist soil standards over the known activity (in dpm) in the standards were determined and an accountability versus SCR curve plotted (figure II.2 and figure II.3).

Accountabilities for the direct counting of soil-borne ^{14}C-lindane were determined to be 55% to 61% for Ap samples and 68% to 73% for Bt samples. These were on average 5% lower than efficiencies determined from the efficiency versus SCR curve. The accountability versus SCR curve was approximately parallel to the efficiency versus SCR curve determined for quenched ^{14}C standards (figure II.2).

The direct counting method was extended to measurement of activity of ^{3}HOH in soil. Accountabilities soil-borne ^{3}HOH were 15% to 20%, and were consistently 5% lower than efficiencies determined from the standard efficiency versus SCR curve. The accountability curve for soil-borne ^{3}HOH was also parallel to the efficiency versus SCR curve for soilless standards in the SCR range encountered (figure II.3).

Because of the uncertainty involved in extrapolating on the accountability curves the standard efficiency versus SCR curves were used to determine activities for both ^{14}C-lindane and ^{3}HOH. Samples which contained both ^{14}C and ^{3}H activities were counted on a dual channel program and efficiencies determined from efficiency versus external standards ratio (ESR) as described in the instrument manual (Searle Analytical Inc., 1974).

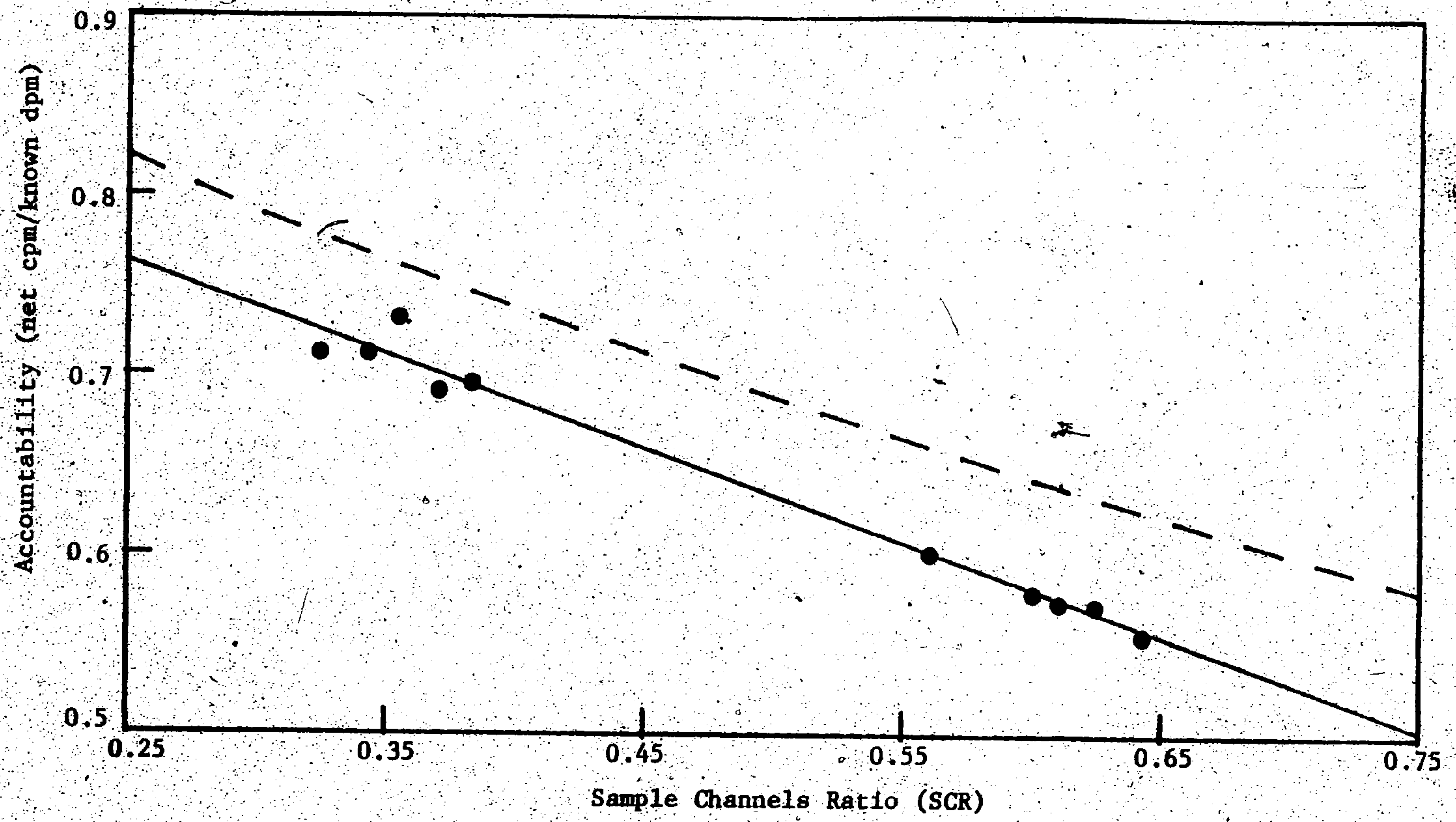

Figure II.2. Accountability (net cpm/known dpm) vs SCR curve (——) for direct liquid scintillation radioassay of ^{14}C-lindane in soil-scintillation cocktail mixture. Upper points in Ap horizon soil samples, lower in Bt horizon samples, Breton Loam. Efficiency vs SCR curve for soilless samples shown for comparison (— —).

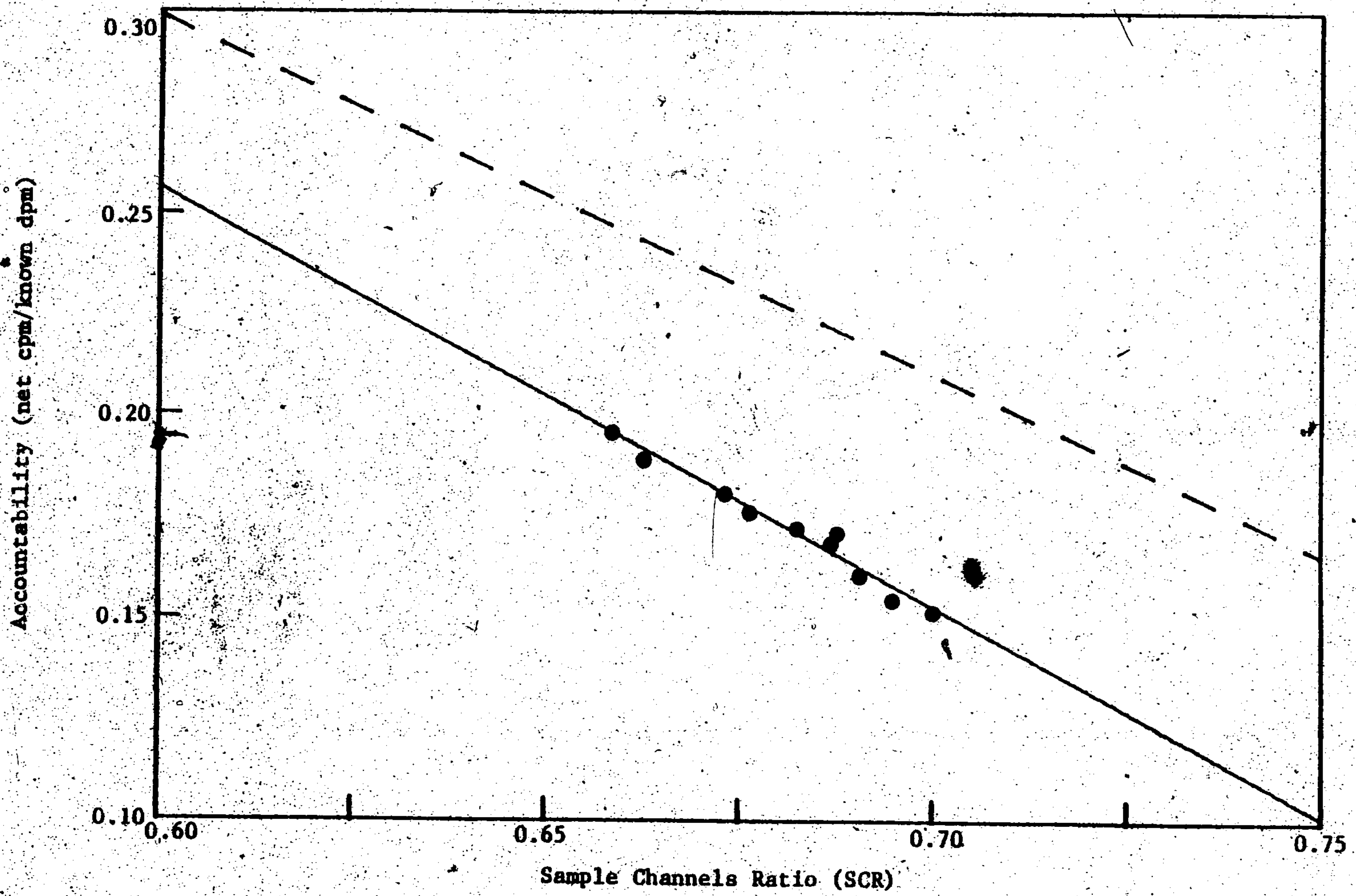

Figure II.3. Accountability vs SCR curve (——) for direct LSC of ^{3}HOH in soil-scintillation cocktail mixture. Upper points Bt horizon soil samples, lower Ap horizon, Breton Loam. Efficiencey vs SCR curve (— —) shown for comparison.

III. RESULTS AND DISCUSSION

A. SIMULATION EXPERIMENTS

1. Relative Sizes of Mobile and Stagnant Pools

The distribution between mobile and stagnant solution pools defines the influence of soil structure on leaching patterns in this simulation model. Ratios of WM:WR varying between 0:1 and 9:1 were used in a simulation experiment to examine sensitivity to this ratio. The amount of water in the mobile pool, WM, was set at WMCAP, the storage capacity of this pool, and WT, Δz, and water flux density were held constant (table III.1). (Time step, Δt, for this and all other simulations is one day).

Table III.1 Data used in simulation experiment 1a: Influence of size of mobile and stagnant moisture pools (WM and WR, respectively) on solute distribution.

SIMULATION	Δz cm	TIME days	WATER FLUX DENSITY ml/cm²-d	cm/layer WT	WM	WR	WR:WM
A	2.54	40	0.5	1.0	1.0	0.0	0:1
B	2.54	40	0.5	1.0	0.5	0.5	1:1
C	2.54	40	0.5	1.0	0.25	0.75	3:1
D	2.54	40	0.5	1.0	0.1	0.9	9:1

The simulation approaches the analytical solution at low WR:WM ratios (figure III.1). For WR:WM of 1:1 or less,

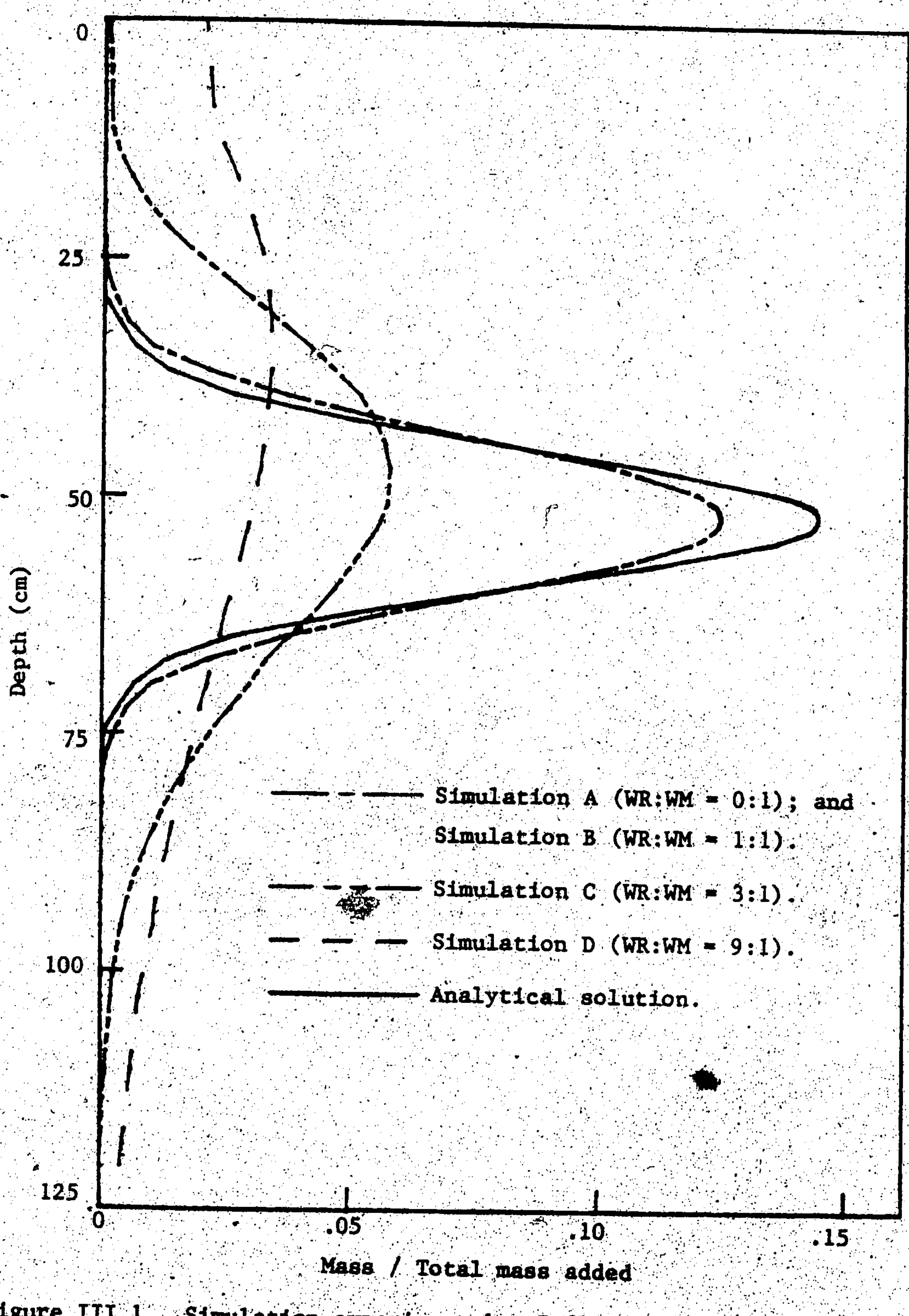

Figure III.1. Simulation experiment 1a: Influence of relative sizes of stagnant (WR) and mobile (WM) water pools on distribution of solute added to the surface layer (0 - 2.5 cm) of a structured soil after simulated leaching by 20 cm of water.

simulated solute distributions are identical and the numerical solution is approximately equal to the analytical solution. Viewed qualitatitively this means that low WR/WM values simulate the situation in which structure plays a decreasing role in affecting leaching patterns. WR/WM approaches zero for structureless media. This is illustrated in figure III.1 by the special case of WR:WM of 0:1 (simulation A). High WR/WM values, representative of highly aggregated soils, are illustrated in simulations C and D.

Increasing the influence of soil structure (increasing WR/WM) is accompanied by both a shift in the solute concentration profile toward the soil surface (positive skewness) and greater spreading. These effects are produced by a fast leaching routine in the simulation program which causes channeling of soil solution through the macropores when the incremental infiltration inputs exceed the mobile water capacity (WMCAP).

This fast leaching routine reduces the degree of equilibration between mobile and stagnant solution pools. Where the rapidly flowing solution moves through a region in which stagnant pool concentrations are higher than in the infiltrating solution, diffusional mass transfer from the stagnant pool is reduced and less solute mass is transported than for slowly infiltrating waters. In regions where concentration in the stagnant pool is lower than in the moving solution reduced mass transfer between pools results in transport of greater mass to greater depths than would occur under low flow rates.

Thus the net effect of the fast leaching routine is to cause deeper penetration of a small amount of solute but holdback of a greater proportion of the mass of the solute at the same time as indicated by the upwardly skewed concentration versus depth profile and the the tailing of the profile at greater depth. This phenomenon was observed by Dekkers and Barbera (1977) in column leaching experiments with initially dry aggregated soil.

The analytical solution in figure III.1 provides a check on the accuracy of the numerical techniques used in the simulation model. The concentration peaks are at the same position in the soil column for the analytical solution and the structureless system. Slightly more spreading occurs in the simulation, however.

The dispersion coefficient, E, used in the analytical solution (Kirkham and Powers, 1972):

$$C/C_0 = 0.5[(\mathrm{erf}(z'+z_0-\nu t)/2\sqrt{(Et)})- \mathrm{erf}(z'-\nu t)/2\sqrt{(Et)}] \quad (41),$$

where $z' = z - 2.54$ cm;

$z_0 = -1.27$ cm;

ν = fluid velocity

$= 1.27$ cm/d;

$t = 40$ d.

was determined as the numerical spreading coefficient using the approximation formula given by Reiniger and Frissel (1974):

$$Dspr = \upsilon \cdot \Delta z/2 \qquad (42).$$

Using this approximate value of E introduces error into the analytical solution. Values for E determined from (41) and the maximum concentration from the profiles obtained from simulations A or B yield curves that effectively coincide with the analytical solution.

Determination of WR and WM

Soil aggregation influences leaching patterns because of the heterogeneous pore structure it produces. Therefore it is important to divide mobile and stagnant pools on the basis of pore size distribution. The moisture retention curve (θ versus soil moisture tension) is one way of quantifying pore size distribution, since soil moisture tension is a function of pore radius.

To assign values for WR and WM a moisture tension characteristic of the pore size range of each pool is chosen and volumetric values assigned on the basis of the moisture retention curve. In this way a standard theoretical criterion for dividing soil moisture pools can be used. The moisture tension used to assign WR/WM should be the same for all soils (Addiscott, 1977). Addiscott (1977) has used 200 kPa tension as a working approximation.

Sensitivity to the moisture tension value used in the allocation of WR:WM was examined using the data in table III.2. The upper limit of WMCAP was defined as field capacity (θ at 33 kPa soil moisture tension) and WM was set at WMCAP. The upper limit of WR was set at 500 kPa, 200 kPa, and 100 kPa for separate simulation runs. Values of θ were determined from a soil moisture retention curve for undisturbed soil cores taken from the field. A complete set of soil physical properties were determined for this experiment by field and laboratory measurements (table III.9).

Table III.2 Data used in simulation experiment 1b: Influence of soil tension value used to assign WR:WM on solute distribution.

				cm/layer			
SIMULATION	Δz cm	TIME days	WATER FLUX DENSITY ml/cm^2-d	WT	WM	WR	WR:WM set at
B	2.54	40	0.5	varies	varies	varies	500kPa
C	2.54	40	0.5	varies	varies	varies	200kPa
D	2.54	40	0.5	varies	varies	varies	100kPa

The results of this simulation experiment (figure III.2) were in qualitative agreement with the previous experiment. Choosing a low soil tension to assign WR and WM resulted in a high WR:WM ratio, causing a greater positive skewness in the solute concentration profile (simulations C and D). The skewed profiles indicate greater penetration of solute and lower net movement of solute mass, as described in the previous simulation experiment. Increasing the tension value (simulation B) moves the solute concentration toward the analytical solution (A).

The abrupt change in slope of the solute concentration profile at 15 cm depth coincides with the boundary between

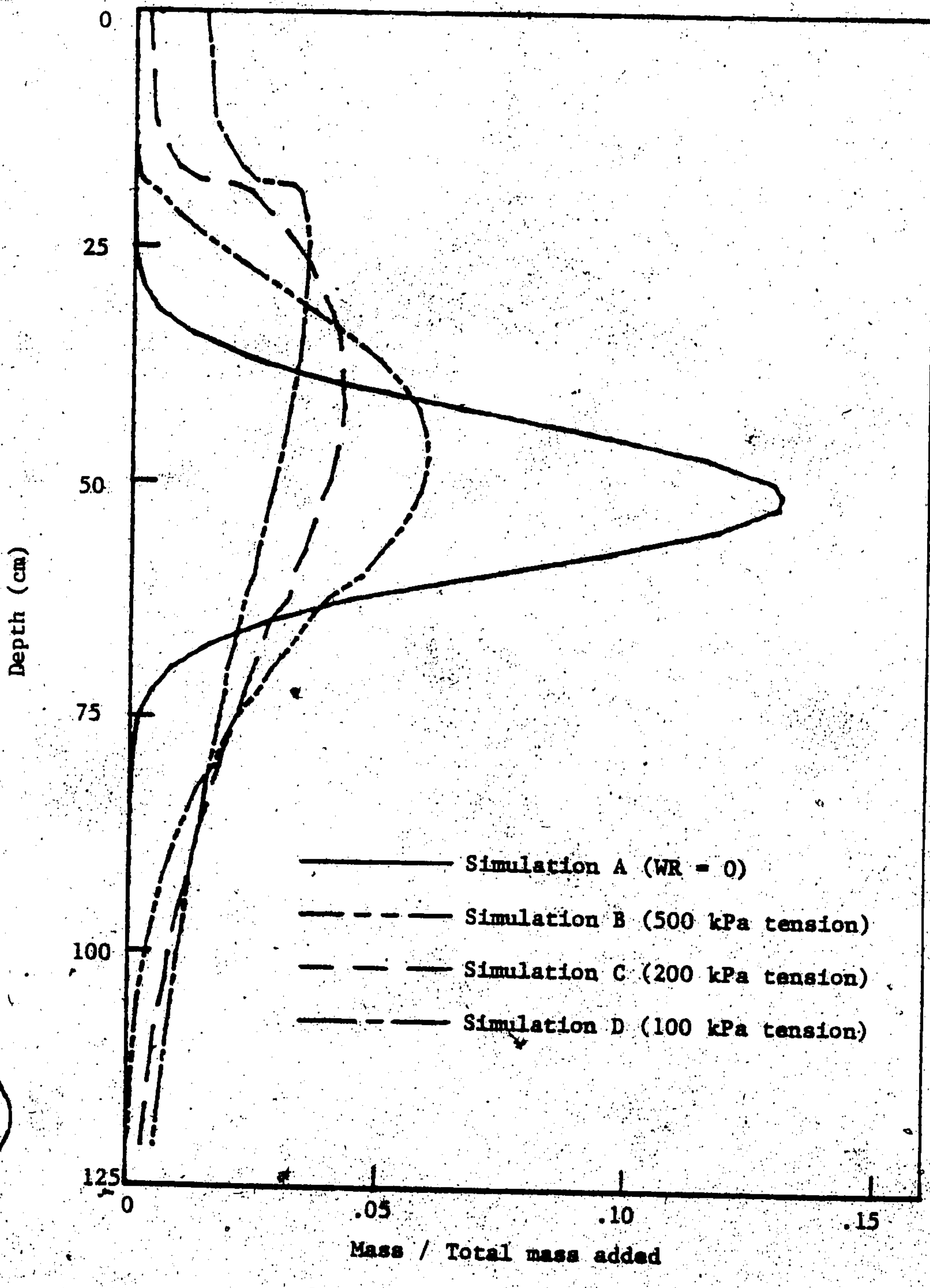

Figure III.2. Simulation experiment 1b: Influence of soil moisture tension values used to assign sizes of stagnant (WR) and mobile (WM) water pools on distribution of solute added to the surface layer (0 - 2.5 cm) of a structured soil after simulated leaching by 20 cm of water.

Ap and Bt horizons and reflects the differences in moisture retention characteristics between these horizons. The higher clay content of the Bt horizon and accompanying larger micropore volume result in a higher WR:WM ratio in the Bt. Consequently a greater proportion of solute is retained in the stagnant pool in the Bt than in the Ap horizon. This feature causes a sharp increase in solute mass held in the stagnant pool at about 15 cm depth.

Such identifiable features can be used to assess the influence of structure on field experiments. Existence of similar sharp changes in slope of the solute concentration profile observed in field experiments would confirm the relative importance of structure in leaching and aid in determining the appropriate distribution of WR and WM. Other diagnostic features of the leaching system which show up in the simulation runs are the position and magnitude of the solute concentration peak, and the depth of solute penetration.

2. Rate and Pattern of Infiltration

High infiltration rates, simulated using the data in table III.3, have an influence on the system similar to that of low WR:WM ratios.

Table III.3 Data used in simulation experiment nr. 2a: Influence of infiltration rate on solute distribution.

SIMULATION	Δz cm	TIME days	WATER FLUX DENSITY ml/cm²-d	cm/layer WT	cm/layer WM	cm/layer WR	WA/WMCAP
A	2.54	80	0.25	1.0	0.5	0.5	0.50
B	2.54	40	0.50	1.0	0.5	0.5	1.0
C	2.54	20	1.0	1.0	0.5	0.5	2.0
D	2.54	8	2.5	1.0	0.5	0.5	5.0

The quantitative relationship between the size of water inputs, WA (WA = flux X Δt), and the mobile water capacity, WMCAP, determines whether solution is channelled through soil macropores by the fast leaching routine (WM is set at WMCAP). For WA/WMCAP greater than 1, solution moves through the soil column with limited equilibration between SR and SM. This mechanism simulates channelling of solution (figure III.3).

Increasing WA/WMCAP to two and five (simulations C and D, respectively) causes an increasing upward skewness in the solute concentration profile. The simulation mechanism causing this skewness is discussed in the previous simulation experiment. Increasing WA/WMCAP has an effect similar to increasing WR/WM.

Simulation B is the special case in which incremental infiltration inputs are equal to WM (and WM = WMCAP) at each layer. The effects of this situation on numerical dispersion were described by Leistra (1973). Mobile solution pools are displaced by exactly one layer thickness for each time increment and, therefore, no mixing occurs in the mobile

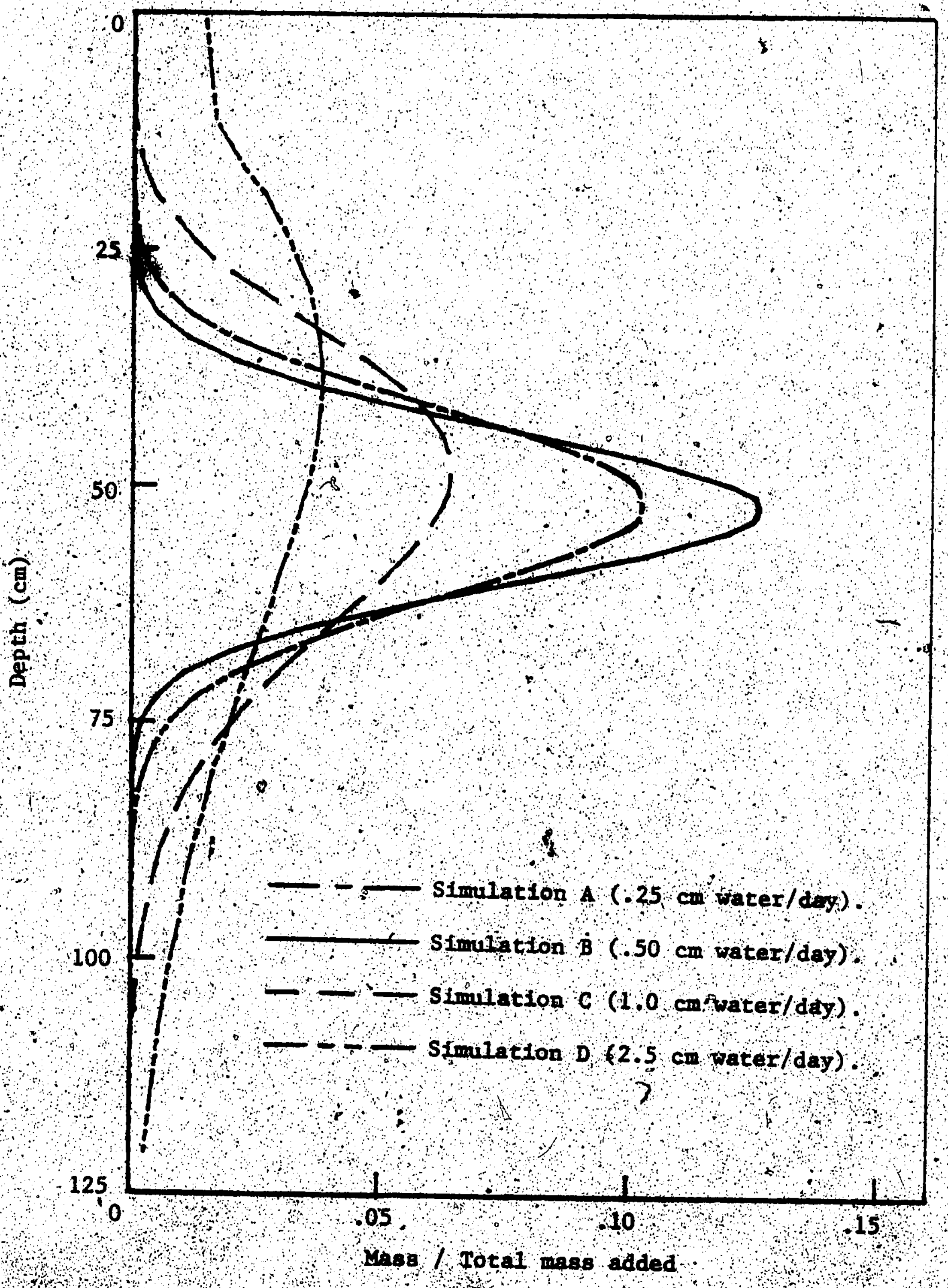

Figure III.3. Simulation experiment 2a: Influence of infiltration rates on distribution of solute applied to the surface layer (0 - 2.5 cm) of a structured soil after simulated leaching by 20 cm of water.

pool. The spreading observed in this case is entirely due to holdback of solution in the stagnant pool. This is why B exhibits less spreading than A.

For simulations A and B, WA/WMCAP is less than or equal to one, so that slow leaching, which permits more complete equilibration between SR and SM, is the only transport mechanism. A and B are symmetrical about a peak concentration located at a depth equal to the product of the fluid velocity and time. These plots approach the analytical solution. This implies that for WA/WMCAP less than one the system approaches an ideal chromatographic system: that is, soil structure has little influence on the leaching pattern which develops. This fact can be illustrated with box diagrams representing simulation of a simplified system (figure III.4). Diagrams A, i) to iv), represent a model of leaching of layered soil column. This is a single solution pool model with a uniform pore size. Diagrams B, i) to vii), represent a layer model of a structured soil possessing two solution pools, equal in volume and representing two distinct pore size ranges.

At time, t_o, 100% of the solute present in both models is located in the top layer. In the non-structured system, A, the entire solution is mobile. In the structured system, B, 50% of the solute is contained in the mobile pool, SM, and 50% is in the stagnant pool, SR.

If a water volume equal to 25% of the layer pore volume moves into layer one then 25% of the solute in layer one is

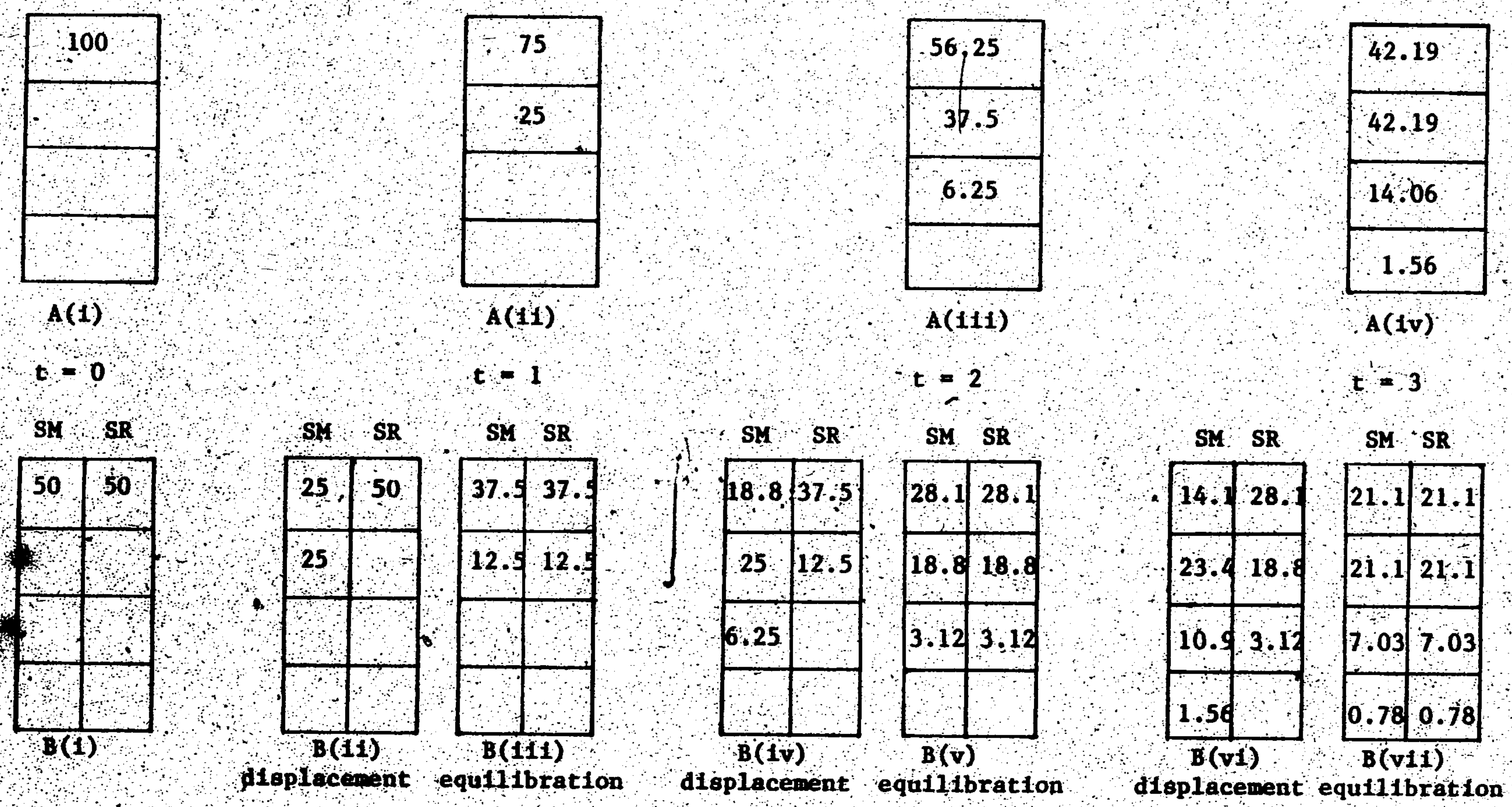
100
A(i)
t = 0
75
25
A(ii)
t = 1
56.25
37.5
6.25
A(iii)
t = 2
42.19
42.19
14.06
1.56
A(iv)
t = 3
SM
SR
50
50
B(i)
25
50
25
B(ii)
displacement
37.5
37.5
12.5
12.5
B(iii)
equilibration
18.8
37.5
25
12.5
6.25
B(iv)
displacement
28.1
28.1
18.8
18.8
3.12
3.12
B(v)
equilibration
14.1
28.1
23.4
18.8
10.9
3.12
1.56
B(vi)
displacement
21.1
21.1
21.1
21.1
7.03
7.03
0.78
0.78
B(vii)
equilibration

Figure III.4. Simple numerical simulation of solute transport. A. Structureless system.

B. Structured system (WR = WMCAP).

Water added at each time step = 1/4 pore volume (A) = 1/2 WMCAP (B).

displaced into the next lower layer. If the same volume of water moves into the structured system 25% of total solute, or 50% of SM, is displaced. The resulting solute mass distribution for each system, at t_1, given in A ii) and B iii), are equal. Repeating the above steps for two more time intervals result in the solute distributions shown in A iii) and iv) and B v) and vii). Solute distribution is the same for each system at each time step. Solute distributions for case A can be determined from the analytical solution. Distributions for the structured system, B, can also be predicted by the analytical solution of system A, provided WA is always less than WMCAP.

When WA exceeds WMCAP the amount of solute displaced at any time step in the structured system can never be more than SM, whereas all the solute in the non-structured system is subject to displacement. The structured system causes holdback of solute in the stagnant pool and at the same time reduces the effective conducting porosity so that greater solution velocity results from the same flux density. Both these features can be seen by comparing simulations A and D of figure III.3, which represent WA/WMCAP values of 0.5 and 5, respectively.

This simulation experiment illustrates the relative leaching efficiency of different infiltration rates. Heavy rainfall events would transport proportionally less soil-borne solute than would gentle precipitation. Greater mass of rain-borne solutes, such as sulfate and radioactive fallout, would be carried to a greater depth by more intensive precipitation events.

The results of this simulation experiment also point out the influence of the time step on simulated leaching patterns. Activation of the fast leaching routine depends on the infiltration rates. The time step used must be small enough to detect short events of high intensity. If large time intervals are chosen the information on rates of infiltration will be hidden in an infiltration rate averaged over the entire time interval.

Simulation experiments were performed to assess the effect of pattern of infiltration on a structured soil system using data summarized in table III.4.

Table III.4 Data used in simulation experiment 2b: Influence of infiltration patterns on solute distribution.

			cm/layer			
SIMULATION	Δz cm	TIME days	WT	WM	WR	WATER FLUX DENSITY ml/cm^2-d
A	2.54	40	1.0	0.25	0.75	s.fig.III.5
B	2.54	100	1.0	0.25	0.75	0.2
C	2.54	40	1.0	0.25	0.75	0.5
D	2.54	16	1.0	0.25	0.75	1.25

An infiltration pattern similar to figure III.5 was observed in experimental plots by γ-densitometer scanning during spring melt of the snowpack. To assign variable daily infiltration rates a smooth curve was plotted through the rates measured; the area under the curve was taken to be

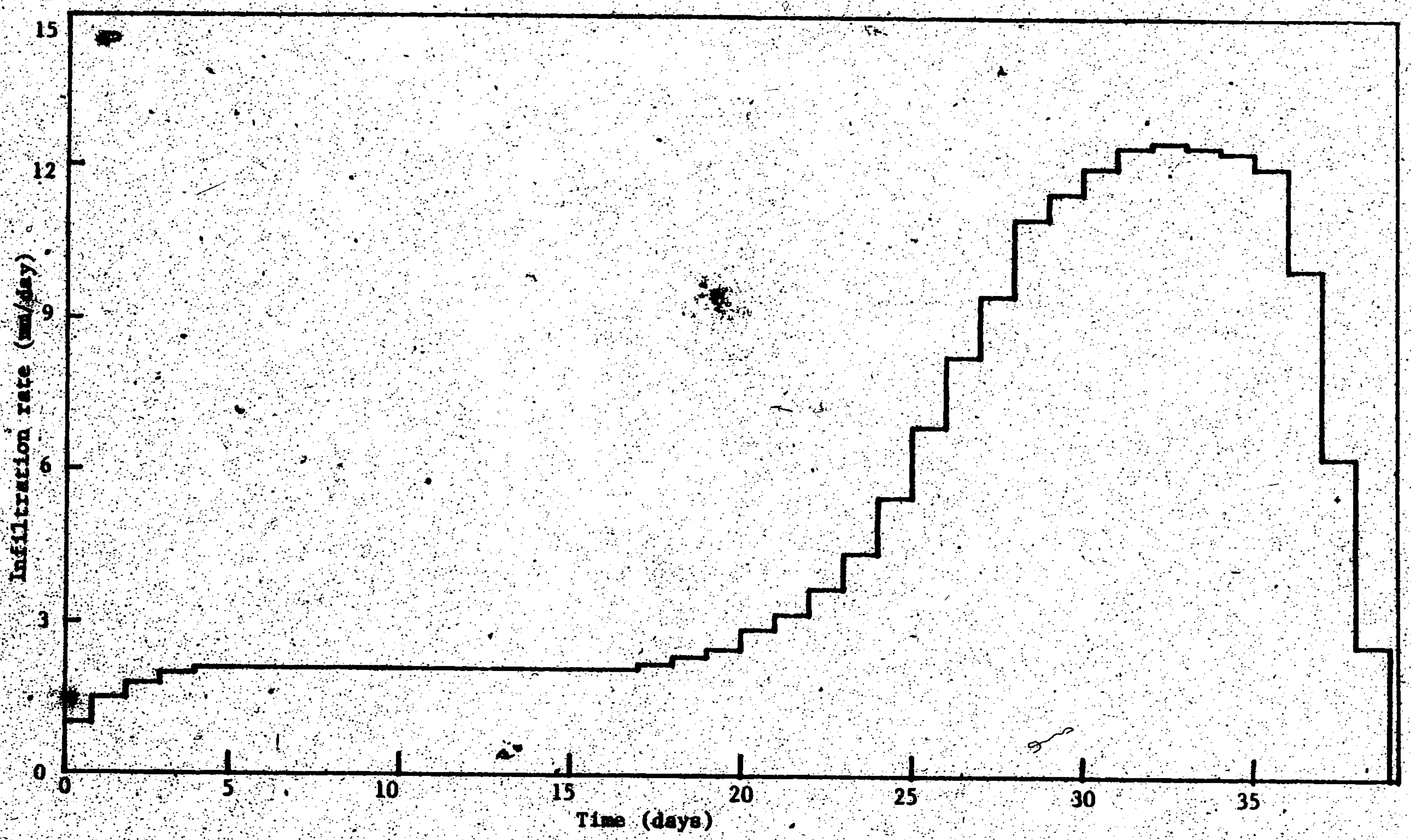

Figure III.5. Infiltration pattern used in simulation experiment 2b (simulation A.). Step-wise rates represent points of interpolation on infiltration vs time curve determined by gamma-densitometry.

20.0 cm of water; and daily infiltration was determined by interpolation.

The simulation for varying infiltration rates (figure III.6, simulation A) is intermediate between the average rate simulated (C) and the maximum rate simulated (D). The position and magnitude of the solute peak concentration for A bear closest resemblence to D (maximum infiltration rate). The poorest fit occurs between A and B (the minimum infiltration rate).

Results of this simulation experiment indicate that relatively few infiltration events of high intensity may dominate over more numerous events of low intensity as shown by the the relative agreement of simulation A to B and D. It also indicates that the model is sensitive to the degree of resolution of the infiltration data as shown by the differences between plot A and plot C, the simulation of averaged infiltration rates.

3. Layer thickness

The influence of layer thickness, Δz, on numerical chromatographic models was discussed in Chapter I, under "plate theories". Leistra (1973), and Frissel and Reiniger (1974) have explained how layer thickness affects spreading of the solute concentration band in numerical models of solute transport based on chromatographic theory.

The influence of layer thickness on simulated leaching patterns (figure III.7) was assessed for three different

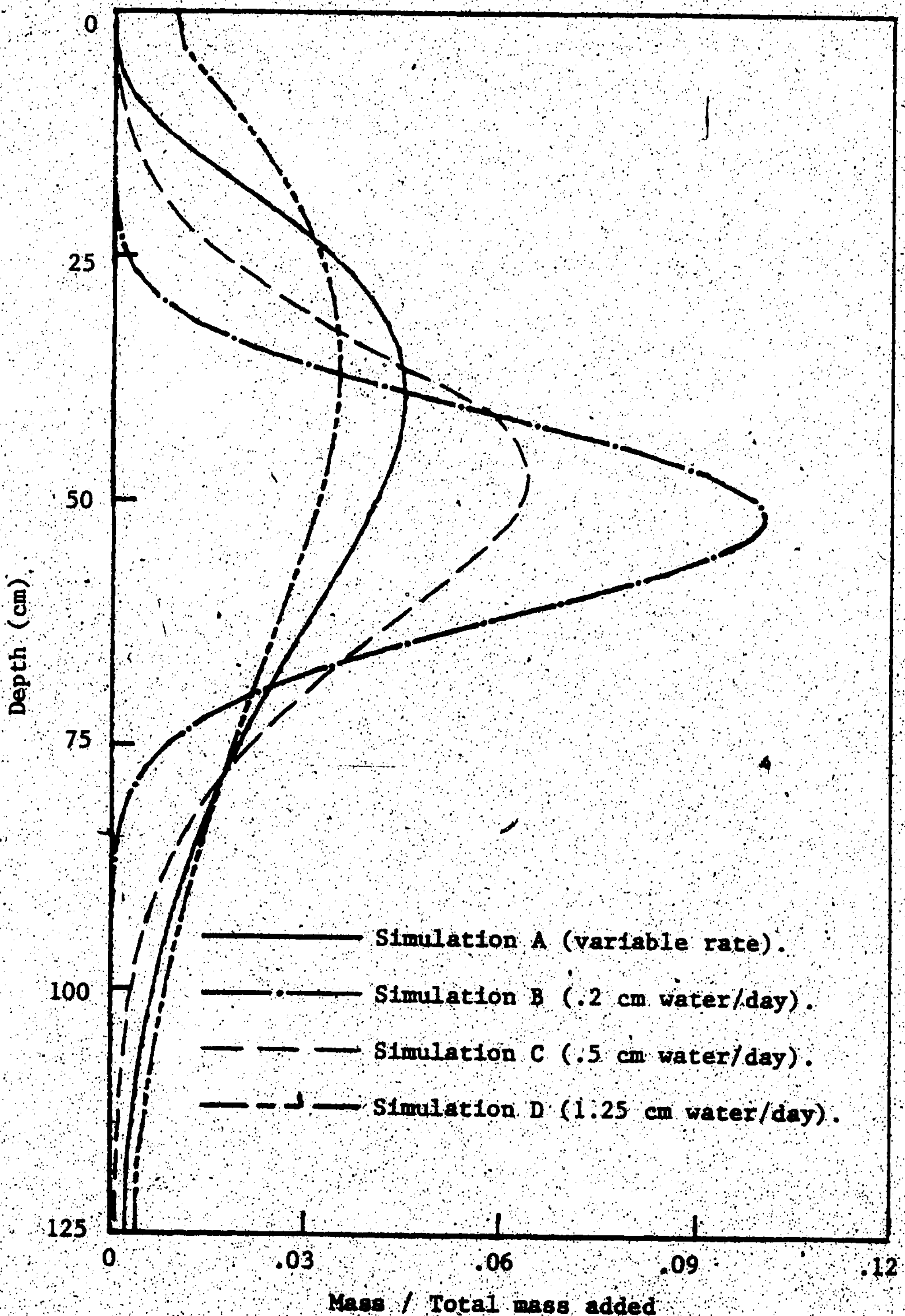

Figure III.6. Simulation experiment 2b: Influence of infiltration pattern on distribution of solute added to the surface layer of a structured soil after simulated leaching by 20 cm of water.

thicknesses using the data in table III.5.

Table III.5 Data used in simulation experiment 3: Influence of layer thickness on solute distribution.

SIMULATION	Δz cm	TIME days	WATER FLUX DENSITY ml/cm^2-d	cm/layer WT	cm/layer WM	cm/layer WR
A	1.27	20	1.0	0.5	0.25	0.25
B	2.54	20	1.0	1.0	0.5	0.5
C	10.16	20	1.0	4.0	2.0	2.0

For this simulation WM was set equal to WMCAP. Simulations A, B, and C exhibit slightly different amounts of spreading and net solute transport. The smallest layer thickness, 1.27 cm, caused more spreading than did 2.54 cm. This seems to contradict the prediction of the analytical solution. This anomaly can be explained with reference to the previous subsections. Fast leaching in this model depends on the relationship between WMCAP and WA. WMCAP is directly proportional to layer thickness. A small layer thickness will reduce WMCAP and thus increase the frequency of use of the fast leaching routine. This results in greater spreading of the solute profile and greater positive skewness of the solute concentration profile. Slightly greater positive skewness can be observed in plot A (layer thickness = 1.27 cm) than occurs in plots B and C, for greater thicknesses.

Differences in plots A, B, and C resulting from differences in layer thickness, are small. Reducing layer

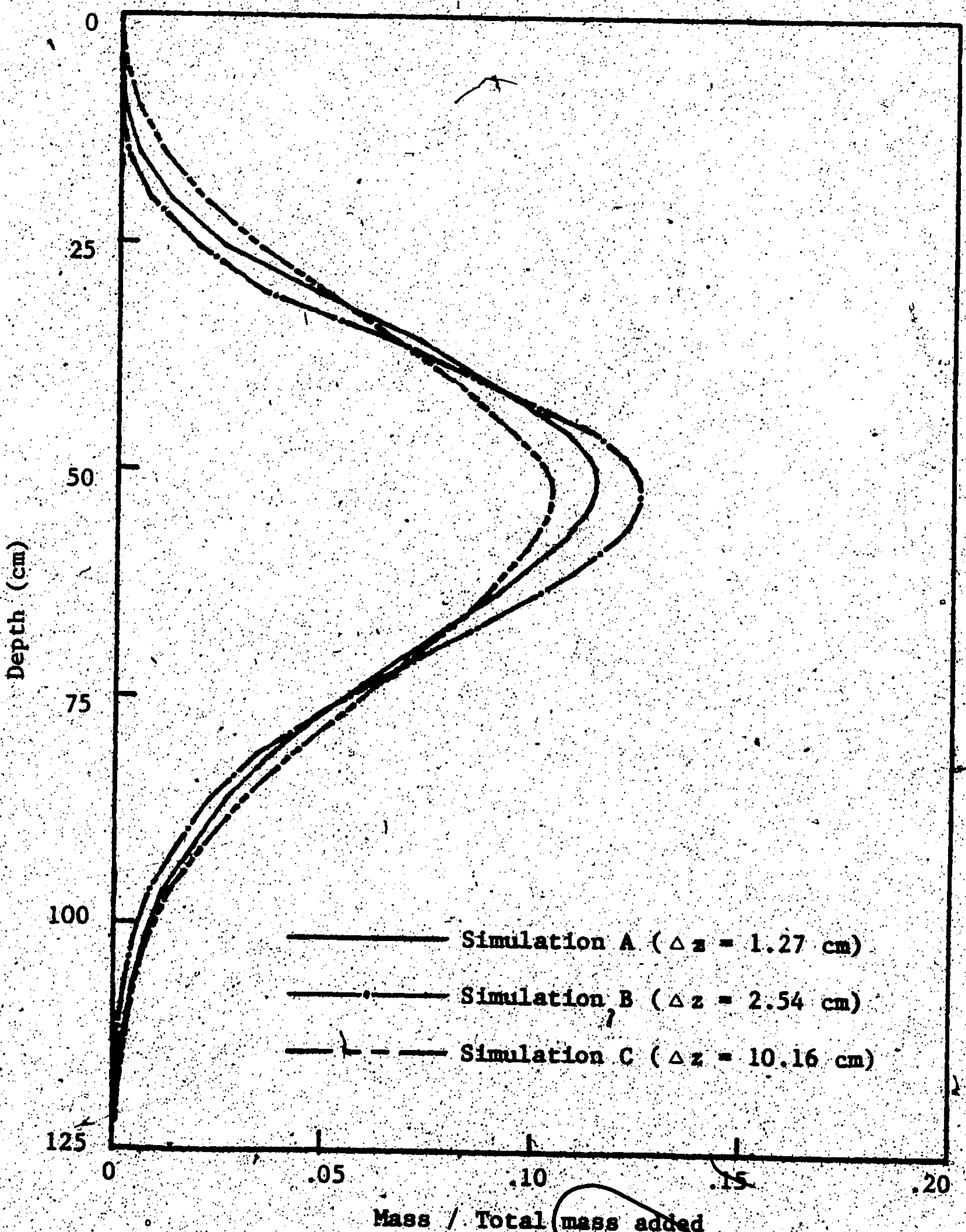

Figure III.7. Simulation experiment 3: Influence of layer thickness on distribution of solute added to the surface layer (0 - 2.5 cm) after simulated leaching by 20 cm of water.

thickness by 1/8, from 10.16 cm to 1.27 cm, results in a change in peak concentration of about 10%, and a shift in depth of the peak concentration of about one cm. Reference to figure III.1 shows that a change in WR/WM of a similar scale (plots III.1.B and III.1.D) reduces peak height by 2/3 and shifts peak concentration position by 20 cm. Inspection of figure III.4 shows that the infiltration rate also has a much greater influence on simulated leaching patterns than does layer thickness.

This relative insensitivity to layer thickness occurs because changing layer thickness brings opposite forces to bear on spreading. Increasing layer thickness increases numerical spreading by increasing the mixing height of the system, but at the same time reduces spreading resulting from channelling through macropores, affected by fast leaching.

In theory, layer thickness should be selected on the basis of a physical experiment. The simulation experiment described above indicates that the model is not highly sensitive to layer thickness between 1.27 cm and 10.16 cm and a guesstimate value may be adequate.

4. Frozen Soil

A frozen layer can influence solute transfer by restricting infiltration rates. Four simulations were run to assess the effects of infiltration into a partially frozen soil (figure III.8) using the data is presented in table III.6.

Table III.6. Data used in simulation experiment 4: Influence of frozen soil on solute distribution. (Infiltration rates are 0.5 cm/day in all cases. Flow rates vary because of the influence of frozen layer).

			cm/layer			
SIMULATION	Δz cm	TIME days	WGRCAP	WM & WMCAP	WR	RATE OF THAW cm/d
A	2.54	25	0.25	0.25	0.75	5.0
B	2.54	25	0.25	0.25	0.75	7.5
C	2.54	25	0.25	0.25	0.75	10.0
D	2.54	25	0.25	0.25	0.75	-

In simulation A, a perched saturated zone forms above the impermeable frozen layer and extends upward above the soil surface. Downward movement behind the receding frozen layer is entirely due to movement of gravity water (WGRAV). This water represents a smaller fraction of the total than in the thawed soil because there is more water present in this saturated zone. Though equal volumes move at each time step in each case, a smaller fraction of the total solution present moves above the frozen zone. Therefore a smaller fraction of the solute is transported in the partially frozen soil.

For simulations B and C the ice recedes much faster than in A. The saturated zones in these cases do not extend as far as in A. Therefore solution moving in the unsaturated upper regions of systems B and C represent a greater proportion of the total solution than in A, thus

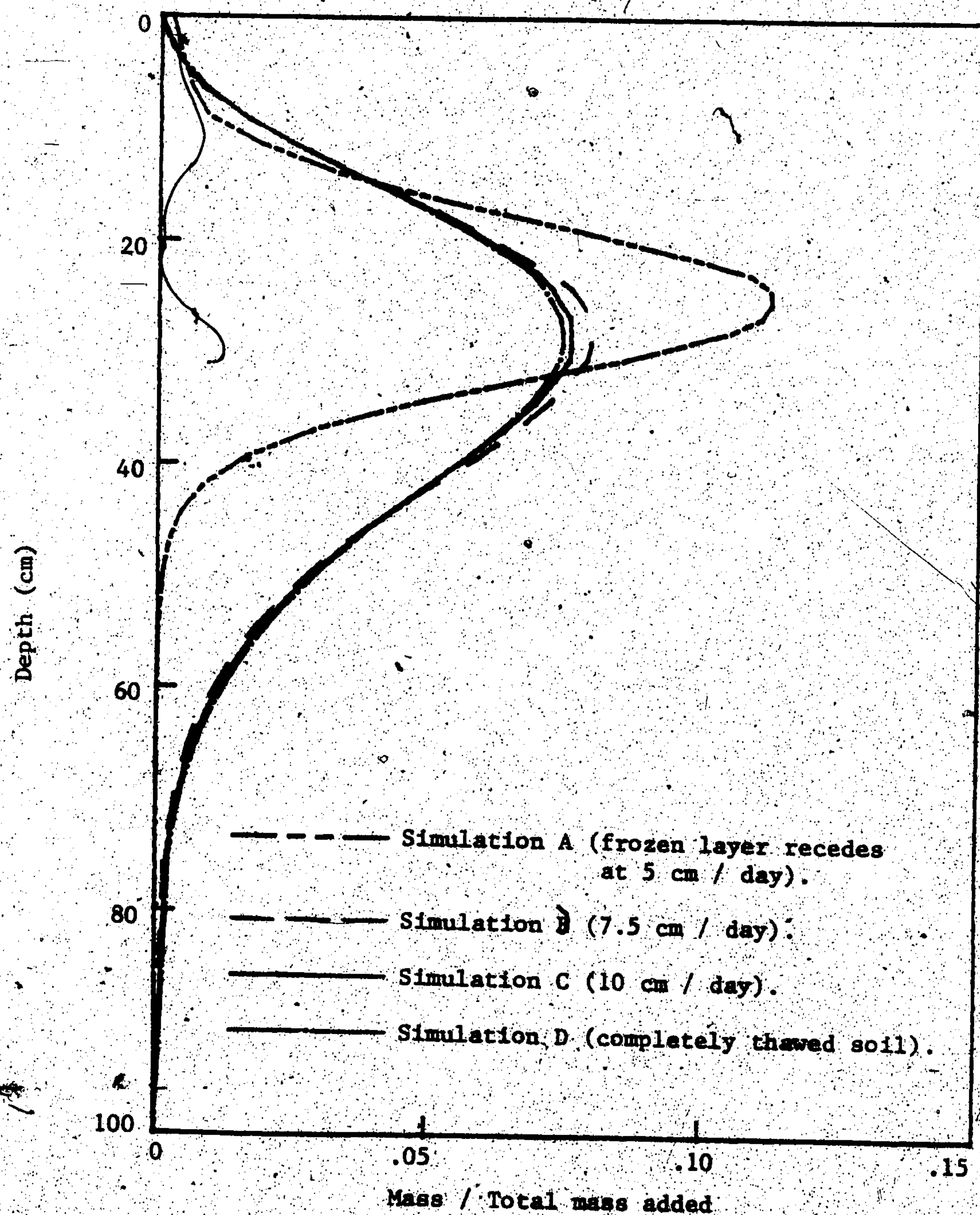

Figure III.8. Simulation experiment 4: Influence of a frozen layer on distribution of solute added to the surface layer (0 – 2.5 cm) of a structured soil after simulated leaching by 12.5 cm of water.

transporting a proportionately larger mass of solute.

The other major distinguishing feature of these plots is the symmetry in plot A and the skewness in B, C, and D. Solution flow rate is reduced by the frost layer in case A so that greater equilibration between SR and SM occurs. In cases B through D the influence of the frozen layers on flux rates is reduced so that fast leaching is more dominant, producing the greater skewness evident.

When a frozen layer has the effect of reducing the solution flow rates and therby causing greater equilibration between mobile and stagnant solution pools, it can cause leaching of a greater solute mass than would occur in thawed soil with the same infiltration rate. An illustration of this phenomenon is discussed in the final section of this chapter (figure III.20).

5. Adsorption

Adsorption affects retention of solute in opposition to the influences of [illegible] flow and diffusion. Quantitative effects of adsorption on solute distribution were simulated using data [illegible] table III.7. Solute was added to the first layer of [illegible] 2.54 cm thickness) and equilibrated between solution phase pools and adsorbed phase according to a linear adsorption isotherm.

Table III.7. Data used in simulation experiment 5a: Influence of adsorption during leaching on solute distribution. (Layer thickness and time step were 2.54 cm and one day, respectively, for all simulations.)

			cm/layer			
SIMULATION	TIME days	WATER FLUX DENSITY ml/cm^2-d	WM	WR	Db g/cm^3	Kads ml/g
A	80	0.25	0.25	0.75	1.5	0.0
B	80	0.25	0.25	0.75	1.5	1.0
C	80	0.25	0.25	0.75	1.5	5.0
D	80	0.25	0.25	0.75	1.5	25.0

It is assumed that adsorption of the hypothetical solute is defined by a linear isotherm and that equilibrium between adsorbed and dissolved phases is attained at each layer between time steps. Therefore the relationship between mass (q) of adsorbed solute per unit mass of soil and concentration of dissolved solute (c) can be defined as:

$$q = Kads \cdot c.$$

The values of Kads used cover a range of conditions encountered in soil. Adsorption of some anions to some soils can be defined by a Kads of 0. Kads of 1, 5, and 25 represent weak, moderate and strong adsorbate-soil affinities, as, for example, lindane adsorbed to sand B horizon, loam B horizon, and loam Ap (O.M. = 4%) horizon soils, respectively.

The most striking feature of the plots of these simulations (figure III.9) is the low mobility of adsorbed solutes. (Solute distributions in figure III.9 are expressed as mass per unit bulk volume rather than concentrations because part of the solute present is not in solution phase.) Nearly 100% of the non-adsorbed solute has moved beyond the furthest extent of even the weakly adsorbed solute. Peak concentration of the non-adsorbed solute (simulation A) moved 50 cm, while for the adsorbed solutes peak concentrations moved ten cm (Kads = 1 ml/g), one cm (Kads = 5 ml/g) and zero cm (Kads = 25 ml/g).

Examining simulation B in detail reveals the reason for the immobility of adsorbed solutes. At each time interval in the simulation, solute is partitioned between solid and liquid on the basis of Kads and the relative masses of solid and liquid in each layer. Assuming a linear isotherm and local equilibrium, this partition is defined by (39):

$$ST = B*MS/(1+B),$$

where $B = Db \cdot Kads/\theta$,

Db = dry bulk density of soil(g/cm^3); and,

θ = volumetric moisture content(ml/cm^3).

The solute mass, SM, subject to displacement is defined by equation (36) so that:

$$SM = (WM/WT)ST = (WM/WT)B*MS/(1+B).$$

For Kads = 1.0 ml/g, and Db and θ defined in table III.7, B is 3.8, while WM/WT is 1/4, so that:

$$SM \cong MS/20.$$

This means that the mobile solution, WM, transports approximately 1/20 of the total solute mass as it passes through layer 1, where the solute was originally placed. As the solution passes through the next layer approximately .95 of the dissolved solute mass is retained. This partition

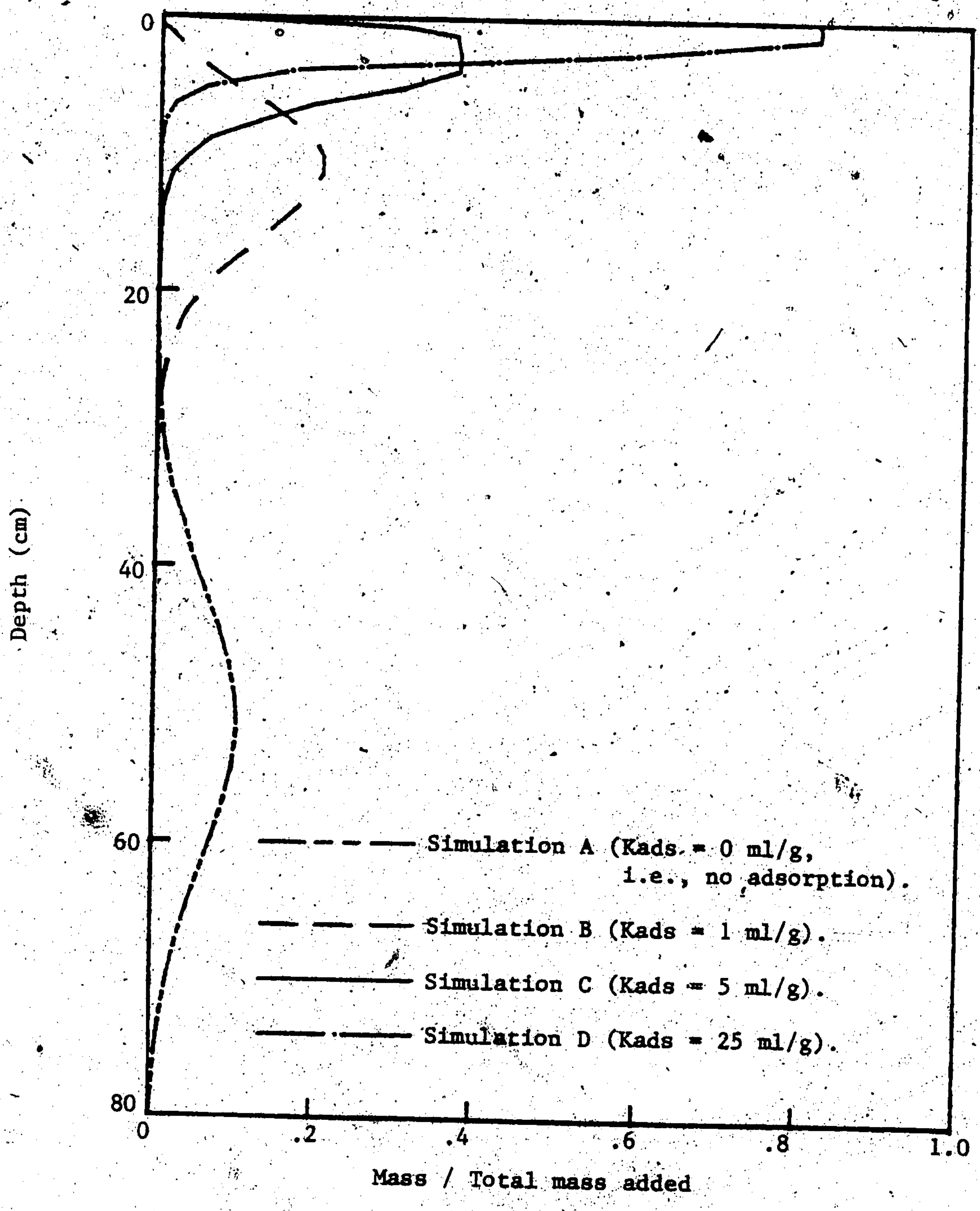

Figure III.9: Simulation experiment 5a: Influence of adsorption on distribution of solute added to the surface layer (0 - 2.5 cm) of a structured soil after simulation leaching by 40 cm of water.

process is repeated for lower layers at each successive time step so that when the solution passes out of the sixth layer (5 time steps later) it contains only $(1/20)^5$, or less than $3X10^{-7}$ of the solute mass which it carried out of layer 1.

The above numerical example illustrates that concentration of leaching solution is an exponential function of the negative product of B and time. This explains why the plot of mass vs depth drops off so sharply for a simulation D, with Kads of 25 ml/g (B = 93.75). This analysis illustrates that adsorption is a dominant control on leaching of solutes through soil.

Water flux was earlier shown to affect leaching patterns of non-adsorbed solute. Transport of a weakly adsorbed solute (Kads = 1.0 ml/g) was simulated at two solution flux densities (table III.8) to assess the influence of flow rate on distribution of adsorbed solute.

Table III.8. Data used in simulation experiment 5b: Influence of solution flow rates on distribution of an adsorbed solute (Layer thickness and time increment were 2.54 cm and one day, respectively, for all simulations).

			cm/layer			
SIMULATION	TIME days	WATER FLUX DENSITY ml/cm^2-d	WM	WR	Db g/cm^3	Kads ml/g
A	100	0.25	0.25	0.75	1.5	1.0
B	50	0.5	0.25	0.75	1.5	1.0

The results (figure III.10) exhibit the same qualitative characteristics as shown in figure III.3

(influence of solution flow rates on leaching of non-adsorbed solutes), that is, the concentration profile is skewed toward the soil surface for higher flow rates (B). In general the phenomena described in the previous simulation experiments performed on non-adsorbed solutes also occur during leaching of adsorbed solutes but the relative importance of their influence is reduced.

B. FIELD LEACHING EXPERIMENTS

Radioactive labelled solutes were applied to the Ap and Bt horizons on Nov. 26 and Dec. 6, 1981, as described in Chapter II (Methods and Materials). Sites were sampled on May 7 to 12, 1982, approximately 10 to 15 days after the snow pack had completely melted. During the first three days of sampling a frozen layer was encountered at 75 to 85 cm. Sampling on May 11 and 12 did not encounter frost. Samples were segmented into 2.5 cm layers from 0 to 75 cm depth and five cm layers from 75 to 100 cm depth.

(Distribution of tracer for experiments discussed in this section is reported as activity per layer over the total activity added, (A/A_0) and is also tabulated in Appendix A.)

Experiment 1: Leaching of Non-reactive Solute (^{3}HOH)

a. ^{3}HOH applied to Ap horizon

Only one site at which ^{3}HOH was applied to the upper layer of the Ap horizon yielded measureable activity

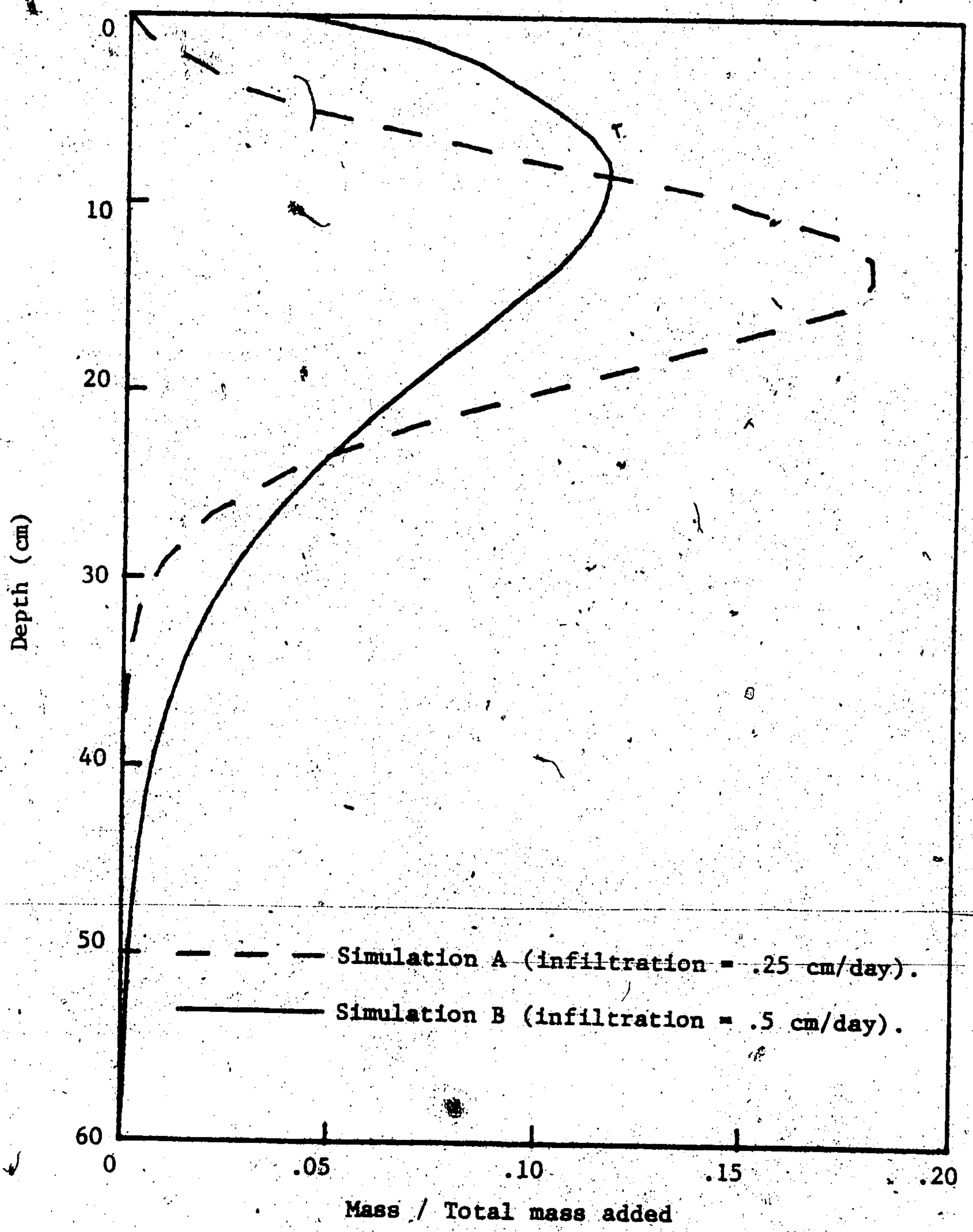

Figure III.10. Simulation experiment 5b: Influence of infiltration rates on distribution of adsorbed solute (Kads = 1.0 ml/g) added to the surface layer (0- 2.5 cm) of a structured soil after simulated leaching by 20 cm of water.

(greater than 100 total counts over background) when sampled in the spring (figure III.11). Tritium could have been lost by evaporation and subsurface lateral flow through the soil. Evaporation occurred early in the winter and late in spring. The plot area was bare of snow for short periods at both these times. The site which retained measureable tritium activities was covered in a snow drift until after Apr. 26, 1982 and so was less subject to evaporative losses than the other sites.

The plots were located on a slope of 2% to 5% (Crown and Greenlee, 1978) and this may have caused subsurface lateral flow, especially when infiltrating water encountered an impermeable frozen layer present during most of the period of this experiment. (Heating duct which marked the location of tracer application did not extend below the level of tracer application and, therefore, did not restrict subsurface lateral flow.)

Tritiated water applied to the soil surface at this site penetrated to a depth of 25 cm. Two tritium peak activities occur in figure III.11: one at the surface layer (0 to 2.5 cm) and one at ten to 12.5 cm. The primary peak at the surface may reflect assimilation of tritium by soil biomass during several days that the tracer-soil mixtures were stored at room temperature before they were applied in the field. Tritium in ^{3}HOH readily exchanges with hydrogen in biological tissue and assimilated tritium would be immobilized against both leaching and evaporation.

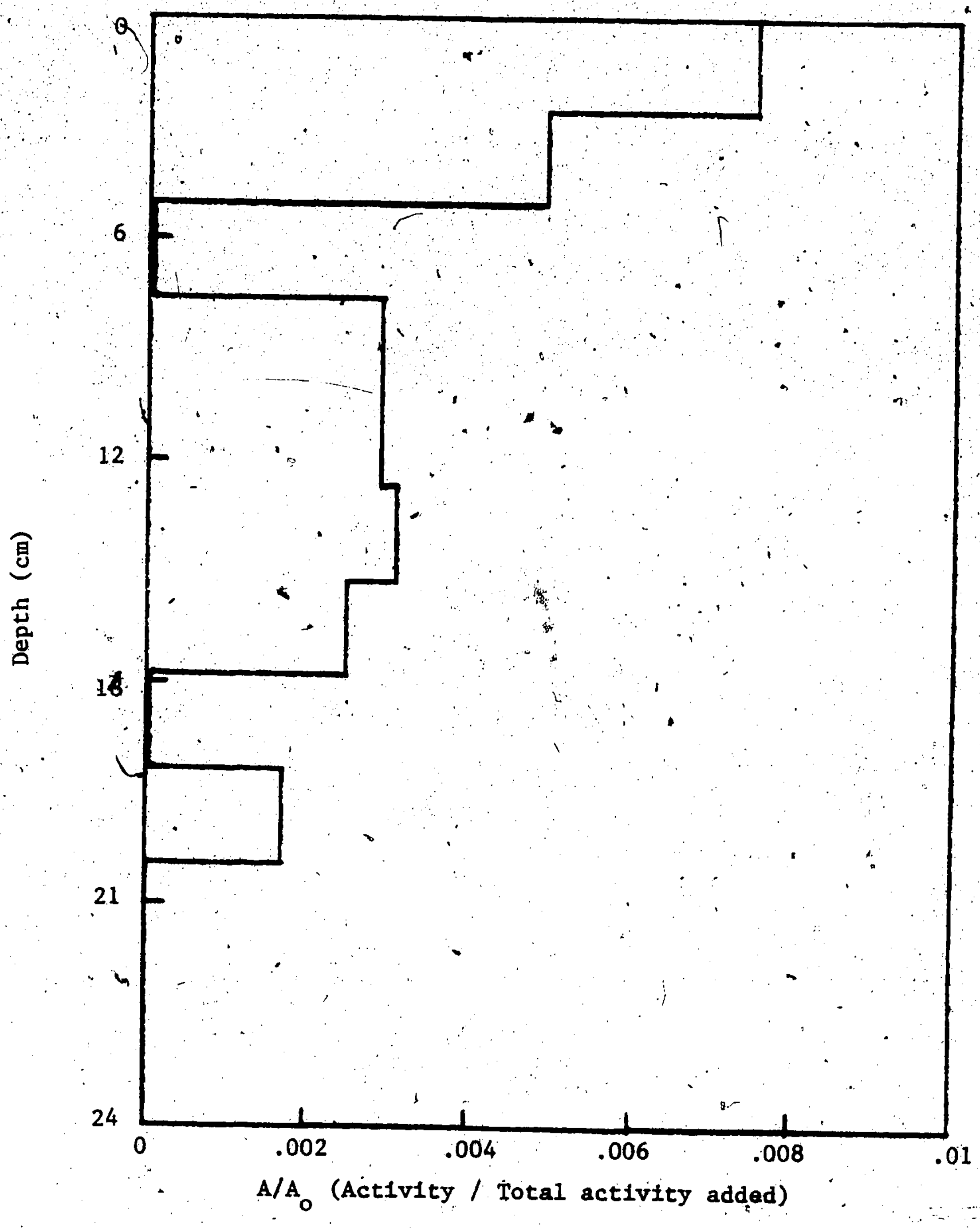

Figure III.11. Tritium activity distribution observed in May, 1982, after ^{3}HOH was applied to the Ap horizon (0 - 2.5 cm) in Dec., 1981, for the one site where tritium activities were detected.

Assimilation of less than 1% of total added tritium activity, or 4 pCi/g soil, would account for all of the activity detected in the surface layer.

b. ^{3}HOH added to Bt horizon

Tritium activity distribution for ^{3}HOH applied to the top of the Bt horizon is summarized as the profile of the mean activities at each layer sampled (figure III.12). The Bt horizon was encountered at different depths and so the ^{3}HOH was applied at different depths. Depths for this plot are therefore expressed as distances from the original placement (0 cm). Distances above this level are expressed as negative values, distances below as positive values.

Data shown are the means of ten sites, except at 0 cm and 2.5 cm where presence of high ^{14}C activities in the same samples made determination of tritium activity impossible. Tritium activities reported for these two levels are the means of four samples.

The peak of the mean ^{3}H activites vs depth plot occurs at 7.5 cm below the level of application. Measureable tritium activity was found at 28 cm below, and at 15 cm above, the level of application. The lower part of the curve shows the typical bell shape also seen in the simulations presented in section A. The amount of tritium activity present in the upper region of the curve did not appear in any simulations. Upward movement of solute could be a result of evaporation or diffusion.

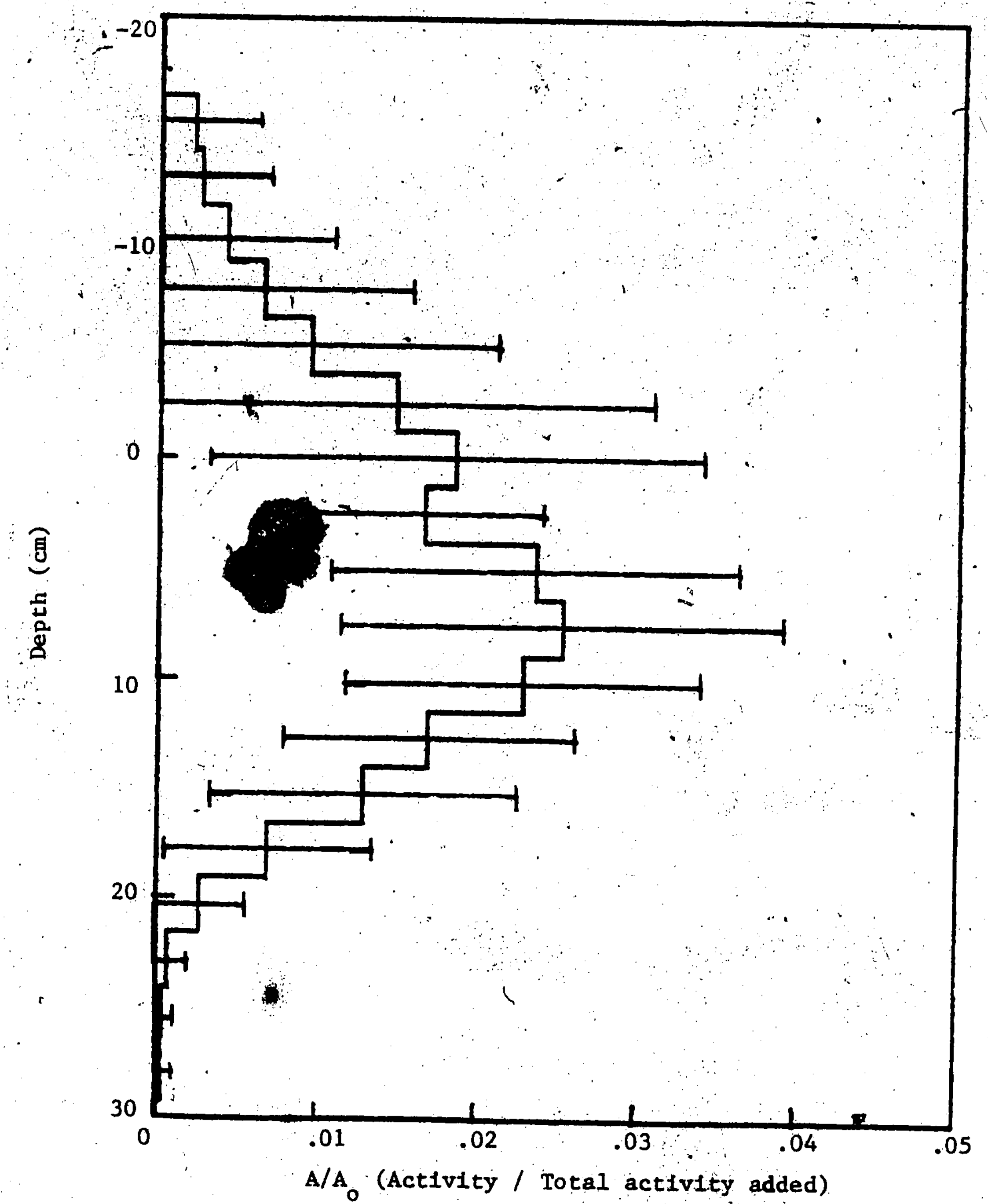

Figure III.12. Mean tritium activity distribution observed in May, 1982, after ^{3}HOH was applied to the upper surface of the Bt horizon in Dec. 1981. Depth coordinate given as distance above (negative values) or below (positive values) level of application. Standard deviations shown.

Measurement of the soil moisture profile by γ-densitometry detected 2.7 cm ~~of~~ water loss by evaporation, between Apr. 26 and May 15, after sampling was completed. Successive θ profiles on Apr. 29 and May 3 showed water depletion to a depth of 45 cm (figure III.13). The upward displacement of ^{3}HOH indicated by figure III.12 could have been caused by water being drawn up through capillaries in response to a soil moisture potential gradient induced by evaporation from the soil surface.

Extra diffusional mixing may have occurred in a zone of high moisture content perched above a frozen layer. Measurement of the θ profile detected a zone of high moisture content which showed up as a bulge in the difference between successive θ profiles. Physical probing of ~~the soil~~ showed that this bulge often coincided with the depth of thawed soil. Gillies (Gray *et al.*, 1970) observed a distinct upper saturated zone of thawed soil above a frozen zone during infiltration of snow meltwater.

A frozen layer was present for nearly the entire period of the experiments. Diffusion of solute in the zone of high moisture content above this layer would be mainly upward because of the ice barrier below. Shearer *et al.* (1973) stated that diffusion rates were approximately proportional to $\theta^{10/3}$. This relationship implies that diffusion would be greatly enhanced in this zone.

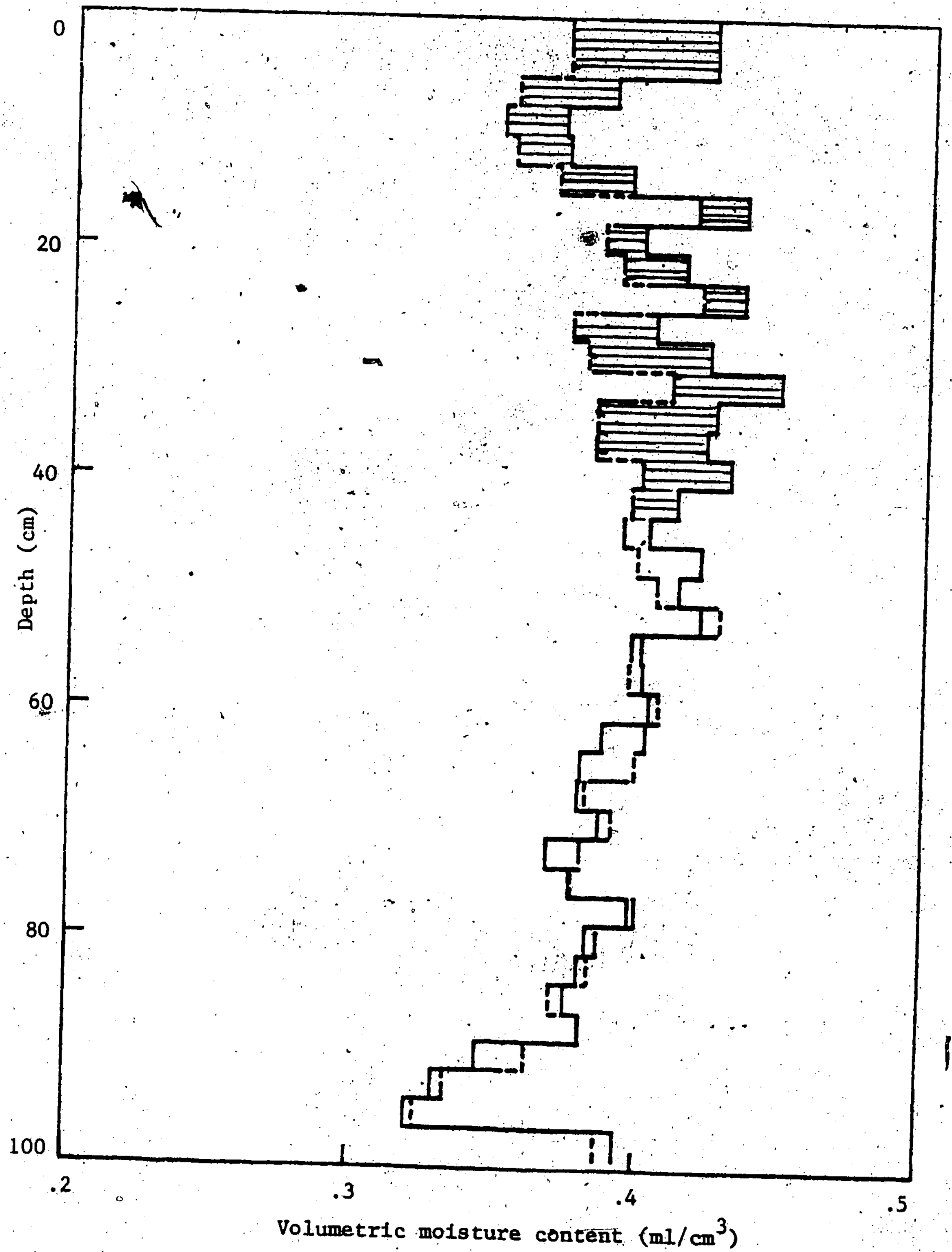

Figure III.13. Determination of evaporation by integration between successive θ profiles on Apr. 29 (——) and May 3 (— — — —), 1982. Cross hatched area is proportional to net evaporation.

Experiment 2: Leaching of Adsorbed Solute (^{14}C-lindane)

Adsorption isotherms were determined for lindane adsorbed to Breton loam Ap and Bt horizon soil (figure III.14). Points plotted show the results of two separate experiments in both cases. Linear isotherms describe the data with a high degree of correlation, as determined by regression analysis ($r^2 = 0.995$ for Ap isotherm; $r^2 = 0.92$ for Bt isotherm). A slight downward concavity is evident in the isotherms and fitting the data to a non-linear Freundlich iostherm ($q = Kads \cdot c^{1/n}$) improved the fit marginally ($r^2 = 0.9995$ for Ap isotherm; $r^2 = 0.992$ for Bt isotherm).

The Kads for lindane adsorbed to Breton Loam Ap and Bt horizon samples were determined to be 12.6 and 5.1 ml/g, respectively, from linear isotherms. These values represent strong and moderate adsorption interactions. Kay and Elrick (1967) determined Kads for lindane adsorbed to soil with higher organic content than Breton loam to be between 17 and 23 ml/g.

a. ^{14}C-lindane applied to Ap horizon

For lindane applied to the surface of the Ap horizon 98.0% of measured activity was found in the zone of application (figure III.15). The observed distribution shows low mobility of adsorbed solute and serves to emphasize the influence of adsorption on solute leaching. The data presented bears strong resemblance to the simulation represented by figure III.9D, for movement of strongly

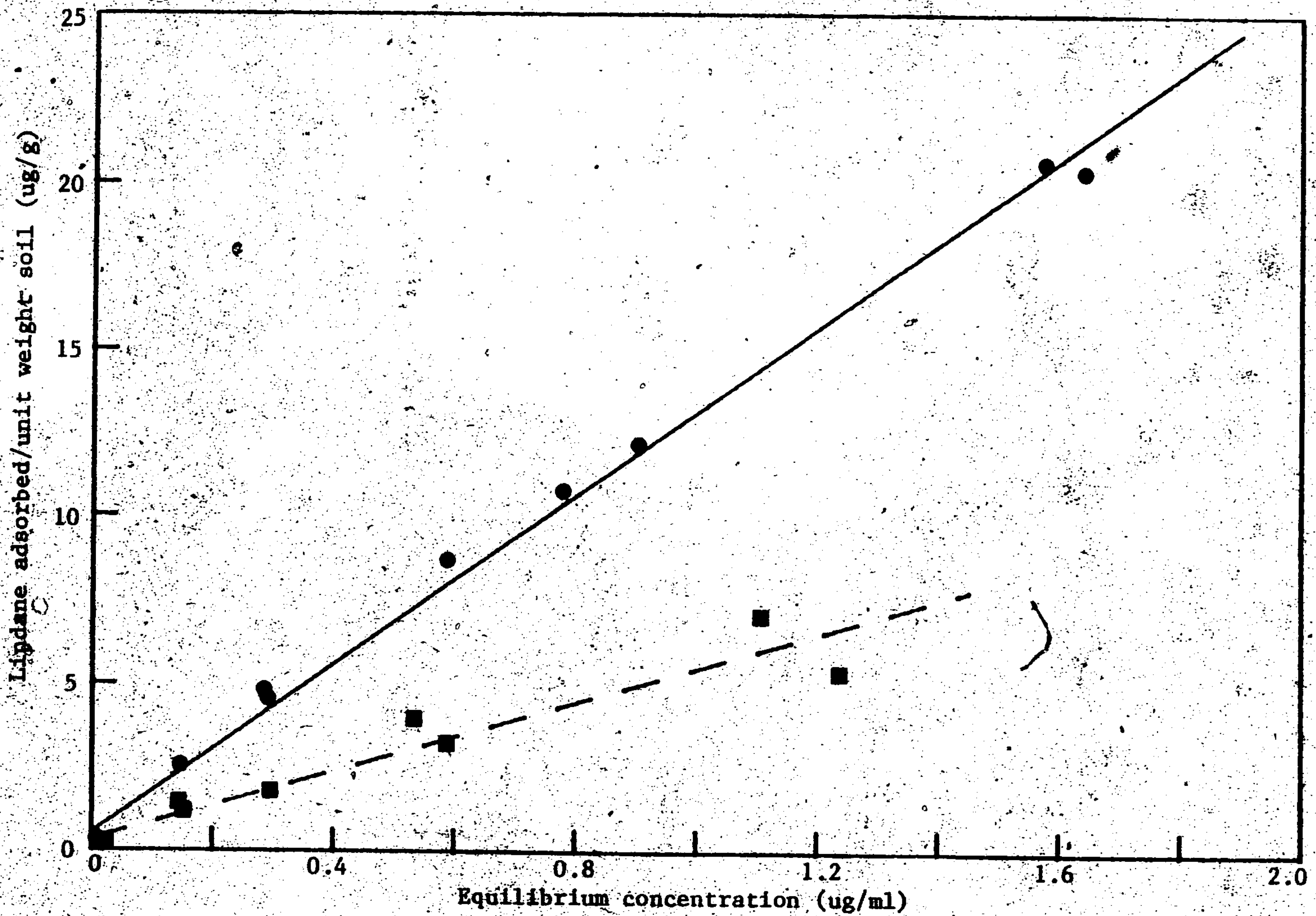

Figure III.14. Lindane isotherms. Lindane adsorbed to Breton Loam Ap Horizon soil (● —— ●) and Bt horizon soil (■ — — ■).

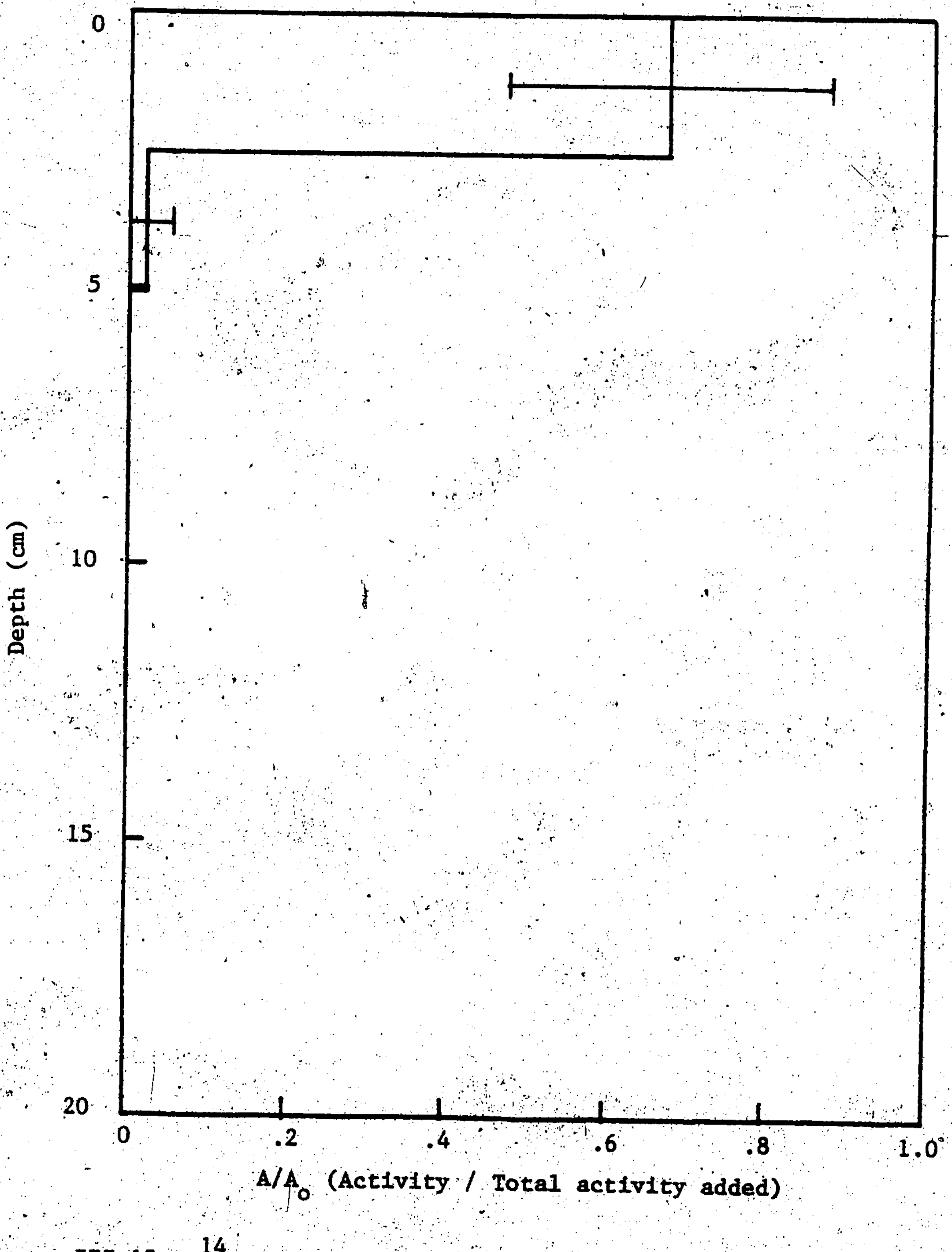

Figure III.15. ^{14}C activity distribution observed in May, 1982, after ^{14}C-lindane was applied to the Ap horizon (0 - 2.5 cm) in Dec., 1981. Standard deviations shown.

adsorbed solute.

69% of ^{14}C-lindane activity applied at the upper surface of the Ap horizon was accounted for by sample activities determined from the efficiency versus SCR curve. It was shown in chapter II that the activities calculated from the efficiency curve underestimated the tracer activity when counts were made in the soil sample-scintillation cocktail mixture. Volatilization would also account for some loss of activity (Kay and Elrick, 1967; Shearer *et al.*, 1973). The relative contribution of each factor can be assessed by comparison with activities calculated for lindane added to the Bt horizon, which was covered in 15 to 22 of moist soil, and would have suffered no volatilization losses. In the latter case 79% of the activity originally added was measured using the direct counting method. The difference between activities accounted for in the Ap and Bt horizons, 10%, suggest some volatilization losses from the surface layer.

b. ^{14}C-lindane applied to Bt horizon

The peak of mean activities of ^{14}C-lindane added to the Bt horizon was also found at the original level of placement (figure III.16). Activity was detected five cm below and two cm above the level of placement. Amounts of ^{14}C activity found below the level of placement may reflect problems in resolving the samples, which makes quantitative interpretation of these data difficult. The high apparent activity observed at 1.3 to 3.8 cm may have resulted from

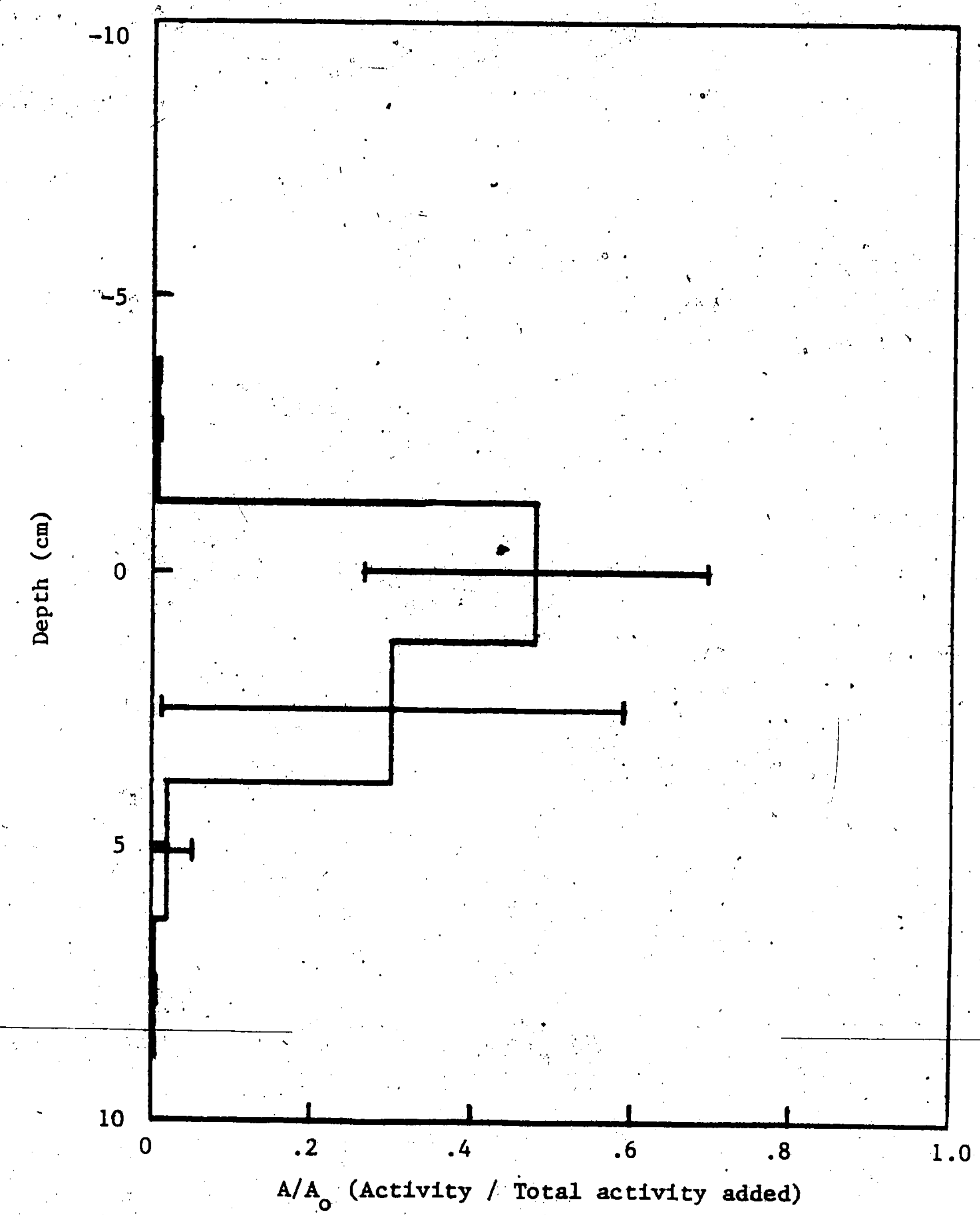

Figure III.16. ^{14}C activity distribution observed in May, 1982, after ^{14}C-lindane was applied to the upper surface of the Bt horizon in Dec. 1981. Standard deviations shown. Depth coordinate given as distance above (negative values) or below (positive values) level of application.

from splitting of the layer of placement into two samples. Nevertheless, it can be concluded from these observations that lindane did not move appreciably in the Bt horizon.

C. SIMULATION OF FIELD EXPERIMENTS

A comparison between the simulation experiments and the field experiments is made in this section. Although the model was based on theoretical principles, it was built with the conditions of the field experiments specifically in mind. Therefore the set of observed experimental conditions does not provide a completely independent objective test of this model.

The test being made is whether the model simulates the effects of this set of conditions on solute transport. The comparison may indicate,what structural modifications to the model are required and what further experiments are necessary, initially to provide information on how to adjust the model, and ultimately, to validate the model.

To test whether the model will simulate the system it was intended to describe, it is necessary to use the same set of physical conditions as occurred in the field experiments. These conditions are discussed in the following subsections.

1: Physical Properties Controlling Simulation Experiments

a. Bulk density.

Dry bulk densities (table III.9) were calculated from wet bulk densities (determined from γ-densitometry) and gravimetric moisture determinations, at 2.5 cm increments, as described in Chapter II.

b. Porosity

Porosities of Ap, Bt, and BC horizons were determined separately because of the structural and textural variation that occurs among them. Porosities, determined from pycnometer determinations of Dp and γ-densitometer determinations of Db, were inconsistent with the moisture retention curve at many layers where α was calculated to be less than θ at five kPa. Rawitz *et al*. (1982) reported errors in γ-densitometry resulting from use of the manufacturer's standards to construct a calibration curve. This is due to inaccuracy introduced by the assumptions that γ absorption in soil can be defined by a universal average attenuation coefficient and that no backscattered radiation was measured by the detector. They reported serious overestimations of Db using the the same model two-probe density gauge as was used in this study.

Overestimation of Db would result in underestimation of α when the equation $\alpha = 1 - Db/Dp$ is used. Using an average Dp value to calculate α within each horizon could also introduce error into calculations of α. Values of α which were calculated to be less than θ at five kPa are marked with an (*) in table III.9.

Table III.9. Physical properties of Breton Loam.

DEPTH cm	Db g/cm^3	Dp g/cm^3	α
0-2.5	1.33	2.59	0.486
2.5-5.1	1.43	2.59	0.445
5.1-7.6	1.50	2.59	*.421
7.6-10.2	1.53	2.59	*.409
10.2-12.7	1.52	2.59	*.412
12.7-15.2	1.50	2.59	*.422
15.2-17.8	1.53	2.59	*.410
17.8-20.3	1.50	2.63	*.437
20.3-22.9	1.46	2.63	*.443
22.9-25.4	1.44	2.63	0.454
25.4-27.9	1.42	2.63	0.457
27.9-30.5	1.42	2.63	0.459
30.5-33.0	1.44	2.63	0.453
33.0-35.6	1.48	2.63	*.435
35.6-38.1	1.47	2.63	*.440
38.1-40.6	1.50	2.63	*.427
40.6-43.2	1.52	2.63	*.422
43.2-45.7	1.56	2.63	*.406
45.7-48.3	1.57	2.63	*.401
48.3-50.8	1.59	2.63	*.394
50.8-53.3	1.66	2.63	*.370
53.3-55.9	1.65	2.63	*.372
55.9-58.4	1.62	2.63	*.382
58.4-61.0	1.61	2.63	*.386
61.0-63.5	1.63	2.64	*.382
63.5-66.0	1.62	2.64	*.385
66.0-68.6	1.62	2.64	*.384
68.6-71.1	1.62	2.64	*.386
71.1-73.7	1.62	2.64	*.381
73.7-76.2	1.59	2.64	*.397
76.2-78.7	1.58	2.64	*.397
78.7-81.3	1.59	2.64	*.398
81.3-83.8	1.61	2.64	*.388
83.8-86.4	1.62	2.64	*.385
86.4-88.9	1.62	2.64	*.387
88.9-91.4	1.59	2.64	*.397
91.4-94.0	1.61	2.64	*.388
94.0-96.5	1.64	2.64	*.379
96.5-99.1	1.63	2.64	*.380
99.1-102.	1.63	2.64	*.381

To account for this discrepancy in the simulation of field experiments WGRAV was considered to be no less than .072 cm/layer (.028 X bulk volume) in the Bt horizon and no less than .052 cm/layer (.020 X bulk volume) in the BC horizon. These values were estimated from the moisture retention curve (figure III.17) as the difference between θ at 0 kPa and θ at 33 kPa tensions.

c. Soil moisture retention curve

Stagnant and mobile water pools were divided on the basis of soil moisture tension curves as discussed in Section III.A. Moisture retention curves (figure III.17) were determined for Ap, Bt, and BC horizons. Gravimetric values were converted to volumetric by multiplying by the bulk densities given in table III.9.

The stagnant water pool, WR, and the mobile pool capacity, WMCAP, used in the simulation model, are heights of water (mm) corresponding to θ values listed in table III.10. WR was determined as the product of θ at either 200 kPa or 500 kPa, and the layer thickness. WMCAP was determined as θ at 33 kPa moisture tension times layer thickness, less WR.

Table III.10.
Volumetric moisture contents used to determine WR and WMCAP.

HORIZON	DEPTH (cm)	θ at soil tension of:		
		33 kPa	200 kPa	500 kPa
Ap	0 - 18	0.366	0.290	0.237
Bt	18 - 60	0.418	0.371	0.332
BC	60	0.384	0.331	0.295

d. Infiltration

Initial conditions for the simulations of field experiments were based on θ profiles measured on Mar. 9, Mar. 20, and Mar.25. Net infiltration occurred from Mar.20 to Apr. 26, while net evaporation occcurred from Apr. 26 until the end of the experiment (table III.11).

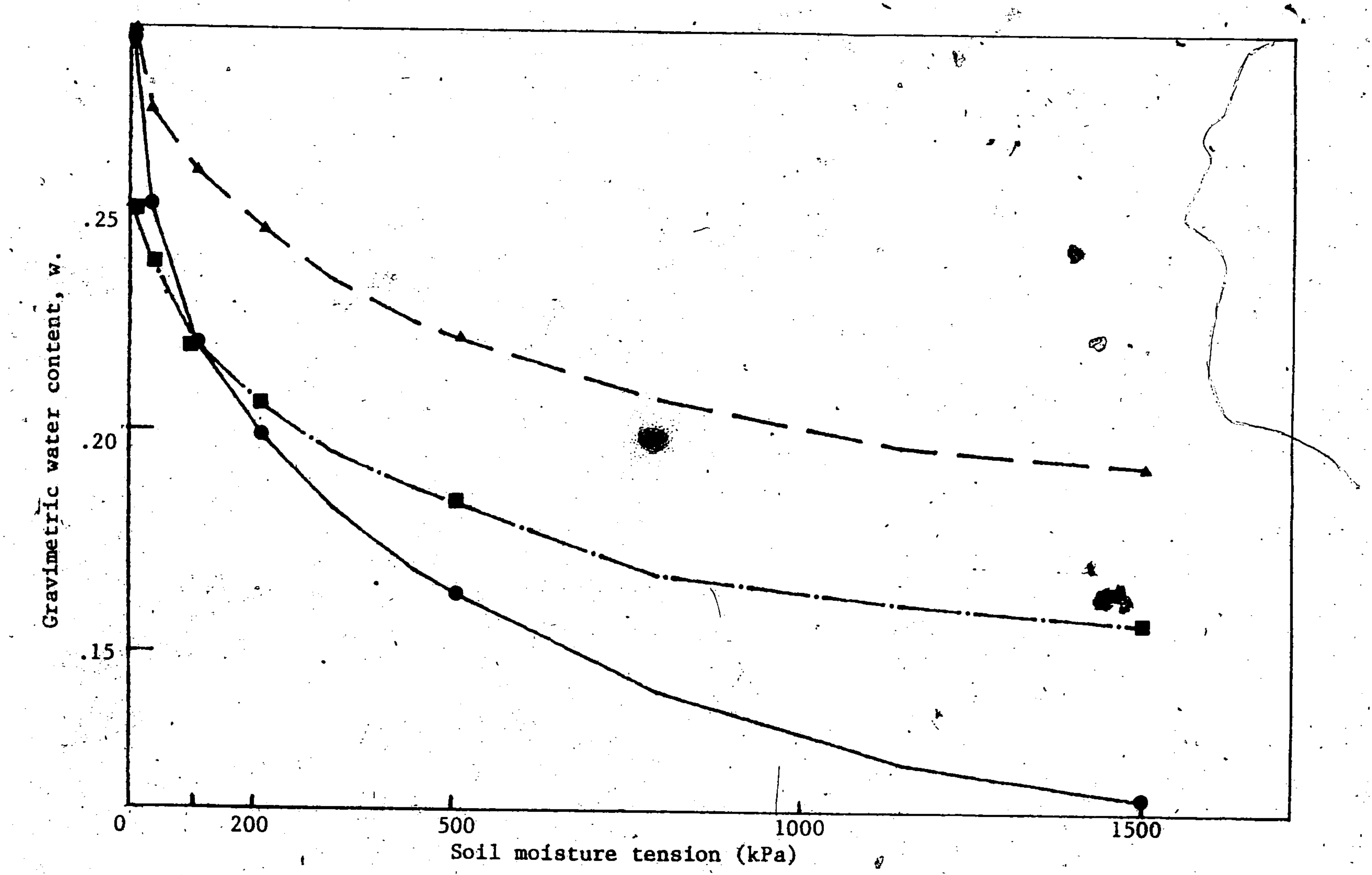

Figure III.17. Soil moisture retention curve, Breton Loam: Ap horizon (● —— ●); Bt horizon (▲ — — ▲); and BC horizon (■ —·— ■).

Table III.11. Infiltration measured at experimental plots.

Measurement period	Total change in water content (mm)	Average daily infiltration (mm/day)	Average daily evaporation (mm/day)
Mar.9 - 20	0.00	-	-
Mar.20 - 25	(+)2.05	0.41	-
Mar.25-Apr.17	(+)11.7	0.51	-
Apr.17 - 20	(+)7.50	2.5	-
Apr.20 - 23	(+)9.6	3.2	-
Apr.23 - 26	(+)9.2	3.07	-
Apr.26 - 29	(-)0.72	-	0.24
Apr.29-May 3	(-)12.4	-	3.1
May 3 - 15	(-)16.7	-	1.39

The sensitivity of the model to the resolution of infiltration data was discussed in section III.A. During the period of most intense infiltration, from Apr. 17 to Apr. 26, θ profiles were measured every three days. The relative daily rates of infiltration were determined by plotting the daily rates averaged over the period of each measurement, drawing a smooth curve through the points and interpolating as shown in figure III.5.

Runoff occurred under the snowpack at the γ-densitometer access tubes. No runoff occurred at the points of application of the tracers because these sites were contained by heating duct extending above the soil surface. Infiltration where the tracers were applied was therefore greater than where infiltration was measured. To account for the difference the daily infiltration rates as determined by γ-densitometry were increased by the factor of the volume of water determined by the Mar. 25 snow survey divided by the total volume of infiltrating water measured at the access tubes.

Snow drifts along the east side of the plot area covered some sites until Apr. 29. As much as two times as much water was held in these drifts as occurred on the west side of the plots. The soil under this snow also thawed more slowly. The γ-densitometer access tubes on the east side of the plots were kinked during installation and so the data necessary to describe leaching here were lacking. Therefore only results obtained for the experiments on the west side of the plots, where a complete set of simulation input variables was available, were compared with the results of simulations.

e. Frozen layers

The depth of thawing was determined by physical probing. However this method did not indicate the maximum depth of thaw, which fluctuated diurnally. The depth to frost measured by probing did, however, coincide approximately with the bulges observed in the differences between successive θ profiles. Gillies (Gray *et al*., 1970) observed that during infiltration of Prairie snowpack two distinct layers developed: an saturated thawed layer overlying an unsaturated frozen layer. The bulges between successive θ profiles was used to approximate the maximum depth of daily thaw in simulations of field experiments.

2. Comparison of Simulations and Field Observations

Simulations were performed which paralleled the field experiments described in Section III.B using the measured and derived parameters and variables described above. Data files for two of the simulation runs (1.b, ^{3}HOH applied to the Bt horizon; and 2.a, ^{14}C-lindane applied to the Ap horizon) are given in Appendix E, along with the final output generated by running these files in the simulation program. The FORTRAN program which implements the simulation model is also printed in Appendix F, with instructions for use in Appendix D.

Observed data used for comparison are expressed as A/A_t, where A is the activity in each layer and A_t is the total activity detected in the soil column. The simulation model is concerned only with vertical transport of solute and relative activities are a truer measure of vertical displacement than absolute activities which reflect both vertical and lateral displacements.

This convention has the additional advantage of correcting for the error introduced by counting activities directly in the soil sample (as described in chapter II). Accountability experiments showed that measured activities were proportional to known activities for standard soil samples (figures II.2 and II.3). Therefore:

$A/A_t = A^*/A_0$,

where A = measured activity in sample,

A_t = total measured activity in soil column,

A^* = actual activity in sample,

A_0 = total actual activity added to soil column.

The data are reported as mean A/A_t values for each layer in the graphs which follow and in the corresponding tables in Appendix C, except for figure III.18, for which only one set of data was obtained.

Test of Fitness

The agreement between observed and simulated data is assessed by regression analysis. The fitness test is whether the regressions of observed on predicted data have intercepts which are close to zero and slopes close to unity (Hillel, 1977). The regression correlation coefficients (r^2) give an indication of the variation in the data from the regression line. Regression analyses were performed on a point-by-point basis, using all samples with measureable activity (100 total counts over background) and all predicted activity greater than 0.1% of A_t.

Experiment 1: Leaching of a non-reactive solute (^{3}HOH)

a. ^{3}HOH applied to Ap horizon

Less than 0.3% of the tritiated water added to the soil surface in November and December, 1981, was accounted for in the samples taken. Simulation of the experimental system with spring evaporation only did not predict this loss. Though drying of the soil surface was observed in early December, no evaporation data were collected at this time. Early winter evaporation was simulated and a better

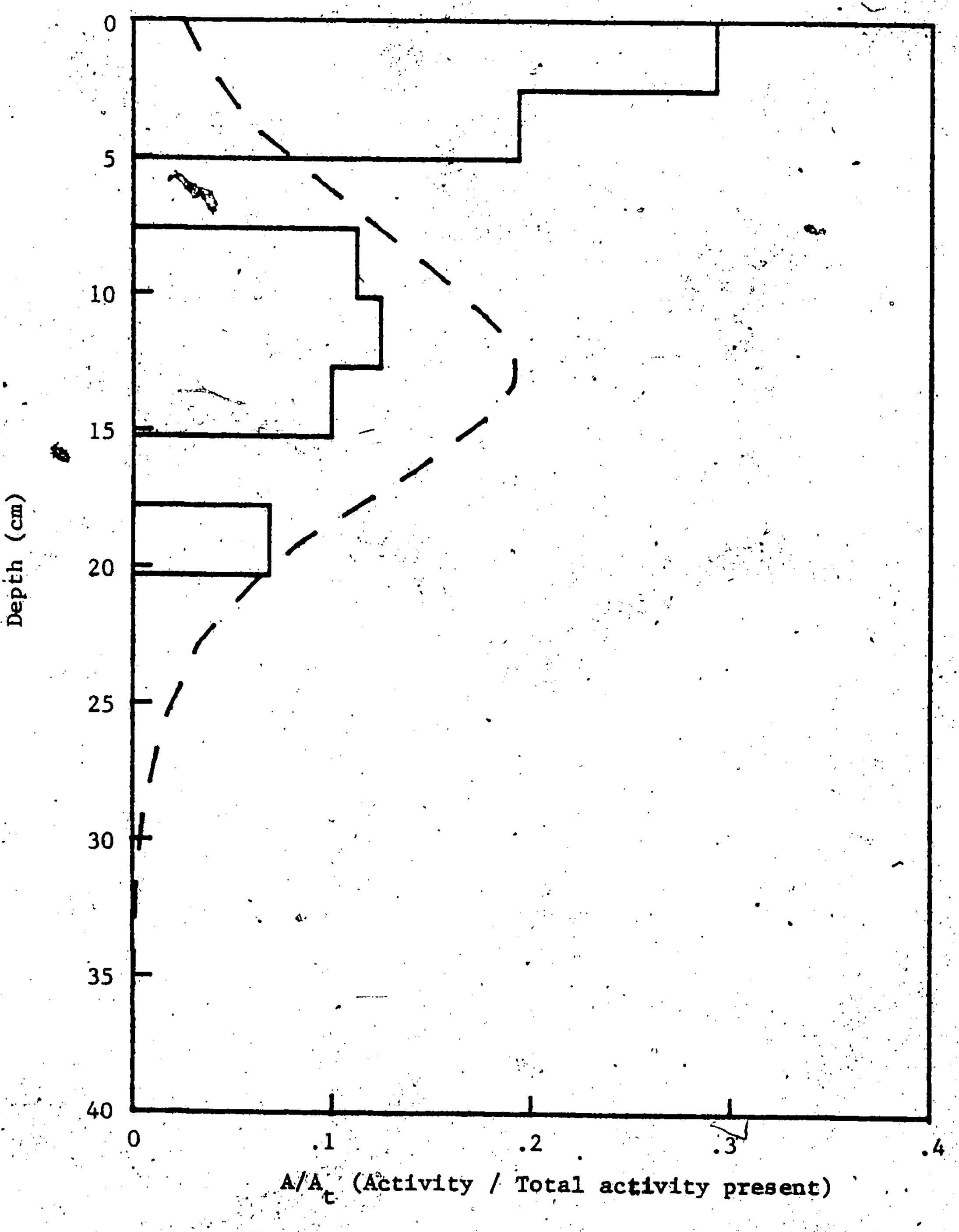

Figure III.18. Observed (——) and predicted (— —) spring tritium activity distribution for ^{3}HOH applied to Ap horizon (0 - 2.5 cm) in the fall, for the one site where activities were detected.

prediction was obtained, though evaporation data for this simulation was speculative. Simulating daily evaporation of 0.1 cm over ten days in December predicted that 76% of the tritium activity would be lost before infiltration began in the spring.

Two activity peaks occur in the observed tritium activity distribution (stepwise plot, figure III.18). The lower peak is approximately predicted by the simulation (smooth curve). The depth of penetration was also reasonably predicted by the simulation. The possibility that the upper peak was caused by microbial assimilation was discussed in the previous section. If this peak activity is disregarded then a much better fit between observed and simulated solute distribution is seen. Regression of observed distribution on predicted is given below.

Including upper peak:

$$Obs = .047 + .17*P, \; r^2 = .04.$$

Excluding upper peak:

$$Obs = -.015 + .59*P, \; r^2 = .62.$$

b. ^{3}HOH applied to Bt horizon

Three different conditions were simulated for comparison with observed distribution of tritium activity for ^{3}HOH added to the Bt horizon: A) using 200 kPa soil moisture tension to assign WR and WMCAP; B) using 500 kPa tension to assign WR and WMCAP; C) disregarding the effects of a frozen layer. One set of the data used in simulation A, along with the output generated, is given in Appendix D. For

B) WR and WMCAP were changed from the values used in A according to θ values given in table III.10. For C internal variables were identical to those used in A, but FLNR was set at zero at all time steps. All three simulations were subject to the same infiltration inputs.

The results of the simulations were compared with the results of the field experiments performed on the west half of the plots (figure III.19). Observed activity distribution at one site indicated that net upward transport of solute had occurred. This data did not fit with the observations at all other sites, where net downward transport occurred. It was concluded that some mechanism other than those being modelled was operating at this site and this data was not used in the comparison with the simulation results.

Comparison of simulations A and B with field observations (figure III.19) showed a qualitative agreement in shape and position of the solute activity profiles. All three solute profiles possess a high degree of symmetry about a point seven to eight cm below the level of tracer application. Simulation A gives a better prediction of the position and value of the mean activity peak. Both A and B accurately predict the depth of solute penetration. Regression of the observed tritium activities on those predicted by the model are given below:

A (WR:WMCAP at 200 kPa tension):

$$Obs = .023 + .73*P, \ r^2 = .726.$$

B (WR:WMCAP at 500 kPa tension):

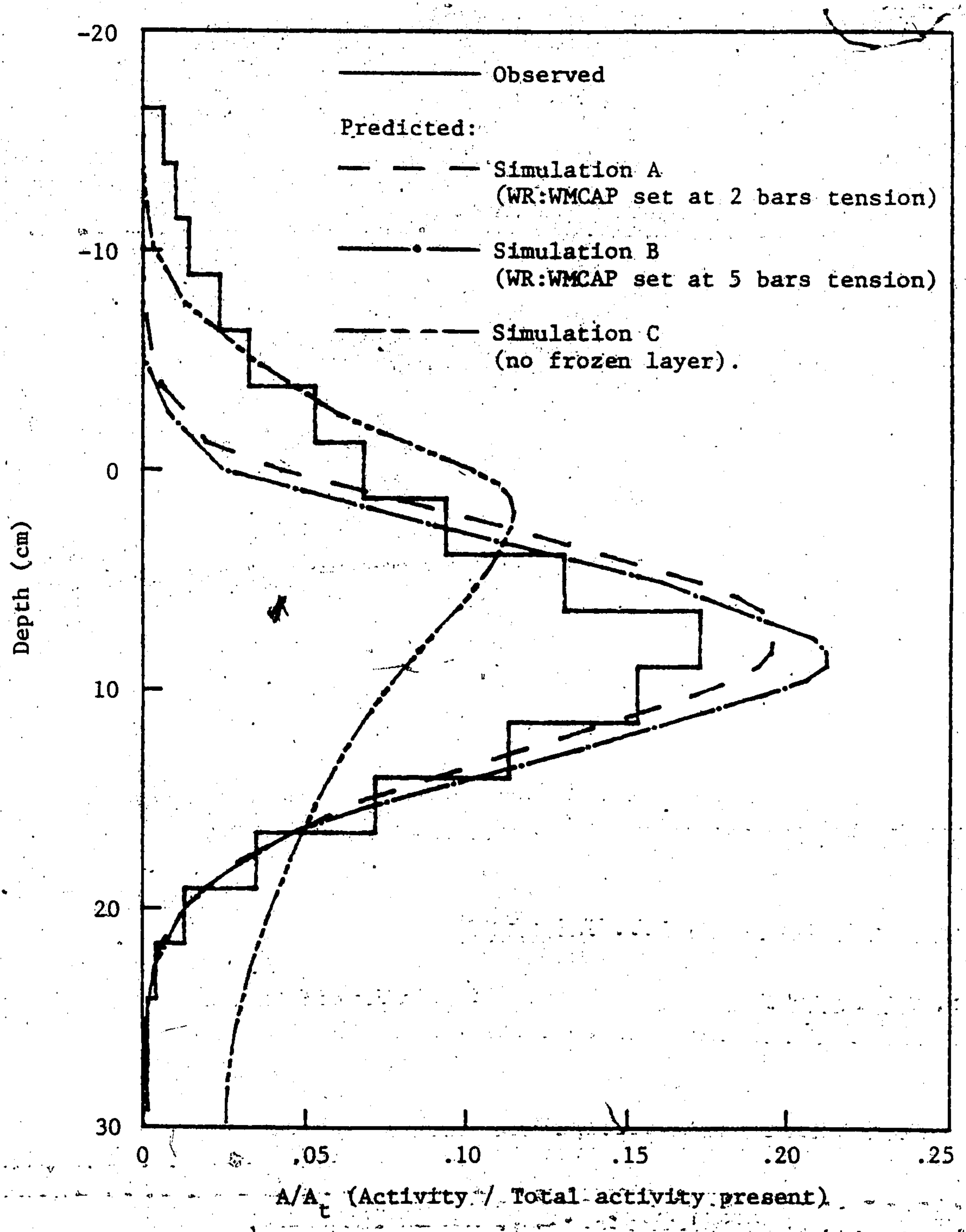

Figure III.19. Mean observed and predicted spring tritium activity distribution for ^{3}HOH applied to upper surface of Bt horizon in fall. Depth coordinate given as distance above (negative values) or below (positive values) level of application.

$$Obs = .022 + .69*P, \ r^2 = .730.$$

Both regressions have intercepts close to zero and the correlation coefficients are nearly the same. The slope of the regression line was closer to 1 for A, indicating a slightly better fit with the observed results.

Comparison of the use of 200 kPa and 500 kPa soil moisture tensions to assign the sizes of the mobile and stagnant pools was inconclusive, mainly because of the influence of the frozen layer discussed below. The 200 kPa value produced a marginally better fit with the observed data and is used for simulations of transport of the adsorbed solute.

Neither simulation A nor B predicted the presence of solute more than five cm above the zone of application, but 5.5% of the activity detected in the soil was found above this depth. The possible causes of the upward displacement are diffusion, evaporation and thermal gradients.

Mixing in the model is achieved by layer thickness and occurs only when there is movement of the soil solution. Total spreading effects were shown in section III.A to be relatively insensitive to layer thicknesses between 1.3 and ten cm so that increasing Δz up to ten cm would not cause a large increase in mixing (see figure III.7). Changing Δz to effect greater diffusional mixing would also spread out the concentration profile at the advancing front where a reasonably good fit is already achieved. To model diffusion more accurately, for both moving and stationary solution, the model would have to incorporate a specific rate law describing diffusion (Fick's law), along with some means to increase diffusivity (D) when moisture content is high, such as the approximation formula presented by Shearer *et al.* (1973) given in the literature review.

The moisture potential gradient produced by evaporation was not measured but large evaporative losses of water were observed in θ profiles. Temperature gradients which occurred in early winter would have been small (soil water temperatures generally vary between 0°C and 5°C at this time). During spring thaw temperature gradients are opposite in sign and would result in downward moisture flux.

No changes should be made to the model to account for the effects of diffusion or evaporation until experiments to isolate their influences have been conducted.

The symmetry of these solute profiles emphasizes the influence of the frozen layer on solute transport. The simulated effects of structure, namely an upwardly skewed solute profile (simulation C), are not evident in the simulated nor in the observed results for the partially frozen structured soil system. The frozen layer acts as a control on infiltration rates causing more complete equilibration of solution between mobile and stagnant pools, and producing the more symmetrical solute profiles seen in A and B.

Comparison of A and C, which possess the same internal properties except for the frozen layer, show that it is possible for solute transport to be greater for leaching of soil-borne solutes during thawing of a partially frozen structured soil than for leaching of an unfrozen structured soil. This effect would occur because the infiltrating water is held in contact with the intra-aggregate solution by the impeding frozen layer thus picking up a greater solute load from the soil. Majka and Lavy (1977) described a similar mechanism to explain observed increased solute transport in packed columns of fine textured soil over coarse soil. They stated that in this case texture exerts a limiting influence on flow rates thereby causing increased equilibration between soil-borne adsorbed solute and solution phase.

The above comparison (A versus C) suggests another possible explanation for the observed solute distribution. During slow infiltration of meltwater clay soils are apt to swell (the Bt horizon of this soil is 33% clay). In such cases the intra-aggregate macropore volume may be sealed off by the expanding soil matrix. Hydraulic conductivity and flow rate are reduced; equilibration is more complete and the resulting activity profile is more symmetrical as shown in A. The symmetry of the observed solute distribution could result from leaching through structure or non-structured partially frozen soil. Because the effects of the frozen layer mask the effects of soil structure it is necessary to study the effects of structure in isolation before definite conclusions can be made about the the influence of structure alone on solute transport in systems with well developed Bt horizons.

Using a solution to the Darcy equation, rather than a water balance equation, to determine flux could possibly have determined the mechanism which caused the symmetrical solute concentration profile observed. This would have necessitated calculation of both saturated and unsaturated hydraulic conductivities (*K*) that vary with swelling of the soil. Because of the heterogeneity of the soil this would be difficult to accomplish in the field. Laboratory measurements could be used to measure *K* for each horizon, but are much less reliable than field measurements.

Experiment 2: Leaching of adsorbed solute (^{14}C-lindane)

a. ^{14}C-lindane added to Ap horizon

Less than 2% of ^{14}C-lindane added to the top 2.5 cm of the Ap horizon was detected as ^{14}C activity beyond this layer (figure III.20). Linear regression analysis of observed data on predicted data generated the following regression equation:

$$Obs = -.043 + 1.125*P, \; r^2 = .992.$$

Eliminating the effects of soil structure from the simulation (that is setting WR=0) predicted the observed lindane distribution almost equally as well, however ($Obs = -.052 + 1.155*P$, $r^2 = .987$). These results point out the importance of adsorption on solute transport. A moderately high adsorption coefficient (12.6 ml/g for Breton

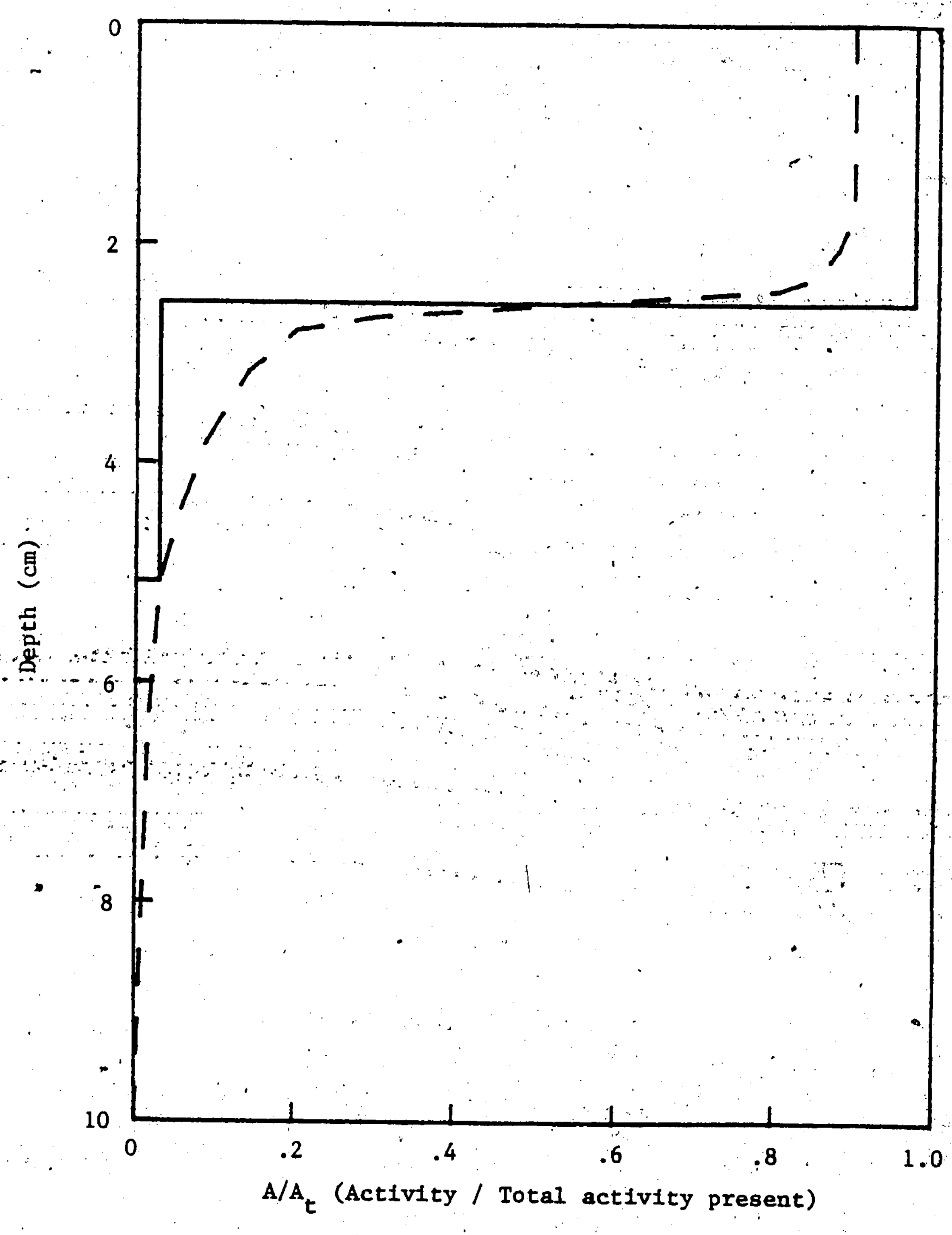

Figure III.20. Mean observed (——) and predicted (— —) spring ^{14}C activity distribution for ^{14}C-lindane applied to the Ap horizon (0 - 2.5 cm) in the fall.

Loam Ap horizon) overrides the effects of soil structure in the simulation experiment (see also figure III.9). The dominant influence of adsorption is also reflected in the observations of the field experiment.

b. ^{14}C-lindane added to Bt horizon

The data obtained from distribution of ^{14}C activity resulting from transport of labelled lindane added to the Bt horizon were less clear cut, mainly because of the difficulties in resolving the field samples. At two of the sites used for comparison with simulations the original layer of placement of lindane may have been split between 2 samples resulting in a mean distribution which may overstate the actual solute movement (stepwise solid line plot, figure III.21). The simulation (smooth curve) predicted that more than 80% of applied lindane would be found in the layer where it was placed. The uncertainty in sample resolution makes interpretation of this experiment difficult, however, it can be seen that adsorption continues to dominated the distribution of solute in the Bt horizon under the leaching conditions studied.

Beyond restating the importance of adsorption in solute transport, little need be said about the experiments with ^{14}C-labelled lindane. Simpler models predicted the observed distribution of solute as well as the structured soil-frozen layer model presented here. Experiments performed under more intense leaching condition are necessary to assess the effects of soil structure on transport of adsorbed solutes.

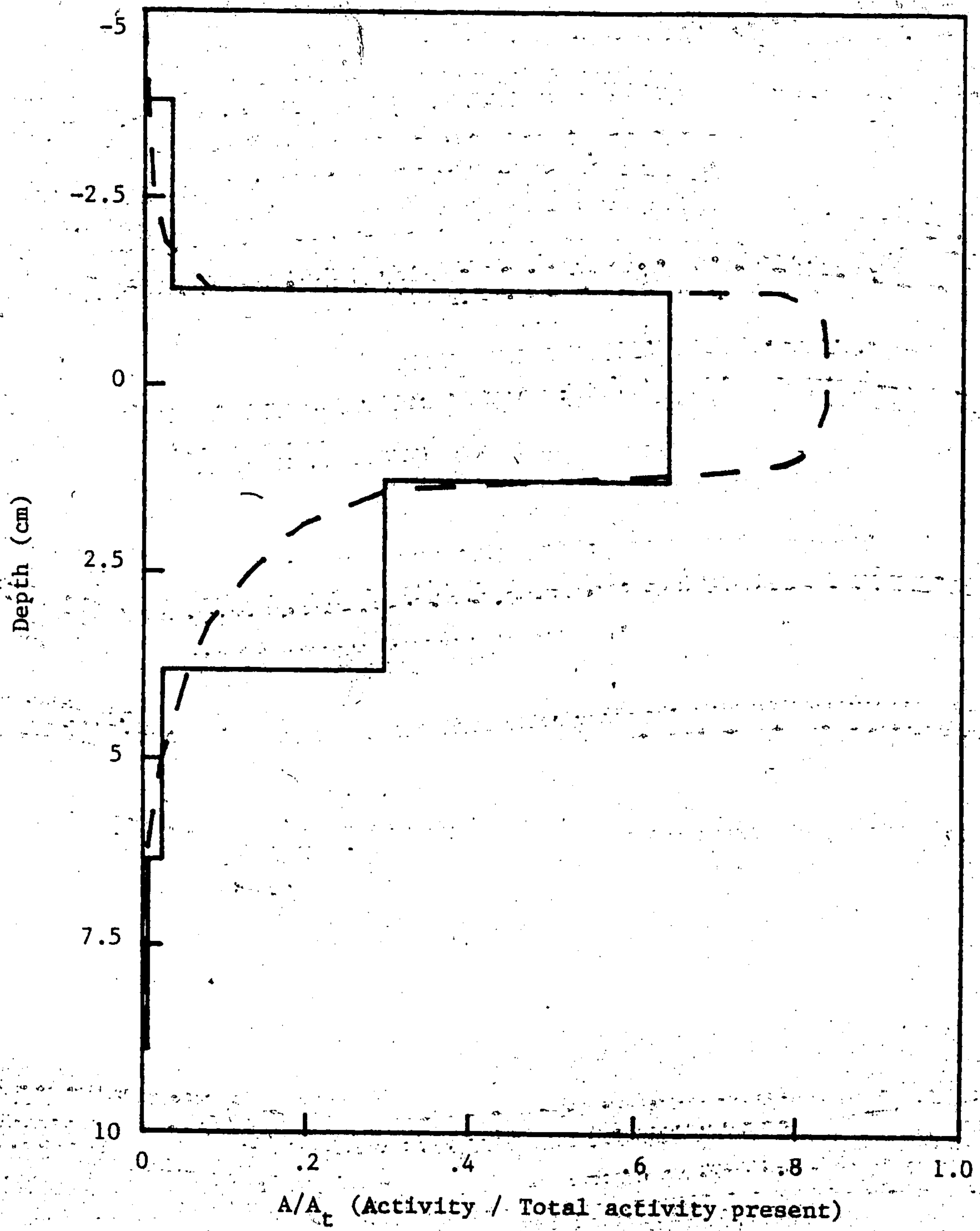

Figure III.21. Mean observed (———) and predicted (— —) spring ^{14}C activity distribution for ^{14}C-lindane applied to upper surface of Bt horizon in the fall. Depth coordinate given as distance above (negative values) or below (positive values) level of application.

Validation testing

The experiments discussed above indicate that the mechanisms modelled in ~~the~~ program require further elucidation before complete structural validation of the model is possible. Experiments designed to study each mechanism in isolation are required. Simulation experiments can prove useful in pointing out the experimental conditions which are likely to provide information necessary to test the model. That is, variation of input which causes definite differences in simulations can be used in physical experiments. The observed results of the physical experiments will then permit conclusions about the structural validity of the simulation model, or parts of it.

Once the important mechanisms have been elucidated and included in the model research should be performed in the field to test the predictive validity of the model.

IV. SUMMARY AND CONCLUSIONS

A. SUMMARY

Model Description

A finite difference simulation model based on the chromatography/continuity equation has been developed to describe solute transport through structured soil, and a 'FORTRAN' computer program written to implement the model. The program can be used to simulate transport of either adsorbed or non-reactive solutes through partially frozen or completely thawed soil.

The model characterizes a heterogeneous soil solution and pore geometry by defining two interactive solution pools: mobile and stagnant, based on the concepts presented by Addiscott (1977). At each infiltration event only the mobile solution is displaced. After each displacement a new equilibrium is established between the pools within each layer.

Transfer of solution between layers is defined by a water balance equation adapted from Burns (1974) to allow for variable water content. The water balance equation is extended to describe the influence of a frozen layer which blocks transmission of water and causes water storage above the frozen layer in excess of field capacity. A first attempt to model the effects of evaporation, based on the method used by Burns (1974), has been incorporated into the model. This method was extended to describe the mechanism of volatilization of solute from the surface layer of the soil system.

Transport of adsorbed solutes is treated by partition of solute between solution and solid phase on the basis of an effective partition coefficient determined from a linear adsorption coefficient, bulk density, and volumetric moisture content.

The computer program which implements the model is reproduced in Appendix F, along with a users' guide and sample input and output data (Appendices D and E, respectively).

Simulation Experiments

Simulation experiments were performed to assess the sensitivity of the model to the relative sizes of mobile and stagnant solution pools; infiltration rates and pattern; layer thickness; frozen layers; and adsorption of solute. It was found that the model was sensitive to adsorption coefficients, infiltration rates, and presence of a frozen layer; but not sensitive to layer thickness variation between 1.3 cm and ten cm.

Simulation of Field Experiments

Transport of tritiated water (non-reactive solute) and ^{14}C-labelled lindane (adsorbed solute) through partially frozen soil during infiltration of snow melt was studied in field experiments performed on a Gray Luvisol. Simulations of the field experiments were run using the data obtained from analysis of the soil physical and chemical properties.

Agreement between predicted and observed results were assessed by regression analysis. The simulation predicted the peak concentrations and downward extent of solute movement reasonably well for both adsorbed and non-reactive solutes. It did not predict the upward extent from the zone of application of the non-reactive solute. This lack of agreement indicates that the mechanisms of upward movement caused by evaporation and/or diffusion should be elucidated and incorporated into the model.

Future Experiments

Conclusions drawn from comparison of simulations and field observations regarding specific mechanisms controlling solute transport are tentative because of interactions between the factors involved (soil structure, frozen layer, infiltration rates, adsorption-desorption). Some of these factors produce opposite effects on solute transport; so[illegible] aggregation causes skewed solute concentration profiles while frozen soil causes symmetrical profiles. Other factors reinforce each other; adsorption and aggregation both cause holdback of solute. Experiments which study each factor in isolation are necessary to validate the treatment of each mechanism by the model and to test the validity of assumptions made in constructing the model. Simulation experiments can be used in this context to indicate the experimental conditions which would best elucidate the factor under consideration, or to "pre-search" for predictive leads (Hillel, 1977).

The assignment of values to define the sizes of the mobile and stagnant solution pools is fundamental to this and other models (Addiscott, 1977) of solute transport through structured soil. Optimization experiments using undisturbed soil columns are necessary to determine the appropriate soil moisture tension on which to base this division. The model makes the assumption that equilibrium between solution pools occurs after each infiltration event. Experiments designed to test the validity of this assumption under various moisture flow rates are also necessary.

After the factors and mechanisms influencing solute transport have been adequately defined and mathematical expressions of their effects included in the model the experimental venue should be moved back into the field to test the predictive validity of the model.

B. CONCLUSIONS

Simulation Experiments

The simulations performed support the following conclusions:

i) Solute held within soil aggregates are less subject to leaching by infiltrating water than are soil-borne solutes in non-structured soil. Solute distribution in structured soils is characterized by an assymetrical concentration profiles (upward skewness) while solute concentration profiles in non-structured soils are symmetrical about the average displacement of the solute.

ii) Adsorption plays a dominant role in controlling solute transport through soil, even when adsorptive forces are relatively weak.

iii) The rate of infiltration influences the leaching pattern which develops in structured soils to a greater degree than in non-structured soils. Intensive infiltration transports less soil-borne solute but carries a small amount to greater depths than low intensity infiltration. This is reflected in skewed solute profiles.

iv) A frozen layer influences solute transport by slowing infiltration and causing more complete equilibration between solution held within aggregates and solution moving between aggregates resulting in symmetrical solute profiles. This can cause transport of greater solute mass under some conditions of leaching in highly stuctured soil. The slow infiltration of meltwater into partially frozen ground may represent the most intensive leaching conditions encountered in some structured soils.

Field Experiments

i) Non-reactive solute:

The simulation of transport of tritiated water through partially frozen, structured soil agreed with the observed distribution of solute from the zone of solute application downward, in peak concentration position; slope; and maximum depth of penetration. Simulations did not adequately describe the solute distribution above the zone of application, indicating the mechanisms of upward solute transport of solute are not adequately defined in the model.

ii) Adsorbed Solute:

Adsorption coefficients of 12.6 and 5.1 ml/g were high enough to exert a dominant controlling influence on transport of ^{14}C-lindane through the Ap and Bt horizons, respectively, for the leaching conditions observed during infiltration of meltwater into a Gray Luvisol. Predicted and observed results both supported this conclusion with a high degree of correlation.

REFERENCES

Addiscott, T.M. 1977. A Simple model for leaching in structured soils. J. Soil Sci. 28:554-563.

Addiscott, T.M., Rose, D.A., and Bolton, J. 1978. Chloride leaching in the Rothampstead drain gauges: Influence of rainfall pattern and soil structure. J. Soil Sci. 28:305-314.

Addiscott, T.M. 1981. Leaching of nitrate in structure soils. *In* M.J. Frissel and J.A. van Veen (ed), Simulation of nitrogen behaviour of soil-plant systems. Centre Agric. Pub. and Docum., Wageningen, Netherlands.

Amoozegar-Fard, A., Nielsen, D.R., and Warrick, A.W. 1982. Soil solute concentration distributions for spatially varying pore water velocities and apparent diffusion coefficients. Soil Sci. Soc. Am. J. 46:3-9.

Blake, G.R. 1965. Particle density. *In* C.A. Black (ed), Methods of Soil Analysis, Part 1. Am. Soc. Agron. Inc., Madison, Wisc., U.S.A.

Burns, I.G. 1973. A model for predicting the redistribution of salts applied to fallow soils after excess rainfall or evaporation. J. Soil Sci. 25:165-178.

Crown, P.H., and Greenlee, G.M. 1978. Soils and land use in the Edmonton area. Guidebook tours E1, E2, and E3. Intl. Soc. Soil Sci. 11th Congress, Edmonton, Canada.

Dekkers, W.A., and Barbera, F. 1977. Effect of aggregate size on leaching of herbicide in soil columns. Weed Res. 17:315-319.

DeVault, D. 1943. The theory of chromatography. J. Am. Chem. Soc. 65:532-540.

Frissel, M.J., and Poelstra, P. 1967. Chromatographic transport through soils. I. Theoretical evaluations. Plant Soil. 26:285-302.

Frissel, M.J., Poelstra, P., and Reiniger, P. 1970. Chromatographic transport through soils. III. A simulation model for evaluation of the apparent diffusion coefficient in undisturbed soils with tritiated water. Plant Soil. 33:161-176.

Frissel, M.J., and Reiniger, P. 1974. Simulation of accumulation and leaching in soils. Centre Agric. Pub.

Docum., Wageningen, Netherlands.

Giles, C.H., MacEwan, T.H., Nakhwa, S.N., and Smith, D. 1960. Studies in adsorption. Part XI. A system of classification of solution adsorption isotherms and its use in diagnosis of adsorption mechanisms in measurement of specific surface area of solids. J. Chem. Soc., London. 1960, Pt.iv:3973-3993.

Giles, C.H. 1970. Interpretation and use of adsorption isotherms. *In* Sorption and transport processes in soils. Soc. Chem. Ind., London. Monograph No. 37.

Glueckauf, E. 1955. Theory of chromatography. 9. The "theoretical plate" concept in column separations. Trans. Farad. Soc. 51:34-44.

Gray, D.M., Norum, D.I., and Wigham, J.M. 1970. Infiltration and the physics of flow through porous media. *In* D.M. Gray (ed), Handbook on the principles of hydrology. Can. Natl. Com. Intl. Hydrol. Decade.

Green, R.E. 1974. Pesticide-clay-water interactions. *In* W.D. Guenzi (ed), Pesticides in soil and water. Soil Sci. Soc. Am. Inc., Madison, Wisc., U.S.A.

Hillel, D. 1977. Computer simulation of soil-water dynamics. Intl. Development Res. Centre, Ottawa, Canada.

Hiltbold, A.E. 1974. Persistence of pesticides in soil. *In* W.D. Guenzi (ed), Pesticides in soil and water. Soil Sci. Soc. Am. Inc., Madison, Wisc., U.S.A.

Howitt, R.W. 1981. Dynamics of a Gray Luvisol. M.Sc. Thesis, University of Alberta, Edmonton, Canada.

Johnson, M.J. 1972. Design of chromatographic procedures. *In* W.W. Umbreit, R.H. Burris, and J.F. Stauffer (ed), Manometric and biochemical techniques. Burgess Pub. Co., Minneapolis, Minn., U.S.A.

Kasten, P.R., Lapidus, L., and Amundson, N.R. 1952. Mathematics of adsorption in beds. V. Effect of intraparticle diffusion in flow systems in fixed beds. J. Phys. Chem. 56:683-688.

Kay, B.D., and Elrick, D.E. 1967. Adsorption and movement of lindane in soil. Soil Sci. 104:314-322.

Kirkham, D., and Powers, W.L. 1972. Advanced soil physics. Wiley-Interscience, New York.

Lapidus, L., and Amundson, N.R. 1952. Mathematics of adsorption in beds. VI. The effect of longitudinal diffusion in ion exchange and chromatographic columns. J. Phys. Chem. 56:984-988.

Lavy, T.L., Messersmith, C.G., and Knoche, H.W. 1972. Direct liquid scintillation radioassay of ^{14}C-labelled herbicides in soil. Weed Sci. 20:215-219.

Leistra, M. 1973. Computation models for the transport of pesticides in soil. Residue Reviews. 49:87-131.

Letey, J., and Farmer, W.J. 1974. Movement of pesticides in soil. *In* W.D. Guenzi (ed), Pesiticides in soil and water. Soil Sci. Soc. Am. Inc., Madison, Wisc., U.S.A.

Lindstrom, F.T., and Boersma, L. 1970. Theory of chemical transport with simultaneous sorption in a water saturated porous medium. Soil Sci. 110:1-9.

Magdoff, F., and Bresler, E. 1973. Evaluation of methods for reclaiming sodic soils with $CaCl_2$. *In* A. Hadas, D. Swartzendruber, P.E. Rijtema, M. Fuchs, and B. Yaron (ed), Physical aspects of soil water and salts. Spring-Verlag Pub., New York.

Majka, J.T., and Lavy, T.L. 1977. Adsorption, mobility, and degradation of cyanazine and diuron in soils. Weed Sci. 25:401-406.

Nash, R.G., and Woolson, E.A. 1967. Persistence of chlorinated hydrocarbon insecticides in soils. Sci. 157:924-927.

Nielsen, D.R., and Biggar, J.W. 1962. Miscible displacement: III. Theoretical considerations. Soil. Sci. Soc. Am. Proc. 26:216-221.

Nkedi-Kizza, P., Rao, P.S.C., Jessup, R.E., and Davidson, J.M. 1982. Ion exchange and diffusive mass transport during miscible displacement through an aggregated oxisol. Soil Sci. Soc. Am. J. 46:471-476.

Oddson, J.K., Letey, J., and Weeks, L.V. 1970. Predicted distribution of organic chemicals in solution and adsorbed as a function of position and time for various chemical and soil properties. Soil Sci. Soc. Am. Proc. 34:412-417.

Rao, P.S.C., Rolston, D.E., Jessup, R.E., and Davidson, J.M. 1980. Solute transport in aggregated porous media: theoretical and experimental evaluation. Soil Sci. Soc. Am. J. 44:1139-1146.

Rawitz, E., Etkin, H., and Hazan, A. 1982. Calibration and field testing of a two-probe gamma gauge. Soil. Sci.

Soc. Am. J. 46:461-468.

Rolland, J.P., and Frissel, M.J. 1974. Leaching of 2,6-dichlorobenzamide (BAM) in soil columns and evaluation of results by simulation. Proc. Third Intl. Cong. Pest. Chem., Helsinki. Assn. Euratom-Ital, Inst. Atomic Sci. Agric., Wageningen, Netherlands.

Scheidegger, A.E. 1974. The physics of flow through porous media. Univ. Toronto Press. Toronto, Canada.

Searle Analytic Inc. 1974. Isocap/300 liquid scintillation system operation manual. G.D. Searle & Co., Des Plaines, Ill., U.S.A.

Shearer, R.C., Letey, J., Farmer, W.J., and Klute, A. 1973. Lindane diffusion in soil. Soil Sci. Am. Proc. 37:189-193.

Skopp, J., Gardner, W.R., and Tyler, E.J. 1981. Solute movement in structured soils: two-region model with small interaction. Soil Sci. Soc. Am. J. 45:837-842.

Smiles, D.E., and Gardiner, B.N. 1982. Hydrodynamic dispersion during unsteady, unsaturated water flow in clay soil. Soil Sci. Am. J. 46:9-14.

Smith, E.M., Tayler, T.H., and Smith, S.W. 1967. Soil moisture measurement using gamma transmission techniques. Am. Soc. Agric. Eng. Trans. 10:205-208.

Soilmoisture Equipment Ltd. Operation of 5 bar pressure plate extractor. Soilmoisture Equipment Ltd., Santa Barbara, Calif., U.S.A.

Soilmoisture Equipment Ltd. Operation of 15 bar ceramic plate extractor. Soilmoisture Equipment Ltd., Santa Barbara, Calif., U.S.A.

Thoma, G., Esser, N., Sonntag, C., Weiss, W., Rudolf, J., and Leveque, P. 1978. New technique of in-situ soil-moisture sampling for environmental isotope analysis applied at Pilat sand dune near Bordeaux. HETP modelling of bomb tritium propagation in ~~the~~ unsaturated and saturated zones. *In* Isotope Hydrology. 1978. v.II. I.A.E.A., Vienna.

Thornthwaite, C.W., Mather, J.R., and Nakamura, J.K. 1960. Movement of radiostrontium in soils. Sci. 131:1015-1019.

Tinsley, I.J. 1979. Chemical concepts in pollutant behavior. Wiley-Interscience, New York.

Troxler Electronic Laboratories, Inc. 1976. Model 2376 two-probe density gauge instrument manual. Troxler Electronic Laboratories, Inc., Raleigh, N.C., U.S.A.

Tyler, D.D., and Thomas, G.W. 1981. Chloride movement in undisturbed soil columns. Soil Sci. Soc. Am. J. 45:459-461.

Van Bavel, C.H.M. 1958. Soil densitometry by gamma transmission. Soil Sci. 87:50-58.

Vose, P.B. 1980. Introduction to nuclear techniques in agronomy and plant biology. Pergamon Press, Toronto, Canada.

de Wit, C.T., and van Keulen, H. 1972. Simulation of transport processes in soils. Centre Agric. Pub. and Docum., Wageningen, Netherlands.

Zimmermann, U., Munnich, K.O., and Roether, W. 1965. Downward movement of soil moisture traced by means of hydrogen isotopes. *In* Isotope techniques in the hydrological cycle. Am. Geophys. Union, Washington.

Zweig, G., and Sherma, J. 1972. Handbook of chromatography. Vol. II. C.R.C. Press, Cleveland, Ohio, U.S.A.

APPENDIX A

List of Symbols Used in Chromatographic Equations

z = vertical distance coordinate (cm).

A = cross-sectional area of soil column (cm^2).

V = volume, $A\Delta z$, of layer of thickness Δz (cm^3).

Vp = pore volume, $\alpha \cdot V$, of layer of thickness Δz (cm^3).

t = time (d).

c = concentration (g/ml).

υ = water flux density (Darcian velocity) (ml/cm^2-d).

ν = water velocity (cm/d).

q = solute mass flux density (g/cm^2-d).

D = solute diffusivity in soil (cm^2/d).

D_0 = solute diffusivity in water (cm^2/d).

E = dispersion coefficient (cm^2/d).

Dspr = spreading coefficient, combining D and E (cm^2/d).

T = tortuosity factor (dimensionless).

α = porosity (cm^3/cm^3).

θ = volumetric water content (ml/cm^3).

θs = saturated volumetric water content (ml/cm^3).

Db = dry bulk density (g/cm^3).

a = mass adsorbate/mass soil (μg/g).

Kads = adsorption coefficient, Freundlich isotherm (ml/g).

B = effective partition coefficient (dimensionless).

$= Db \cdot k/\theta$.

The symbolism used in the simulation program is given in Appendix D.

APPENDIX B

Summary of Field Data

Table B.1. Mean radioisotope activity distributions observed in May, 1982, after labelled solutes applied to the Ap horizon (0 - 2½ cm) in Nov. and Dec., 1981.

Depth (cm)	A/A_0(^{3}HOH)[1]	A/A_0(^{14}C-lindane)
0 - 2½	.0075	.678 ± .206
2½ - 5	.0049	.014 ± .026
5 - 7½	0	0 ± 0
7½ - 10	.0029	
10 - 12½	.0029	
12½ - 15	.0031	
15 - 17½	.0025	
17½ - 20	0	
20 - 22½	.0017	
22½ - 25	0	

A = activity measured in each soil sample layer.

A_0 = total activity added to each site

= 6.25 µCi for ^{3}HOH;

= 2 µCi for ^{14}C-lindane.

[1] Note - activities detected at one site only.

Table B.2. Mean radioisotope activity distributions observed in May, 1982, after labelled solutes applied to the upper surface of Bt horizon in Nov. and Dec., 1981. Depths are given as distances from the centre of the layer of application (negative values above layer of application, positive below).

Depth (cm)	A/A_0(^{3}HOH)	A/A_0(^{14}C-lindane)
- 15	.0021 ± .0041	
- 12½	.0026 ± .0043	
- 10	.0042 ± .0067	
- 7½	.0064 ± .0094	
- 5	.0094 ± .0118	
- 2½	.0148 ± .0160	.0032 ± .0062
0	.0186 ± .0154	.4550 ± .2480
2½	.0167 ± .0074	.2975 ± .2854
5	.0236 ± .0128	.0185 ± .0305
7½	.0253 ± .0138	.0038 ± .0039
10	.0228 ± .0111	
12½	.0175 ± .0091	
15	.0129 ± .0096	
17½	.0069 ± .0066	
20	.0027 ± .0027	
22½	.0008 ± .0012	
25	.0004 ± .0007	
27½	.0004 ± .0007	

A = activity measured in each soil sample layer.
A_0 = total activity added to each site
(6.25 and 10 μCi for ^{3}HOH; 2 μCi for ^{14}C-lindane)

APPENDIX C

Summary of Field Data Used for Comparison with Simulations

Table C.1. Mean radioisotope activity distributions observed on west half of experimental plot area in May, 1982, after labelled solutes applied to Ap horizon (0 - 2½ cm) in Nov. and Dec., 1981.

Depth (cm)	A/At(^{3}HOH)[1]	A/At(^{14}C-lindane)
0 - 2½	.292	.971 ± .044
2½ - 5	.193	.029 ± .044
5 - 7½	0	0 ± 0
7½ - 10	.112	
10 - 12½	.112	
12½ - 15	.124	
15 - 17½	.099	
17½ - 20	0	
20 - 22½	.068	
22½ - 25	0	

A = activity measured in each soil sample layer.
At = total activity measured at each site
= ΣA.

[1] Note - activities detected at one site only.

Table C.2. Mean radioisotope activity distributions observed on west half of plot area in May, 1982, after labelled solutes applied to the upper surface of Bt horizon in Nov. and Dec., 1981. Depths are given as distances from the centre of the layer of application (negative values above layer of application, positive below).

Depth (cm)	A/At(^{3}HOH)	A/At(^{14}C-lindane)
- 15	.0064 ± .0079	
- 12½	.0102 ± .0125	
- 10	.0142 ± .0182	
- 7½	.0238 ± .0245	
- 5	.0327 ± .0167	
- 2½	.0530 ± .0155	.0333 ± .0563
0	.0682 ± .0228	.6402 ± .2469
2½	.0932 ± .0162	.2963 ± .2575
5	.1300 ± .0180	.0234 ± .0290
7½	.1726 ± .0590	.0067 ± .0047
10	.1528 ± .0409	
12½	.113 ± .053	
15	.072 ± .034	
17½	.035 ± .018	
20	.013 ± .008	
22½	.0042 ± .0054	
25	.0016 ± .0032	
27½	.0014 ± .0028	

A = activity measured in each soil sample layer.
At = total activity measured at each site
= ΣA.

APPENDIX D

Manual for use with Simulation Model FORTRAN Program "PFSS2"

DIMENSIONING:

The program is set up for systems of less than 100 layers. If the system to be modelled contains 100 or greater layers the dimensions of the following arrays must be changed.

WT(m), WR(m), WMCAP(m), WGRCAP(m), WM(m), WGRAV(m),
XSWMCP(m), XSWGCP(m), ST(m), SR(m), SM(m), SGRAV(m),
WE(m), SE(m), MS(m), Q(m), DB(m), KADS(m), DEPTH(m)

where m = number of layers in system.

PROBLEM IDENTIFIERS:

TITLE1 = first title line, up to 80 alphanumeric characters

TITLE2 = second title line, up to 80 alphanumeric characters

SYSTEM PARAMETERS:

M = number of layers in system being modelled.

DELTAZ = layer thickness, in mm.

TIME STEP PARAMETERS:

TFIN = time period of simulation, days;
also signals when the final output data is printed.

T1, T2, T3 = times when intermediate results can be printed;
if not required set all equal to TFIN.

LAYER PARAMETERS:

DB(m) = dry bulk density of each layer (g/cm^3); used only for adsorbed solutes, otherwise can be set = 0.

KADS(m) = adsorption coefficient, linear Freundlich isotherm (ml/g); must be specified (for non-adsorbed solute set = 0).

INTERNAL VARIABLES:

Initial values for the following variables must be provided by the user.

MS(m) = total mass of solute in each layer per unit area (e.g., kg/ha, $\mu g/cm^2$); area can be chosen arbitrarily, but must be consistent with units used for S (see DRIVING VARIABLES).

WT(m) = total height equivalent (mm) of water in each layer; determined by user as product of volumetric moisture content and layer thickness in mm.

= DELTAZ*θ

WR(m) = height equivalent (mm) of water in stagnant water pool; determined from moisture retention curve (θ at 200 kPa moisture tension) and layer thickness in mm

= DELTAZ*θ(200 kPa)

WMCAP(m) = mobile water pool capacity, in height equivalent (mm) of water; determined from moisture retention curve and layer thickness in mm.

= DELTAZ*[θ(33 kPa) - θ(200 kPa)]

WGRCAP(m) = gravity water capacity in height equivalent (mm) of water; determined from porosity, moisture retention curve and layer thickness in mm.

= DELTAZ*[porosity - θ(33 kPa)]; used in frozen layer routine only; can be set at 0 at all layers for non-frozen soil.

The simulation program generates the following initial internal variables from those provided above and updates them throughout the program:

WM(m) = water contained in mobile pool, height equivalent (mm).

WGRAV(m) = water contained in gravity pool, height equivalent (mm).

XSWMCP(m) = unfilled capacity in mobile water pool (mm).

XSWGCP(m) = unfilled capacity in gravity water pool (mm).

B = effective partition coefficient (dimensionless);
= DELTAZ*DB(m)*KADS(m)/WT(m).

Q(m) = mass of adsorbed solute (μg) in each layer;
= MS(m)*B/(1+B).

ST(m) = mass of dissolved solute (μg) in each layer;
= MS(m)/(1+B).

SR(m) = mass of dissolved solute (μg) in stagnant pool;
= ST(m)*WR(m)/WT(m).

SM(m) = mass of dissolved solute (μg) in mobile pool;
= ST(m)*WM(m)/WT(m).

SGRAV(m) = mass of dissolved solute (μg) in gravity pool;
= ST(m)*WGRAV(m)/WT(m).

DRIVING VARIABLES

The following input variables must be provided at each time step. There must be TFIN sets of input data.

FLNR = frozen layer number (dimensionless);

the upper limit of frost in the soil;

for unfrozen soil must be set = 0.

W = daily precipation or infiltration (mm); (see note', below).

E = daily evaporation (mm) (see note', below).

S = daily mass of water borne solute applied per unit area of soil; must be compatible with units used for MS(m) (e.g., kg/ha, μg/cm²).

' - Note: Net infiltration is determined from W and E as WA = W - E. WA cannot be 0 because some concentrations are determined by dividing by WA. Therefore W and E must not be equal.

The following driving variables are generated by the simulation program to affect transfer of water and solute mass between layers:

WA, WL = water added from layer above and lost to layer below, respectively, by downward transmission of water infiltrating at surface layer.

SA, SL = solute mass carried by WA and WL, respectively.

WE(m) = water lost to layer above due to capillary flow induced by evaporation; (WE(1)=water lost from surface layer to atmosphere by evaporation).

SE(m) = solute mass carried by WE(m); (SE(1) = solute lost from surface layer to atmosphere by volatilization).

INPUT CARD INSTRUCTIONS.

The data enterred into to the program must follow the following format:

CARD	VARIABLE	FORMAT	COLUMNS
1	TITLE1	80A1	1 - 80
2	TITLE2	80A1	1 - 80
3	M	I5	1 - 5
	TFIN	I5	6 - 10
	T1	I5	11 - 15
	T2	I5	16 - 20
	T3	I5	21 - 25
	DELTAZ	F5.2	26 - 30
4[2]	DB	F10.4	1 - 10
	KADS	F10.4	11 - 20
	MS	F10.4	21 - 30
	WT	F10.4	31 - 40
	WR	F10.4	41 - 50
	WMCAP	F10.4	51 - 60
	WGRCAP	F10.4	61 - 70
5[3]	FLNR	I3	1 - 5
6[3]	W	F10.2	1 - 10
	E	F10.2	11 - 20
	S	F10.2	21 - 30

Notes: [2] - Card 4 is repeated M times, where M is the number of layers in the system being modelled, in order that variable values are supplied for all layers.

[3] - Cards 5 and 6 are repeated TFIN times, where TFIN is the number of time steps simulated. Cards 5 and 6 must be enterred alternately, so that daily FLNR, and W, E, and S are read together.

Examples of complete input files illustrating the correct formatting can be found in Appendix E. Input data are enterred on I/O device unit 5; output data can be enterred on I/O unit 6.

OUTPUT FORMAT

The results of the simulation program are printed in the following format:

1. Model identifier (2 lines).
2. Problem identifiers, reprinted from input file (2 lines).
3. Time step and layer parameters, reprinted from input file (1 line).
4. Data echo: the data for each layer is reprinted as it appears in the data file, under the headings, DB, KADS, MS, WT, WR, WMCAP, WGRCAP, as defined above.
5. Initial conditions, calculated from input data supplied, under the headings, I, DEPTH, XSGMCP, XSWMCP, B, Q, ST, and SM, as defined above.
6. Infiltration/evaporation records (daily), under the headings J (time), FLNR (frozen layer number), FLNRT (previous frozen layer number), W-INPUT (precipitation/infiltration), EVAPN (evaporation), S-INPUT (solute carried by infiltrating water), W-POND (height of ponded water), WA(NETW) (net infiltration/evaporation), and WTOTAL (total infiltration to date), in tabular form.
7. If there is any volatilization loss of solute the above table is interrrupted and the following information is supplied: NET E (always 0); WT(1), WG(1), WM(1), WR(1) (total, gravity, mobile, and stagnant water, respectively, contained in layer 1); WE(1), SE(1) (evaporative water losses and volatilization losses, respectively, from layer

1).

8. Sink losses: water and solute which drain from the bottom layer of the system will also interrupt the data tabulated in 7 (above) under the headings: SINK LOSSES AFTER DAY "J"; VOLUME, AMT. SOLUTE, and CONC. SOLUTE (drainage water, height equivalent; mass of solute drained, per unit area; and solute concentration in drainage, respectively).

8. The solute concentration profile is printed in tabular form under the headings: LAYR (layer number), GRAVHOH, MOBHOH, and RETHOH (gravity, mobile, and stagnant water, respectively, contained in the layer): GRAVSOL, MOBSOL, and RET[illegible]L (solute mass, per layer, contained in gravity pool, mobile pool, and stagnant pool, respectively); DISSOL, ADSOL, TTLSOL (total dissolved solute, adsorbed solute, and total solute mass, respectively, contained in the layer).

Examples of the output data file are found in Appendix E, following their respective input data files.

APPENDIX E

Input Data Used by, and Output Data Generated by Simulation Model Program.

The following pages contain I/O data files used/generated by the FORTRAN program which implements the simulation model. (The program is printed in Appendix F.)

Simulation E1, pages 146 to 149, is for transport of a non-reactive solute (tritiated water) applied to the Bt horizon and is a simulation of field experiment 1b, described in chapter III. Simulation E2, pages 150 to 153, is for transport of an adsorbed solute (^{14}C-lindane) applied to the Ap horizon (0 - 2.5 cm) and is a simulation of field experiment 2a, chapter III.

The output file generated by each simulation follows its respective input data file. Details on formatting of input and output files are given in Appendix D.

INPUT DATA FILE E1:

```
SIMULATION OF FIELD EXPT. 1b: 3HOH APPLIED TO Bt HORIZON.
WR:WMCAP SET AT 2 BARS. LAYERS = 40 X 25.4 MM. SITE 13.
   40   54   30   40   50 25.4
  1.331     0.000     0.00     8.18     7.375     1.92     2.99
  1.437     0.000     0.00     8.18     7.375     1.92     1.96
  1.500     0.000     0.00     8.62     7.375     1.92     1.76
  1.531     0.000     0.00     7.92     7.375     1.92     1.76
  1.523     0.000     0.00     8.45     7.375     1.92     1.76
  1.497     0.000     0.00     8.64     7.375     1.92     1.76
  1.528     0.000     100.     9.42     9.42      1.21     1.00
  1.4975    0.000     0.00     9.42     9.42      1.21     0.72
  1.462     0.000     0.00     9.42     9.42      1.21     0.72
  1.435     0.000     0.00     9.42     9.42      1.21     0.92
  1.425     0.000     0.00     9.42     9.42      1.21     1.02
  1.420     0.000     0.00     9.42     9.42      1.21     1.06
  1.436     0.000     0.00     9.42     9.42      1.21     0.91
  1.483     0.000     0.00     9.42     9.42      1.21     0.72
  1.471     0.000     0.00     9.42     9.42      1.21     0.72
  1.504     0.000     0.00     9.42     9.42      1.21     0.72
  1.519     0.000     0.00     9.42     9.42      1.21     0.72
  1.559     0.000     0.00     9.42     9.42      1.21     0.72
  1.573     0.000     0.00     9.61     9.42      1.21     0.72
  1.592     0.000     0.00     9.99     9.42      1.21     0.72
  1.655     0.000     0.00     9.92     9.42      1.21     0.72
  1.650     0.000     0.00     9.42     9.42      1.21     0.72
  1.622     0.000     0.00     9.63     9.42      1.21     0.72
  1.613     0.000     0.00     9.51     9.42      1.21     0.72
  1.630     0.000     0.00     9.40     8.40      1.34     0.52
  1.620     0.000     0.00     9.24     8.40      1.34     0.52
  1.623     0.000     0.00     9.09     8.40      1.34     0.52
  1.617     0.000     0.00     9.05     8.40      1.34     0.52
  1.618     0.000     0.00     9.02     8.40      1.34     0.52
  1.590     0.000     0.00     9.48     8.40      1.34     0.52
  1.585     0.000     0.00     9.74     8.40      1.34     0.52
  1.587     0.000     0.00     9.74     8.40      1.34     0.52
  1.614     0.000     0.00     9.64     8.40      1.34     0.52
  1.622     0.000     0.00     9.74     8.40      1.34     0.52
  1.616     0.000     0.00     9.50     8.40      1.34     0.52
  1.588     0.000     0.00     8.58     8.40      1.34     0.52
  1.612     0.000     0.00     8.40     8.40      1.34     0.52
  1.636     0.000     0.00     8.40     8.40      1.34     0.52
  1.634     0.000     0.00     8.40     8.40      1.34     0.52
  1.632     0.000     0.00     9.41     8.40      1.34     0.52
002
0.66      0.00      0.0
002
0.66      0.00      0.0
002
0.66      0.00      0.0
002
```

```
0.66      0.00      0.0
002
0.66      0.00      0.0
003
0.66      0.00      0.0
003
0.80      0.00      0.0
003
0.80      0.00      0.0
003
0.80      0.0       0.0
003
0.80      0.0       0.0
003
0.80      0.0       0.0
003
0.80      0.0       0.0
003
0.80      0.0       0.0
003
0.80      0.0       0.0
003
0.80      0.0       0.0
004
0.80      0.0       0.0
004
0.80      0.0       0.0
004
0.80      0.0       0.0
004
0.80      0.0       0.0
004
0.80      0.0       0.0
004
0.80      0.0       0.0
004
0.80      0.0       0.0
005
0.80      0.0       0.0
005
0.80      0.0       0.0
005
0.80      0.0       0.0
005
0.80      0.0       0.0
006
1.00      0.0       0.0
006
1.50      0.0       0.0
007
2.50      0.0       0.0
008
3.50      0.0       0.0
```

```
009
4.20      0.0      0.0
010
4.75      0.0      0.0
011
5.05      0.0      0.0
012
5.30      0.0      0.0
014
5.20      0.0      0.0
016
5.00      0.0      0.0
018
4.50      0.0      0.0
020
3.00      0.0      0.0
022
0.000     1.30     0.0
024
0.00      1.30     0.0
026
0.00      1.30     0.0
026
0.00      4.10     0.0
027
0.00      4.10     0.0
027
0.00      4.10     0.0
028
0.00      1.39     0.0
028
0.00      1.39     0.0
029
0.00      1.39     0.0
030
0.00      1.39     0.0
032
0.00      1.39     0.0
034
0.00      1.39     0.0
000
0.00      1.39     0.0
000
0.00      1.39     0.0
000
0.00      1.39     0.0
000
0.00      1.39     0.0
000
0.00      1.39     0.0
000
0.00      1.39     0.0
```

OUTPUT DATA FILE E1:

```
PFSS2: TWO-POOL MODEL OF SOLUTE TRANSPORT THROUGH
PARTIALLY FROZEN STRUCTURED SOIL.

SIMULATION OF FIELD EXPT. 1b: 3HOH APPLIED TO Bt HORIZON.
WR:WMCAP SET AT 2 BARS. LAYERS = 40 X 25.4 mm. SITE 13.
   40   54   30   40   50 25.4
(NOTE:DATA  ECHO, INITIAL CONDITIONS, INFILTRATION RECORDS,
INTERMDIATE SOLUTE DISTRIBUTION PROFILES, ARE OMMITTED)
..
SOLUTE PROFILE, DAY 54  .
LAYR GRAVHOH MOBHOH RETHOH GRAVSOL MOBSOL RETSOL DISSOL ADSOL TTLSOL
 1    0.0     0.0    7.38    0.0    0.0    0.0    0.0    0.0    0.0
 2    0.0     0.0    7.38    0.0    0.0    0.00   0.00   0.0    0.00
 3    0.0     0.0    7.38    0.0    0.0    0.01   0.01   0.0    0.01
 4    0.0     0.0    7.38    0.0    0.0    0.08   0.08   0.0    0.08
 5    0.0     0.0    7.38    0.0    0.0    0.40   0.40   0.0    0.40
 6    0.0     0.0    7.38    0.0    0.0    1.28   1.28   0.0    1.28
 7    0.0     0.0    9.42    0.0    0.0    3.93   3.93   0.0    3.93
 8    0.0     0.0    9.42    0.0    0.0    8.38   8.38   0.0    8.38
 9    0.0     1.05   9.42    0.0    1.49  13.37  14.86   0.0   14.86
10    0.0     1.21   9.42    0.0    2.09  16.26  18.35   0.0   18.35
11    0.0     1.21   9.42    0.0    2.03  15.84  17.88   0.0   17.88
12    0.0     1.21   9.42    0.0    1.64  12.74  14.37   0.0   14.37
13    0.0     1.21   9.42    0.0    1.11   8.66   9.77   0.0    9.77
14    0.0     1.21   9.42    0.0    0.65   5.07   5.72   0.0    5.72
15    0.0     1.21   9.42    0.0    0.33   2.58   2.91   0.0    2.91
16    0.0     1.21   9.42    0.0    0.15   1.15   1.30   0.0    1.30
17    0.0     1.21   9.42    0.0    0.06   0.45   0.51   0.0    0.51
18    0.0     1.21   9.42    0.0    0.02   0.16   0.18   0.0    0.18
19    0.0     1.21   9.42    0.0    0.01   0.05   0.06   0.0    0.06
20    0.0     1.21   9.42    0.0    0.00   0.01   0.02   0.0    0.02
21    0.0     1.21   9.42    0.0    0.00   0.00   0.00   0.0    0.00
22    0.0     1.21   9.42    0.0    0.00   0.00   0.00   0.0    0.00
23    0.0     1.21   9.42    0.0    0.00   0.00   0.00   0.0    0.00
24    0.0     1.21   9.42    0.0    0.00   0.00   0.00   0.0    0.00
25    0.0     1.34   8.40    0.0    0.00   0.00   0.00   0.0    0.00
26    0.0     1.34   8.40    0.0    0.00   0.00   0.00   0.0    0.00
27    0.0     1.34   8.40    0.0    0.00   0.00   0.00   0.0    0.00
28    0.0     1.34   8.40    0.0    0.00   0.00   0.00   0.0    0.00
29    0.0     1.34   8.40    0.0    0.00   0.00   0.00   0.0    0.00
30    0.0     1.34   8.40    0.0    0.00   0.00   0.00   0.0    0.00
31    0.0     1.34   8.40    0.0    0.00   0.00   0.00   0.0    0.00
32    0.0     1.34   8.40    0.0    0.00   0.00   0.00   0.0    0.00
33    0.0     1.34   8.40    0.0    0.00   0.00   0.00   0.0    0.00
34    0.0     1.34   8.40    0.0    0.00   0.00   0.00   0.0    0.00
35    0.0     1.34   8.40    0.0    0.00   0.00   0.00   0.0    0.00
36    0.0     1.34   8.40    0.0    0.00   0.00   0.00   0.0    0.00
37    0.0     1.34   8.40    0.0    0.00   0.00   0.00   0.0    0.00
38    0.0     1.34   8.40    0.0    0.00   0.00   0.00   0.0    0.00
39    0.0     1.34   8.40    0.0    0.00   0.00   0.00   0.0    0.00
40    0.0     1.34   8.40    0.0    0.00   0.00   0.00   0.0    0.00
```

INPUT DATA FILE E2:

```
SIMULATION OF FIELD EXPT. 2a: 14C-LINDANE APPLIED TO Ap HORIZON.
WR:WMCAP SET AT 2 BARS. LAYERS = 40 X 25.4 MM. SITE 10.
  40   48   30   40   45 25.4
 1.331    12.60    100.     8.18    7.375    1.92    2.99
 1.437    12.60    0.00     8.18    7.375    1.92    1.96
 1.500    12.60    0.00     8.62    7.375    1.92    1.76
 1.531    12.60    0.00     7.92    7.375    1.92    1.76
 1.523    12.60    0.00     8.45    7.375    1.92    1.76
 1.497    12.60    0.00     8.64    7.375    1.92    1.76
 1.528    5.100    0.00     9.42    9.42     1.21    1.00
 1.4975   5.100    0.00     9.42    9.42     1.21    0.72
 1.462    5.100    0.00     9.42    9.42     1.21    0.72
 1.435    5.100    0.00     9.42    9.42     1.21    0.92
 1.425    5.100    0.00     9.42    9.42     1.21    1.02
 1.420    5.100    0.00     9.42    9.42     1.21    1.06
 1.436    5.100    0.00     9.42    9.42     1.21    0.91
 1.483    5.100    0.00     9.42    9.42     1.21    0.72
 1.471    5.100    0.00     9.42    9.42     1.21    0.72
 1.504    5.100    0.00     9.42    9.42     1.21    0.72
 1.519    5.100    0.00     9.42    9.42     1.21    0.72
 1.559    5.100    0.00     9.42    9.42     1.21    0.72
 1.573    5.100    0.00     9.61    9.42     1.21    0.72
 1.592    5.100    0.00     9.99    9.42     1.21    0.72
 1.655    5.100    0.00     9.92    9.42     1.21    0.72
 1.650    5.100    0.00     9.42    9.42     1.21    0.72
 1.622    5.100    0.00     9.63    9.42     1.21    0.72
 1.613    5.100    0.00     9.51    9.42     1.21    0.72
 1.630    5.100    0.00     9.40    8.40     1.34    0.52
 1.620    5.100    0.00     9.24    8.40     1.34    0.52
 1.623    5.100    0.00     9.09    8.40     1.34    0.52
 1.617    5.100    0.00     9.05    8.40     1.34    0.52
 1.618    5.100    0.00     9.02    8.40     1.34    0.52
 1.590    5.100    0.00     9.48    8.40     1.34    0.52
 1.585    5.100    0.00     9.74    8.40     1.34    0.52
 1.587    5.100    0.00     9.74    8.40     1.34    0.52
 1.614    5.100    0.00     9.64    8.40     1.34    0.52
 1.622    5.100    0.00     9.74    8.40     1.34    0.52
 1.616    5.100    0.00     9.50    8.40     1.34    0.52
 1.588    5.100    0.00     8.58    8.40     1.34    0.52
 1.612    5.100    0.00     8.40    8.40     1.34    0.52
 1.636    5.100    0.00     8.40    8.40     1.34    0.52
 1.634    5.100    0.00     8.40    8.40     1.34    0.52
 1.632    5.100    0.00     9.41    8.40     1.34    0.52
002
0.66      0.00     0.0
002
0.66      0.00     0.0
002
0.66      0.00     0.0
```

```
002
0.66      0.00      0.0
002
0.66      0.00      0.0
003
0.66      0.00      0.0
003
0.80      0.00      0.0
003
0.80      0.00      0.0
003
0.80      0.0       0.0
003
0.80      0.0       0.0
003
0.80      0.0       0.0
003
0.80      0.0       0.0
003
0.80      0.0       0.0
003
0.80      0.0       0.0
003
0.80      0.0       0.0
004
0.80      0.0       0.0
004
0.80      0.0       0.0
004
0.80      0.0       0.0
004
0.80      0.0       0.0
004
0.80      0.0       0.0
004
0.80      0.0       0.0
004
0.80      0.0       0.0
005
0.80      0.0       0.0
005
0.80      0.0       0.0
005
0.80      0.0       0.0
005
0.80      0.0       0.0
006
1.00      0.0       0.0
006
1.50      0.0       0.0
007
2.50      0.0       0.0
008
```

```
3.50      0.0       0.0
009
4.20      0.0       0.0
010
4.75      0.0       0.0
011
5.05      0.0       0.0
012
5.30      0.0       0.0
014
5.20      0.0       0.0
016
5.00      0.0       0.0
018
4.50      0.0       0.0
020
3.00      0.0       0.0
022
0.000     1.30      0.0
024
0.00      1.30      0.0
026
0.00      1.30      0.0
026
0.00      4.10      0.0
027
0.00      4.10      0.0
027
0.00      4.10      0.0
028
0.00      1.39      0.0
028
0.00      1.39      0.0
029
0.00      1.39      0.0
030
0.00      1.39      0.0
032
0.00      1.39      0.0
034
0.00      1.39      0.0
000
0.00      1.39      0.0
000
0.00      1.39      0.0
000
0.00      1.39      0.0
000
0.00      1.39      0.0
000
0.00      1.39      0.0
000
0.00      1.39      0.0
```

0.0	0.0
0.0	0.0
0.0	0.0
0.0	0.0
0.0	0.0
0.0	0.0
0.0	0.0
1.30	0.0
1.30	0.0
1.30	0.0
4.10	0.0
4.10	0.0
4.10	0.0
1.39	0.0
1.39	0.0
1.39	0.0
1.39	0.0
1.39	0.0
1.39	0.0
1.39	0.0
1.39	0.0
1.39	0.0
1.39	0.0
1.39	0.0
1.39	0.0

0.0	0.0
0.0	0.0
0.0	0.0
0.0	0.0
0.0	0.0
0.0	0.0
0.0	0.0
1.30	0.0
1.30	0.0
1.30	0.0
4.10	0.0
4.10	0.0
4.10	0.0
1.39	0.0
1.39	0.0
1.39	0.0
1.39	0.0

```
      DOUBLE PRECISION SA, SL, DELTAS, B
      DOUBLE PRECISION WT(99), WGRAV(99), WM(99), XSWMCP(99),
     1XSWGCP(99), SR(99), SM(99), SGRAV(99), ST(99),
     2WE(99), SE(99), MS(99), Q(99)
      REAL NETEVN, WPOND, W, E, S, WA, WL, WDRAIN,
     1DCONC, DELTAZ, DB(99), KADS(99), DEPTH(99),
     2WGRCAP(99), WMCAP(99), WR(99)
      DIMENSION TITLE1(80), TITLE2(80)
      WRITE(6,608)
  608 FORMAT('PFSS2: TWO-POOL MODEL OF SOLUTE TRANSPORT THROUGH'/
     *'PARTIALLY FROZEN STRUCTURED SOIL.'/)
      READ(5,500) TITLE1,TITLE2
      WRITE(6,500) TITLE1,TITLE2
  500 FORMAT(80A1/80A1)
      READ(5,501) M, TFIN, T1, T2, T3, DELTAZ
      WRITE(6,501) M, TFIN, T1, T2, T3, DELTAZ
  501 FORMAT(5I5, F5.2)
  502 FORMAT(7F10.4)
  503 FORMAT(I3)
  504 FORMAT(3F10.2)
  601 FORMAT(1X,'TOO MANY LAYERS -- CHECK DIMENSIONS')
  602 FORMAT('DATA ECHO: INITIAL CONDITIONS'/'      DB        KADS',
     *'      MS        WT        WR       WMCAP      WGRCAP')
  606 FORMAT(1X,I2,2X,I2,2X,I2,2X,F6.3,2X,F6.3,2X,F6.3,2X,F6.3,
     *2X,F6.3,2X,F7.3)
  607 FORMAT('J FLNR FLNRT W-INPUT EVAPN  S-INPUT  W-POND',
     *'   WA(NETW) WTOTAL')
      IF(M.LT.100)GO TO 50
         WRITE(6,601)
      GO TO 9999
   50 READ(5,502) ((DB(K),KADS(K),MS(K),WT(K),WR(K),WMCAP(K),
     *WGRCAP(K)),K=1,M)
      WRITE(6,602)
      WRITE(6,502) ((DB(K),KADS(K),MS(K),WT(K),WR(K),WMCAP(K),
     *WGRCAP(K)),K=1,M)
C+------------------------------------------------------------+
C|  INITIALIZE SOIL VARIABLES (WGRAV, XSWGCP, XSWMCP, WM, ST,  |
C|                            Q, SR, SM, SGRAV).               |
C|  INITIALIZE PROGRAM VARIABLES (J, FLNRT).                   |
C+------------------------------------------------------------+
      WRITE(6,2001)
      DO 51 K=1,M
         B = DELTAZ*DB(K)*KADS(K)/WT(K)
         ST(K) = MS(K)/(1+B)
         Q(K) = MS(K)*B/(1+B)
         SR(K) = WR(K)*ST(K)/WT(K)
         WM(K) = WT(K) - WR(K)
         SM(K) = WM(K)*ST(K)/WT(K)
         WGRAV(K) = 0.0
         SGRAV(K) = 0.0
         XSWGCP(K) = WGRCAP(K) - WGRAV(K)
         XSWMCP(K) = WMCAP(K) - WM(K)
         DEPTH(K) = DELTAZ*(-FLOAT(K) + 0.50)
      WRITE(6,2000) (K,DEPTH(K),XSWGCP(K),XSWMCP(K),WM(K),B,
     *Q(K),ST(K),SR(K),SM(K))
 2000 FORMAT(1X,I2,F6.0,8(2X,F6.2))
 2001 FORMAT('  I DEPTH    XSWGCP  XSWMCP  WM     B        Q ',
     *'     ST      SR      SM')
   51 CONTINUE
      J = 0
      WPOND = 0.0
      FLNRT = 0
      WTOTAL = 0.0
      WRITE(6,607)
    1 J = J + 1
      DO 11 K=1,M
        XSWMCP(K) = WMCAP(K) - WM(K)
        XSWGCP(K) = WGRCAP(K) - WGRAV(K)
   11 CONTINUE
      I = 1
      IF(FLNRT.GT.0)GO TO 310
C  CHECK PREVIOUS POSITION OF FROZEN LAYER AND GO TO
C  REDISTRIBUTION ROUTINE IF NECESSARY.
           READ(5,503) FLNR
           IF(FLNR.LE.M)GO TO 2
              WRITE(6,609) M, FLNR
  609         FORMAT('SYSTEM CONTAINS ONLY ',I3,'LAYERS;',
     *          'SYSTEM NOT DEFINED FOR FLNR = ',I3)
              GO TO 9999
C  RESET FLNRT TO FLNR AND READ IN PRECIP., EVAPN, PRECIP-BORNE
C  SOLUTE CONCENTRATION.
    2 FLNRT = FLNR
      I = 1
      READ(5,504) W, E, S
      WTOTAL = WTOTAL + W
      WA = W - E + WPOND
      S = (S*W + SPOND*WPOND)/WA
      WRITE(6,606) J, FLNR, FLNRT, W, E, S, WPOND, WA, WTOTAL
      WPOND = 0.0
      SPOND = 0.0
      IF(WA.GE.0.0)GO TO 99
        NETEVN = -WA
        GO TO 400
   99 IF(WGRAV(I).GT.0.0)GO TO 299
      IF(I.EQ.FLNR)GO TO 300
C+-----------------------------------------------------+
C|  SLOW LEACHING ROUTINE.                              |
C+-----------------------------------------------------+
  100 IF(WA.GT.XSWMCP(I))GO TO 101
        WM(I) = WM(I) + WA
        WT(I) = WR(I) + WM(I) + WGRAV(I)
      DELTAS = S*WA
      MS(I) = MS(I) + DELTAS
      B = DELTAZ*DB(I)*KADS(I)/WT(I)
      ST(I) = MS(I)/(1+B)
      Q(I) = MS(I)*B/(1+B)
```

```
C+-------------------------------------------------------+
C| EQUILIBRATION OF SOLUTE AMONG RET,MOB,&GRAV POOLS:|
C| SOL CONCN. IS THE SAME IN EACH WITHIN EACH LAYER. |
C+-------------------------------------------------------+
         SR(I) = ST(I)*WR(I)/WT(I)
         SM(I) = ST(I)*WM(I)/WT(I)
         SGRAV(I) = ST(I)*WGRAV(I)/WT(I)
C+-------------------------------------------------------+
C|  RESET WA, SA, S: THESE VARIABLES CARRY WATER AND |
C|                    SOLUTE INTO THE NEXT LAYER.     |
C|  RESET EXCESS MOBILE WATER CAPACITY AND CONTINUE. |
C+-------------------------------------------------------+
         WA = 0.0
         SA = 0.0
         S = 0.0
         XSWMCP(I) = WMCAP(I) - WM(I)
         GO TO 999
  101 IF(WA.GT.WMCAP(I))GO TO 200
         WL = WA - XSWMCP(I)
         SL = ST(I)*WL/WT(I)
         SA = S*WA
       DELTAS = SA - SL
       MS(I) = MS(I) + DELTAS
       WM(I) = WM(I) + WA - WL
       WT(I) = WR(I) + WM(I) + WGRAV(I)
C  PARTITION OF SOLUTE, SOLUTION/ADSORBED PHASES.
       B = DELTAZ*DB(I)*KADS(I)/WT(I)
       ST(I) = MS(I)/(1+B)
       Q(I) = MS(I)*B/(1+B)
C  EQUILIBRATION OF DISSOLVED SOLUTE AMONG POOLS.
         SR(I) = ST(I)*WR(I)/WT(I)
         SM(I) = ST(I)*WM(I)/WT(I)
         SGRAV(I) = ST(I)*WGRAV(I)/WT(I)
         WA = WA - XSWMCP(I)
         SA = SL
         S = SA/WA
         XSWMCP(I) = WMCAP(I) - WM(I)
       IF(I.EQ.M)GO TO 900
         I = I + 1
         GO TO 99
C      ********************************************
C+-------------------------------------------------------------+
C|  FAST LEACHING ROUTINE(200).                                |
C+-------------------------------------------------------------+
  200 WL = WM(I)
      SL = SM(I)
      SA = S*WMCAP(I)
      WM(I) = WMCAP(I)
      DELTAS = SA - SL
      MS(I) = MS(I) + DELTAS
      WT(I) = WR(I) + WM(I) + WGRAV(I)
      B = DELTAZ*DB(I)*KADS(I)/WT(I)
C  PARTITION
```

```
      ST(I) = MS(I)/(1+B)
      Q(I) = MS(I)*B/(1+B)
C  EQUILIBRATION
      SR(I) = ST(I)*WR(I)/WT(I)
      SM(I) = ST(I)*WM(I)/WT(I)
      SGRAV(I) = ST(I)*WGRAV(I)/WT(I)
C  RESET WA,SA,S,XSWMCP(I)
      WA = WA - XSWMCP(I)
      SA = SL + S*(WA-WL)
      S = SA/WA
      XSWMCP(I) = WMCAP(I) -WM(I)
      IF(I.EQ.M)GO TO 900
      I = I + 1
      GO TO 99
C     ******************************************
C+-----------------------------------------------+
C|  FROZEN LAYER ROUTINE                         |
C+-----------------------------------------------+
  299 IF(WGRCAP(I).GT.WGRAV(I))GO TO 301
  300   I = I - 1
  301 IF(I.EQ.0)GO TO 309
      IF(WA.GT.XSWGCP(I))GO TO 302
        WGRAV(I) = WGRAV(I) + WA
      DELTAS = S*WA
      MS(I) = MS(I) + DELTAS
        WT(I) = WR(I) + WM(I) + WGRAV(I)
      B = DELTAZ*DB(I)*KADS(I)/WT(I)
C PARTITION OF SOLUTE MASS -- ADSORBED-DISSOLVED.
      ST(I) = MS(I)/(1+B)
      Q(I) = MS(I)*B/(1+B)
C  EQUILIBRATION OF DISSOLVED SOLUTE.
        SR(I) = ST(I)*WR(I)/WT(I)
        SM(I) = ST(I)*WM(I)/WT(I)
        SGRAV(I) = ST(I)*WGRAV(I)/WT(I)
C  RESET FEED VARIABLES
        WA = 0.0
        SA = 0.0
        S = 0.0
        XSWGCP(I) = WGRCAP(I) - WGRAV(I)
        FLNRT = FLNR
        GO TO 999
  302 WGRAV(I) = WGRCAP(I)
      DELTAS = S*XSWGCP(I)
      MS(I) = MS(I) + DELTAS
      WT(I) = WR(I) + WM(I) + WGRAV(I)
      B = DELTAZ*DB(I)*KADS(I)/WT(I)
C PARTITION OF SOLUTE MASS -- ADSORBED-DISSOLVED.
      ST(I) = MS(I)/(1+B)
      Q(I) = MS(I)*B/(1+B)
C EQUILIBRATION OF DISSOLVED SOLUTE.
      SR(I) = ST(I)*WR(I)/WT(I)
      SM(I) = ST(I)*WM(I)/WT(I)
      SGRAV(I) = ST(I)*WGRAV(I)/WT(I)
```

```
C RESET FEED VARIABLES.
      WA = WA - XSWGCP(I)
      SA = S*WA
      S = SA/WA
C     WRITE(6,606) J, FLNR, FLNRT, W, E, S, WPOND, WA, WTOTAL
      XSWGCP(I) = WGRCAP(I) - WGRAV(I)
      GO TO 300
C+-----------------------------------------------------+
C| IF WGRAV BUILDS UP ABOVE I=1, WA IS PONDED(WPOND=WA). |
C|         WPOND IS THEN ADDED TO WA AT NEXT TIME STEP.  |
C+-----------------------------------------------------+
  309 WPOND = WA
      SPOND = S
      WA = 0.0
      S = 0.0
      I = 1
      FLNRT = FLNR
      GO TO 999
C+---------------------------------------------------+
C|  REDISTRIBUTION OF WATER AND SOLUTE WHEN FROST LAYER |
C|  MOVES DOWNWARD BETWEEN SUCCESSIVE TIME STEPS.       |
C+---------------------------------------------------+
  310 READ(5,503) FLNR
C IF FROZEN LAYER HAS MELTED, CLEAR WGRAV FROM THE PROFILE.
      IF(FLNR.EQ.0)GO TO 314
C IF FROZEN LAYER HAS NOT MOVED DOWNWARD THERE IS NO REDISTRIBUTN.
      IF(FLNR.LE.FLNRT)GO TO 2
C IF THERE IS NO WGRAV TO REDISTRIBUTE RETURN TO 2.
      DO 312 K=1,FLNRT
         IF(WGRAV(K).GT.0.0)GO TO 314
  312 CONTINUE
         GO TO 2
C REDISTRIBUTE WGRAV, STARTING AT THE LAYER ABOVE THE PREVIOUS FROZEN LAYER.
  314 IR = FLNRT - 1
      IF(IR.EQ.0)GO TO 2
        WA = WGRAV(IR)
        IF(WGRAV(IR).EQ.0.0)GO TO 320
        S = SGRAV(IR)/WGRAV(IR)
        WGRAV(IR) = 0.0
        XSWGCP(IR) = WGRCAP(IR) - WGRAV(IR)
        WT(IR) = WR(IR) + WM(IR)
          MS(IR) = MS(IR) - SGRAV(IR)
           B = DELTAZ*DB(IR)*KADS(IR)/WT(IR)
C  PARTITION
           ST(IR) = MS(IR)/(1+B)
           Q(IR) = MS(IR)*B/(1+B)
C  EQUILIBRATION
             SR(IR) = WR(IR)*ST(IR)/WT(IR)
             SM(IR) = WM(IR)*ST(IR)/WT(IR)
             SGRAV(IR) = WGRAV(IR)*ST(IR)/WT(IR)
      I = IR + 1
      FLNRT = -1
      GO TO 99
```

```
C MOVE TO THE NEXT HIGHER LAYER AND REDISTRIBUTE WGRAV DOWNWARD.
  320 IR = IR - 1
         IF(IR.EQ.0) GO TO 2
            WA = WGRAV(IR)
            IF(WGRAV(IR).EQ.0.0)GO TO 320
            S = SGRAV(IR)/WGRAV(IR)
            WGRAV(IR) = 0.0
         XSWGCP(IR) = WGRCAP(IR) - WGRAV(IR)
         WT(IR) = WR(IR) + WM(IR)
            MS(IR) = MS(IR) - SGRAV(IR)
            B = DELTAZ*DB(IR)*KADS(IR)/WT(IR)
            ST(IR) = MS(IR)/(1+B)
            Q(IR) = MS(IR)*B/(1+B)
              SR(IR) = WR(IR)*ST(IR)/WT(IR)
              SM(IR) = WM(IR)*ST(IR)/WT(IR)
              SGRAV(IR) = WGRAV(IR)*ST(IR)/WT(IR)
            I = IR + 1
            GO TO 99
C *****************************************************
C +---------------------------------------------------+
C |  EVAPORATION ROUTINE: WATER IS REMOVED FROM        |
C |   TOP LAYER (I=1) FIRST. WATER AND SOLUTE          |
C |   MOVE UP THE PROFILE TO REPLENISH WR(1) ONLY.     |
C |   SOLUTE VOLATILIZED FROM LAYER 1 ONLY.            |
C |   UPWARD MOVEMENT CONTINUES UNTIL NET EVAPORATN    |
C |   LOSSES ARE SATISFIED BY WGRAV + WM.              |
C |   UPWARD MOVEMENT OF WATER IS ACCOMPANIED BY       |
C |   UPWARD MOVEMENT OF SOLUTE.                       |
C |   WHERE NETEVN IS NOT SATISFIED BY WT(1), THE      |
C |   PROCESSES ABOVE ARE REPEATED UNTIL NETEVN = 0.   |
C +---------------------------------------------------+
  400 IF(NETEVN .LE .WT(1)) GO TO 4001
        NETEVN = NETEVN - WT(1)
        WE(1) = WT(1)
        GO TO 4002
 4001 WE(1) = NETEVN
      NETEVN = 0.0
 4002 SE(1) = WE(1)*ST(1)/WT(1)
      WRITE(6,474)
  474 FORMAT('NET E  WT(1)  WG(1)  WM(1)  WR(1)  WE(1)  SE(1)')
  475 FORMAT(7(F5.2,2X))
      WRITE(6,475)NETEVN,WT(1),WGRAV(1),WM(1),WR(1),WE(1),SE(I)
      WGMSUM = WGRAV(1) + WM(1)
      I = 1
  401 IF(WE(1) .LE. WGMSUM)GO TO 402
        I = I + 1
        WGMSUM = WGMSUM + WGRAV(I) + WM(I)
        GO TO 401
  402 ELLAST = I
      IF(ELLAST.EQ.1)GO TO 405
      K = ELLAST - 1
      DO 403 L=1,K
         LNEXT = L + 1
         WE(LNEXT) = WE(L) - WM(L) - WGRAV(L)
         SE(LNEXT) = WE(LNEXT)*ST(LNEXT)/WT(LNEXT)
  403 CONTINUE
      K = ELLAST - 1
      DO 404 L=1,K
         LNEXT = L + 1
         WT(L) = WT(L) - WE(L) + WE(LNEXT)
      DELTAS = -SE(L) + SE(LNEXT)
      MS(L) = MS(L) + DELTAS
         WM(L) = 0.0
         SM(L) = 0.0
         WGRAV(L) = 0.0
         SGRAV(L) = 0.0
         WR(L) = WT(L)
      B = DELTAZ*DB(L)*KADS(L)/WT(L)
C PARTITION OF SOLUTE MASS.
      ST(L) = MS(L)/(1+B)
      Q(L) = MS(L)*B/(1+B)
         SR(L) = ST(L)
  404 CONTINUE
  405 WT(ELLAST) = WT(ELLAST) - WE(ELLAST)
      DELTAS = -SE(ELLAST)
      MS(ELLAST) = MS(ELLAST) + DELTAS
      B = DELTAZ*DB(ELLAST)*KADS(ELLAST)/WT(ELLAST)
C PARTITION OF SOLUTE MASS.
      ST(ELLAST) = MS(ELLAST)/(1+B)
      Q(ELLAST) = MS(ELLAST)*B/(1+B)
      WGRAV(ELLAST) = WT(ELLAST) - WM(ELLAST) - WR(ELLAST)
      IF(WGRAV(ELLAST).LT.0.0)GO TO 406
        WM(ELLAST) = WMCAP(ELLAST)
        GO TO 499
  406 WGRAV(ELLAST) = 0.0
      WM(ELLAST) = WT(ELLAST) - WR(ELLAST)
  499 SGRAV(ELLAST) = WGRAV(ELLAST)*ST(ELLAST)/WT(ELLAST)
      SM(ELLAST) = WM(ELLAST)*ST(ELLAST)/WT(ELLAST)
      SR(ELLAST) = WR(ELLAST)*ST(ELLAST)/WT(ELLAST)
      IF(NETEVN .GT. 0.0)GO TO 400
        GO TO 999
C**************************************************************
C+------------------------------------------------------------+
C| DRAINAGE ROUTINE:. IF WATER IS LOST FROM THE BOTTOM LAYER,  |
C|                    IT IS REMOVED RROM THE SYSTEM AS DRAINAGE.|
C+------------------------------------------------------------+
  900 WDRAIN = WA
      SDRAIN = SA
      DCONCN = S
      WRITE(6,603)J
      WRITE(6,604)
      WRITE(6,605) WDRAIN, SDRAIN, DCONCN
  603 FORMAT(2X,'DRAINAGE WATERS AFTER DAY',I2)
  604 FORMAT('VOLUME     AMT.SOLUTE  CONC. SOLUTE')
  605 FORMAT(3F10.3,2X)
  999 IF(IR.GT.0)GO TO 320
```

```
      IF(FLNRT.LT.0)GO TO 2
      FLNRT = FLNR
      IF(J.NE.T1.AND.J.NE.T2.AND.J.NE.T3.AND.J.NE.TFIN)GO TO 1
      WRITE(6,699) J
      WRITE(6,698)
      WRITE(6,697)((K,WGRAV(K),WM(K),WR(K),SGRAV(K),SM(K),SR(K),ST(K
     *),Q(K),MS(K)),K=1,M)
  699 FORMAT(1X/,'SOLUTE PROFILE, DAY ',I2)
  698 FORMAT('LAYR GRAVHOH MOBHOH  RETHOH  GRAVSOL  MOBSOL'
     *,'  RETSOL  DISSOL  ADSOL TTLSOL')
  697 FORMAT(1X,I2,2X,F6.2,2X,F6.2,2X,F6.2,2X,F6.2,2X,F6.2,2X,F6.2
     *,2X,F6.2,2X,F6.2,2X,F6.2)
      WRITE(6,607)
      IF(J.LT.TFIN)GO TO 1
 9999 STOP
      END
```